

Streambed Sediments of Virginia Eastern Shore Streams Are Poised for Pore-Water
Denitrification

George Stillman McFadden
Charleston, South Carolina

B.A., University of Virginia, 2007

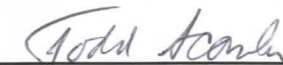
A Thesis presented to the Graduate Faculty
of the University of Virginia in Candidacy for the Degree of
Master of Science

Department of Environmental Sciences

University of Virginia
May, 2013 Degree **will be Conferred**







Abstract

Beneath Virginia Eastern Shore (VAES) streams are extensive biologically active zones poised for denitrification, which have the potential to decrease high groundwater nitrate loads to coastal receiving waters. Leached fertilizer from dense agricultural land use on the VAES has resulted in nitrate concentrations exceeding the Federal drinking water standard of $10 \text{ mg NO}_3\text{-N L}^{-1}$ in the underlying, unconfined Columbia aquifer. In addition to human health concerns, large nitrate loads to surface waters can disrupt ecosystems through eutrophication. A part of the riparian buffer system that has recently received attention as a site of substantial denitrification, given the right conditions, is streambed sediment. For this research, four streams on the VAES were selected for a regional study to evaluate the streambed conditions of carbon availability, vertical pore-water velocity, and chemical analysis of pore-water. Many studies cite low carbon supply as a limitation to denitrification at depth in sediment, however an abundant supply of carbon was found throughout streambed sediment at all four streams. At each stream, abundant carbon (total organic matter) existed in 70-90% of the sediment. At three streams the pore-water at the maximum sample depth of ~60 cm had median dissolved oxygen (DO) concentrations ranging from $0.82\text{--}1.30 \text{ mg L}^{-1}$; the depleted DO was taken to indicate microbial activity at depth. The fourth stream had higher DO concentrations in pore water. Two of the streams had low pore-water nitrate concentrations throughout the sediments, while the other two streams, Coal Kiln and Parker Creek, had a transverse pattern of higher nitrate and DO concentrations along the sides of the channel sediments. Coal Kiln and Parker Creek

had positive correlations of DO and nitrate, likely indicating denitrification was inhibited by DO, which is expected as denitrification is an anaerobic microbial process. Prior studies of the Columbia aquifer on the VAES have reported nitrate concentrations more than double the Federal drinking water standard. If the elevated nitrate concentrations are widespread throughout the Columbia aquifer on the VAES, then there is a large amount of nitrate removal along the flow path of groundwater discharging to streams. In the sediments of the four streams, pore-water velocity was slow enough for microbial processes and carbon was abundant to greater depths than previously reported. Throughout the streambed sediments of two streams and in the center channel sediments of the other two streams, the low DO and low nitrate concentrations suggest denitrification at a greater depth than measured. Overall, discharging groundwater diluted stream-water nitrate concentrations at three of the streams. The streambed sediments of the four VAES streams studied have similar characteristics and appear to be an important part of the riparian buffer system.

Table of Contents

1	Introduction.....	1
1.1	Riparian Zones as Water Filters	2
1.1.1	Near-Stream Sediments	3
1.2	Nitrate Contamination on the Virginia Eastern Shore	6
1.3	Research Objectives	9
2	Materials and Methods.....	10
2.1	Field Site Description.....	11
2.1.1	Piezomanometer Construction	16
2.1.2	Hydraulic Head Calculation	18
2.1.3	Manometer Equilibration, Accuracy, and Precision.....	19
2.1.4	Piezomanometer Use in the Field	20
2.2	Alternative Measurements of Pore-Water Velocity.....	22
2.3	Fieldwork and Sampling Design.....	23
2.4	Streambed Sediment Analysis	26
2.4.1	Estimation of Hydraulic Conductivity	28
2.5	Nitrogen Transport and Fate.....	30
2.6	Repeated Measures ANOVA	31
3	Results.....	33
3.1	Streambed Sediments	33
3.2	Flow Regime	35
3.3	Chemical Conditions in Streambed Sediments.....	47
3.3.1	Total Organic Matter.....	47
3.3.2	Pore-Water Dissolved Oxygen.....	50
3.3.3	Pore-Water Nitrate.....	54
3.4	Nitrate Transport	60
3.5	Nitrate Fate.....	61
4	Discussion.....	69
4.1	Streambed Sediment Architecture and Effects of Fluvial Processes.....	69
4.2	Flow Regime	73
4.3	Chloride as a Chemical Marker of Water Bodies	75
4.4	Streambed Sediment Denitrification and Nitrate Loads.....	79
5	Conclusion	84
6	References	86
7	Appendix A	93
8	Appendix B	98

List of Figures

Figure 2-1. Watersheds of the twelve streams sampled in the 1 st iteration of fieldwork.....	12
Figure 2-2. Location of the four streams selected for the 2 nd iteration of fieldwork.....	14
Figure 2-3. Picture of the oil-water piezomanometer drive-point inserted into a streambed.	15
Figure 2-4. Tip of the drive-point.	16
Figure 2-5. Comparison of known and manometer-measured hydraulic head differences in the laboratory.....	20
Figure 2-6. The aligned square grid sampling design performed in the 2 nd iteration.	25
Figure 3-1. All streams: Histogram of sediment grain size.	33
Figure 3-2. All streams: Mean K per depth interval of each stream, with Standard Error of the Mean (SEM) bars.....	34
Figure 3-3. All streams: Mean effective grain size per depth interval of each stream, with SEM bars.....	35
Figure 3-4. All streams: Boxplot of dh per depth interval of each stream.	36
Figure 3-5. All streams: Cubic spline interpolated contour maps of hydraulic head per depth interval at each stream. Pore-water hydraulic head was measured relative to overlying surface water in the stream.....	39
Figure 3-6. Mean q of each depth interval at each stream, with SEM bars.....	41
Figure 3-7. Boxplots of chloride concentration per depth interval of each stream. The vertical dashed green line represents the surface water chloride concentration.....	42
Figure 3-8. Interpolated contour maps of pore-water Cl^- mg L^{-1} per depth interval at each stream.	45
Figure 3-9. Histogram of all pore-water Cl^- concentrations at Coal Kiln in the left panel and Parker Creek in the right panel. The vertical dashed red line represents the Cl^- concentration discontinuity.....	47
Figure 3-10. Histogram showing the frequency of maximum TOM per sediment core for each depth interval.	49
Figure 3-11. Boxplots of TOM% per depth interval of each stream.....	50
Figure 3-12. Boxplots of DO per depth interval of each stream.	51
Figure 3-13. Interpolated contour maps of pore-water DO per depth interval at each stream.	54
Figure 3-14. Boxplots of nitrate concentration per depth interval of each stream. The vertical dashed green line represents the surface water nitrate concentration.....	55
Figure 3-15. Interpolated contour maps of pore-water nitrate mg L^{-1} per depth interval at each stream.....	58
Figure 3-16. Scatter plot of Cl^- to nitrate-nitrogen at Coal Kiln and Parker Creek, left panel and right panel respectively.	59
Figure 3-17. Mean J per depth interval of each stream, with SEM bars.....	61

Figure 3-18. Vertical profiles of nitrate mg L^{-1} at each stream. The vertical red line represents stream water nitrate concentration.	63
Figure 3-19. Mean nitrate removal rate between depth intervals (between 10 and 30 cm and between 30 and 60 cm) organized by vertical flow direction at each stream, with SEM bars. The sample size of each bar is featured directly above the bar.	65
Figure 3-20. Mean nitrate removal rate between depth intervals (between 10 and 30 cm and between 30 and 60 cm) for each stream, with SEM bars.	65
Figure 3-21. Scatter plot of DO to nitrate-nitrogen of pore-water at Coal Kiln and Parker Creek, left panel and right panel respectively.	66
Figure 3-22. Scatter plot of DO to nitrate-nitrogen and a least squares linear regression trendline of pore-water at all depths of Parker Creek.	67
Figure 4-1. Mean chloride concentration of stream water and groundwater at each stream, with SEM bars.	77
Figure 4-2. Chloride concentration of surface water, groundwater, and precipitation on the Delmarva Peninsula from numerous studies.	77
Figure 7-1. Boxplots of K by depth interval at each stream.	93
Figure 7-2. Boxplots of K by location in channel, the stream stretch, at each stream.	93
Figure 7-3. Boxplots of TOM% by location in the channel, stream stretch at each stream.	94
Figure 7-4. Chloride concentration vertical profiles at each stream.	95
Figure 7-5. Scatter plot of DO to R . Nitrate removal rate, R , between depth intervals (between 10 and 30 cm and between 30 and 60 cm) was calculated according to flow direction, upward or downward. A corresponding DO value was calculated by averaging the DO of the two associated depth intervals (the mean DO at 10 and 30 cm or the mean DO at 30 and 60 cm).	96
Figure 7-6. Scatter plot of TOM% to R . The same methods explained in Figure 7-2 were used here, but with TOM% instead of DO	97
Figure 8-1. Pore-water velocity measured by the piezomanometer device compared to pore-water velocity calculated from temperature profiles using a Matlab program by <i>Flewelling</i> [2009].	99
Figure 8-2. A comparison of methods for measuring pore-water velocity. The Schmidt method was completed using the Matlab program Ex-Stream; the Bredehoeft method was completed using a model by <i>Flewelling</i> [2009]; and the Piezomanometer method is also presented.	100

List of Tables

Table 2-1. Overview of fieldwork performed at specific streams.....	13
Table 2-2. Mean porosity value of each stream.....	29
Table 2-3. <i>K</i> values from specific depth intervals were averaged to provide values for calculation of pore-water velocity.....	30
Table 3-1. Descriptive statistics of repeated measures ANOVA between stream stretches A, C, and E, at Coal Kiln and Parker Creek.....	46
Table 3-2. Descriptive statistics of TOM content of all depth intervals at each stream.....	48
Table 3-3. Descriptive statistics of <i>DO</i> per depth interval from repeated measures ANOVA between stream stretches A, C, and E, at Parker Creek.....	51
Table 3-4. Descriptive statistics of nitrate-nitrogen mg L ⁻¹ per depth interval from repeated measures ANOVA between stream stretches A, C, and E, at Coal Kiln and Parker Creek.....	58
Table 3-5. Pearson correlation coefficient of chloride and nitrate of specific depth intervals at Coal Kiln and Parker Creek.....	59
Table 3-6. Pearson's correlation coefficient, <i>r</i> , of <i>DO</i> to NO ₃ ⁻ and Cl ⁻ to NO ₃ ⁻ for specific depth intervals of Coal Kiln and Parker Creek.....	67

1 Introduction

Human production of reactive nitrogen now exceeds the global amount of natural biological nitrogen fixation [Galloway *et al.*, 2003]. Most of human produced reactive nitrogen is from the Haber-Bosch process, of which 85% is utilized for fertilizers [Galloway *et al.*, 2003]. Cheap and abundant fertilizers have resulted in greater agricultural productivity, helping feed a growing global population. However, the more than doubling of reactive nitrogen available to ecosystems has also caused negative externalities of water body acidification [Galloway *et al.*, 2003], human health issues [Prasad and Power, 1995], greenhouse gas production [Wagner-Riddle *et al.*, 1996], and eutrophication [Nixon, 1996]. The problems caused when reactive nitrogen enters water in excess motivated this research.

Nitrate has been designated as the most ubiquitous water contaminant in the world [Spalding and Exner, 1993]. Nitrogen in fertilizers is typically in the form of ammonia, which can easily be converted into nitrate via nitrification when it is applied to the soil. Nitrate is readily transported by water because nitrate is highly soluble and does not adsorb to most soils since most soils have a negative charge as well. The high mobility of nitrate has led to extensive contamination in U.S. waters in areas with agricultural activities that used fertilizers [Winter, 1998]. Nitrate is the most significant pollutant of coastal waters [Justic *et al.*, 1995; Howarth *et al.*, 2000; NRC, 2000; Rabalais *et al.*, 2002; Galloway *et al.*, 2003]. Howarth *et al.* [2000] concluded that 60% of coastal bays and rivers of each coastal state in the contiguous U.S. has moderate to severe degradation of the ecosystem from nutrient contaminants. For mid-Atlantic coastal waters, human activities have increased the

nitrogen load by 5.1 fold [Howarth *et al.*, 2000]. The consequences of excess nutrients in water bodies are human health risks, eutrophication, hypoxia, loss of biodiversity, and habitat degradation [Galloway *et al.*, 2003]. Human health risks can be caused by the ingestion of nitrates in drinking water, which leads to methemoglobinemia, commonly known as blue baby syndrome. Children are more susceptible to the condition. Nitrate in the blood stream hinders the transport of oxygen in the body and can cause in tissue hypoxia [Meek, 1996]. The worse incidents of coastal eutrophication in the U.S. have occurred in the Gulf of Mexico and the mid-Atlantic [Bricker *et al.*, 1999].

1.1 Riparian Zones as Water Filters

Riparian areas have been identified as natural water filters for receiving waters. Gregory *et al.* [1991] defined the riparian zone as the area surrounding streams where terrestrial and aquatic ecosystems intersect, delineated by the floodplain of the stream. The forestry industry utilized riparian areas to mitigate disturbances to stream ecosystems, and then other practices such as agriculture adopted the practice [Lowrance *et al.*, 1997]. Over time, the riparian area became known as the riparian buffer zone when used for water quality purposes. The riparian buffer zone has been shown to substantially decrease the flux of nitrate to streams [Peterjohn and Correll, 1984; Jacobs and Gilliam, 1985; Cooper, 1990; Haycock and Pinay, 1993]. The two mechanisms in a riparian buffer zone decreasing nitrate fluxes are denitrification [Hill, 1996] and autotrophic uptake [O'Neill and Gordon, 1994].

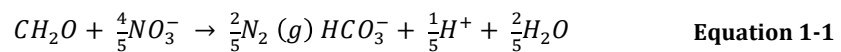
Riparian buffer zones can remove 0 – 99% of groundwater nitrate traveling towards streams, typically removing at least 80%, a large potential [Hill, 1996]. Hill *et al.* [2000] noted the wide range of possible riparian conditions and the consequent uncertainty of denitrification extent. The many factors of a riparian zone such as landscape features, sediments, and vegetation, contribute to making the extent of nitrate removal as well as the amount removed by uptake versus denitrification, unique to each site [Young and Briggs, 2005]. The riparian buffer zone can be bypassed by overland flow during precipitation events or by groundwater flow paths deeper than the soil horizons and root zone [Böhlke and Denver, 1995; Hill, 1996; Gold *et al.*, 2001; Vidon and Hill, 2004]. However, overland flow typically constitutes a small portion of water input to a stream. A part of the riparian system that has gained attention for decreasing nutrient loads is streambed sediments.

1.1.1 Near-Stream Sediments

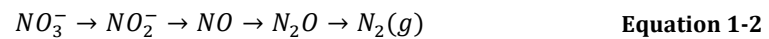
The sediments adjacent to stream water are typically an environment with low turbulence, abundant surface area for microorganism habitat, and a continuous flux of aqueous solution, in which microorganisms can flourish. The influence of groundwater-surface water interactions on ecosystems has recently gained attention and become a major hydrology research topic [Kennedy *et al.*, 2008]. The heterogeneity of sediments presents tortuous flow paths, as well as interconnected and disconnected pore-waters. Streambed sediment architecture allows exclusive microbial processes like nitrification and denitrification to occur in close proximity [Fischer, 2005]. Kennedy *et al.* [2009] reported that denitrification in streambed

sediments decreased the nitrate load of groundwater discharging to surface water by 50%.

Denitrification is mainly performed by facultative bacterial heterotrophs in an anaerobic environment, given an ample supply of electron donors [Maier *et al.*, 2009]. A generalized view of denitrification in sediments is the oxidation of organic carbon by facultative heterotrophs and the reduction of nitrate (Equation 1-1) [Freeze and Cherry, 1979].



Denitrification reduces nitrate to unreactive nitrogen, N_2 , with the following intermediate steps:



Complex channel morphology influences the hydraulic head gradient in sediments. The near-stream sediment that experiences surface water input is called the hyporheic zone. Triska *et al.* [1989] precisely defined the hyporheic zone as the sediment where stream water and groundwater mix, with at least 10% of the water from stream water. Microbial activity in the streambed sediments is aided by carbon and oxygen inputs to the sediments from seeping surface water [Brunke and Gonser, 1997; Brunke and Fischer, 1999; Battin, 2000]. Complex flow paths in the sediments and hyporheic exchange is caused by channel characteristics such as meanders [Wroblicky, 1998], changes in streambed slope [Harvey and Bencala, 1993], stream sinuosity [Cardenas, 2009], as well as streambed topography features like bedform geometry, and obstacles of woody debris and boulders [Wondzell and Swanson, 1999; Marion *et al.*, 2002; Zarnetske *et al.*, 2007]. The more heterogeneous

the channel morphology, the more complicated pore-water flow paths become [Cardenas *et al.*, 2004].

Fluvial processes create patterns in channel morphology that affect pore-water flow. Deposition of fines in zones of slower stream water velocity, such as along stream banks, clog sediments and result in decreased hydraulic conductivity (K) [Genereux *et al.*, 2008]. Lower K decreases the ease of flow through the porous medium, and can reduce the throughput volume. Birgand *et al.* [2007] noted that agricultural streams are prone to sediment clogging because of an abundant supply of fines and organic particulates input to streams from adjacent land.

The amount of denitrification in streambed sediments is often limited by carbon availability [Kristensen *et al.*, 1995; Bastviken *et al.*, 2001; Bradley *et al.*, 1992; Groffman, 1996; Hedin *et al.*, 1998; Birgand *et al.*, 2007]. Due to carbon limitations, denitrification in streambed sediments is often reported as restricted to shallow sediments or the hyporheic zone [Inwood *et al.*, 2007; Stelzer *et al.*, 2011]. In other riparian settings, microbial activity in sediments occurs in the soil-stream interface where terrestrially derived water with high dissolved organic carbon (DOC) meets deeper groundwater loaded with electron acceptors [Hedin *et al.*, 1998]. And Hill *et al.* [2000] observed denitrification along flow paths 2-5 m deep in a riparian zone, associated with localized buried river deposits of organic matter. The processes governing carbon input to sediments vary in riparian zones, and ultimately determine the location and magnitude of microbial activity.

1.2 Nitrate Contamination on the Virginia Eastern Shore

The Delmarva Peninsula has been the site of numerous studies investigating water quality. The Virginia Eastern Shore (VAES) makes up the southern tip of the Delmarva Peninsula and is part of the Atlantic Coastal Plain physiographic province. The Delmarva Peninsula is topographically flat and underlain by the unconfined Columbia aquifer, composed of Pleistocene-aged sands, generally 8-30 m thick [Sinnott and Tibbits, 1968; Mixon *et al.*, 1989]. The VAES is divided into Accomack and Northampton counties, in which the total land area designated as farmland is 32.6 and 47.1%, respectively; and 80% of the farmland is cultivated with row crops [USDA, 2009]. High nitrate concentrations in the groundwater have been observed throughout the Delmarva, mainly attributed to agricultural practices [Denver *et al.*, 2004]. A water-quality report of the Delmarva Peninsula by Denver *et al.* [2004], sampled shallow wells ranging in depth from 6-8 m below land surface, which terminated in the Columbia aquifer. Groundwater from about one-third of the wells had nitrate concentrations exceeding the Federal drinking water standard of 10 mg NO₃-N L⁻¹ [Denver *et al.*, 2004]. Specifically in the VAES portion of the Columbia aquifer, Hamilton *et al.* [1993], reported the highest nitrate concentrations occurred in shallow groundwater, approximately 6 m under agricultural fields. From sampling a well network at the southern end of the VAES, a maximum groundwater nitrate concentration of 34 mg NO₃-N L⁻¹ was found, which occurred in the Columbia aquifer [Hamilton *et al.*, 1993].

A stream on the VAES, Cobb Mill Creek, has been a study site of denitrification in the riparian zone. Past research at Cobb Mill Creek has shown

large decreases in groundwater nitrate concentrations by denitrification as groundwater travels towards the channel through sediments adjacent to the stream [Galavotti, 2004; Gu, et al., 2007; Mills et al., 2008; Flewelling et al., 2011.] Flewelling et al. [2011] reported groundwater nitrate concentrations below the stream decreased from 15-20 mg NO₃⁻-N L⁻¹ to 1-2 NO₃⁻-N mg L⁻¹ along flow paths to the stream. Denitrification mainly occurred in the shallow sediments of Cobb Mill Creek, concomitant with the highest sediment content of organic matter [Galavotti, 2004]. Sediment cores extracted by Gu [2007] corroborated the concentration of sediment organic matter in the shallow sediments, specifically in the top 20 cm. Laboratory experiments on intact sediment cores from Cobb Mill Creek showed increasing flow rates adversely affected denitrification [Gu et al., 2007]. Pore-water velocity through sediments is an additional factor affecting the amount of denitrification in riparian zones.

Based upon a theoretical groundwater flow model of a riparian zone [Hornberger et al., 1998], two general groundwater flow paths to a stream occur. A shallow flow path travels in a more lateral trajectory through the root zone and soil horizons of the riparian zone. The shallow flow path is expected to consist of groundwater from nitrate and chloride poor precipitation, which recharges into the riparian zone [Böhlke and Denver, 1995; Flewelling et al., 2011]. Along the shallow flow path through the riparian zone, changes to the aqueous chemistry of the groundwater can occur from plant uptake and microbial activity, thus the water is referred to as riparian-influenced groundwater [Flewelling et al., 2011]. The second general groundwater flow path typically travels too deeply to be affected by the root

zone or soil horizons in the riparian zone. The deeper flow path consists of groundwater recharged distal to the stream, in agricultural fields beyond the riparian zone. The groundwater recharged through agricultural fields is expected to have high nitrate and chloride concentrations from leached fertilizers. The deeper flow path is referred to as the riparian-bypass groundwater [Lowrance *et al.*, 1997], along which the aqueous chemistry is not expected to change much. Riparian-influenced groundwater discharges into the stream along the stream sides and riparian-bypass groundwater travels up towards the streambed sediment surface more vertically, typically discharging in the center of the channel [Hornberger *et al.*, 2008].

The two general groundwater flow paths in the riparian zone have been observed to have distinct chemical identities at Cobb Mill Creek [Gu *et al.*, 2008; Flewelling *et al.*, 2011]. On average, riparian-influenced groundwater had low nitrate and high chloride concentrations, whereas the riparian-bypass groundwater had the opposite concentration scheme [Gu *et al.*, 2008]. The low nitrate concentration in riparian-influenced groundwater is likely explained by plant uptake and microbial denitrification occurring along a shallow flow path towards the stream. Comparatively, the main opportunity to remove nitrate in riparian-bypass groundwater occurs by denitrification in the streambed sediments. Gu *et al.* [2007] estimated that greater than 80% of nitrate traveling through streambed sediments at Cobb Mill Creek was removed by denitrification. Overall, the riparian zones on the VAES, which include the streambed sediments, can improve water quality by reducing nutrient loads input to streams.

Streams on the eastern side of the VAES discharge to the ecologically productive, yet sensitive coastal estuaries. The coastal estuaries are part of the Virginia Coast Reserve (VCR), which is home to the longest stretch of undeveloped coastline on the east coast of the U.S. Input of nitrogen to the estuaries can cause eutrophication. Denitrification in streambed sediments could be providing an essential service in decreasing the load of leached fertilizers to the VCR. Environmental degradation to the VAES estuaries would harm the natural resources as well as hurt local economies. The collective interest in riparian zone nitrate removal motivates this research.

1.3 Research Objectives

The transport and fate of nitrate has been well studied in the riparian zone of Cobb Mill Creek on the VAES. The present research aimed to expand understanding of VAES streams beyond Cobb Mill Creek to a more regional level. The main objectives of this research were to visit VAES streams to evaluate nitrate transport and fate in near-stream sediments, to examine the flow regime, and to examine the spatial layout of the biologically active zone of streambed sediments. This research aimed to compare the denitrification potential of streambed sediments of VAES streams and report the range of these conditions regionally. Pore-water and sediment characteristics were analyzed for within as well as among-stream patterns.

2 Materials and Methods

The geographical region of this study is the southern tip of the Delmarva Peninsula, the Virginia Eastern Shore (VAES). The VAES is part of the Atlantic Coastal Plain Province, characterized by low relief topography and underlain by unconsolidated sediments. The underlying sediment ranges in thickness from 0 to 2440 m and dips to the south and southeast [Hamilton *et al.*, 1993]. The VAES is underlain by the unconfined surficial Columbia aquifer [Hamilton *et al.*, 1993; Richardson, 1994]. The Columbia aquifer is composed of unconsolidated Pleistocene sediments ranging from very fine silty sands to gravelly clean sands, with discontinuous clay and silt lenses throughout [Richardson, 1994]. Most of the Columbia aquifer consists of sands with high infiltration rates [Sinnott and Tibbitts, 1968; Lowrance *et al.*, 1997]. The Columbia aquifer ranges in thickness from 0 to 50 meters, typically 10 to 20 meters thick [Phillips, 1993]. A continuous clay-silt unit under the sediments ends the unconfined Columbia aquifer [Meng and Harsh, 1988]. The VAES is topographically divided by a ridge that runs north to south along the center of the peninsula with an elevation of approximately 15 m [Sinnott and Tibbitts, 1968]. This study exclusively focuses on the eastern half of this divide, the Atlantic Ocean side.

Agricultural land-use occupies a large portion of the VAES. A 2007 census reported that the two counties of VAES, Northampton and Accomack, consisted of 47% and 33% farmland by area, respectively [USDA, 2009]. The farmland of Northampton and Accomack counties was 82% and 95% harvested cropland, respectively [USDA, 2009]. Harvested cropland was predominantly row crops of soy

bean and corn. A study of the Delmarva by the National Water Quality Assessment Program (NAWQA) reported fertilizer application accounts for 95% of available nutrients [Denver *et al.*, 2004]. The NAWQA investigation found nitrate concentrations exceeding the EPA Primary Contaminant level of 10 mg NO₃⁻-N L⁻¹ to be widespread in the surficial aquifer [Denver *et al.*, 2004]. The high nitrate concentrations in the aquifer are attributed to leached fertilizers from agricultural lands [Denver, 1989]. A U.S. Geological Survey report of water quality found nitrate concentrations as high as 34 mg NO₃⁻-N L⁻¹ in the Columbia aquifer at the southern tip of the VAES [Hamilton *et al.*, 1993]. Nitrate is transported through the Columbia aquifer with limited chemical transformation at depth due to oxic conditions and minimal labile carbon availability, precluding microbial transformation [Hamilton *et al.*, 1993; Mills *et al.*, 2008]. Groundwater transported through the riparian zone or streambed sediments passes through a biogeochemically active zone that can significantly decrease nitrate levels.

2.1 Field Site Description

Nearly all of the streams transecting the eastern section of the VAES were initially investigated. Streams of the VAES eastern section are typically 1st and 2nd order gaining streams and flow direction is generally oriented west to east, flowing from the central ridge to the Atlantic Ocean. All of the 17 streams of the ongoing synoptic survey led by Professors Janet Herman and Aaron Mills were visited and sampled if there was appreciable surface water. In addition to the synoptic survey streams, two other streams were sampled. The majority of fieldwork was performed from July through October 2011. Fieldwork was completed in 2

segments referred to as the 1st and 2nd iterations. During the 1st iteration, streams were investigated for appreciable surface water flow, to review fluvial characteristics, and to test instruments, particularly how deep an instrument could penetrate the streambed sediments. Twelve streams were sampled during the 1st iteration (Figure 2-1) and stream details are presented in Table 2-1. Using the sampling location as the catchment outlet, watershed size was calculated using ArcMap™ software by Esri. Watersheds ranged in area from 92 – 1546 ha, with a mix of land uses.

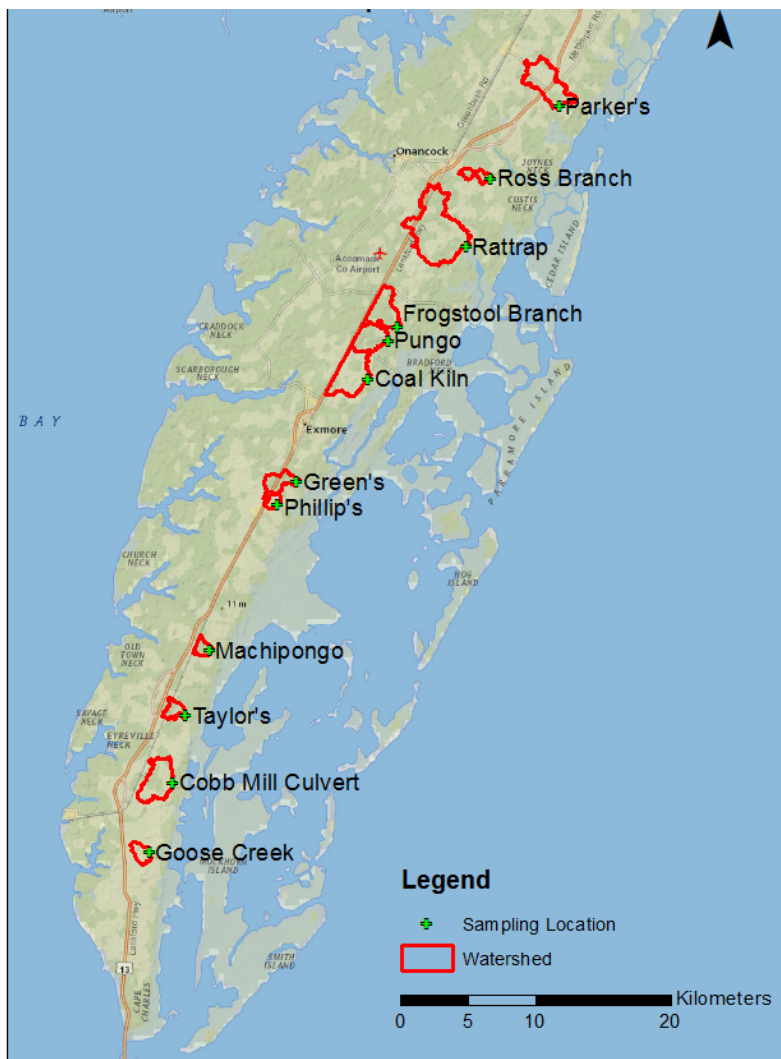


Figure 2-1. Watersheds of the twelve streams sampled in the 1st iteration of fieldwork.

Table 2-1. Overview of fieldwork performed at specific streams.

Stream name (north to south)	Watershed area (ha)	3-point sampling scheme	15-point sampling scheme	Water		Sediment cores collected
				Major anions	Dissolved oxygen	
Parker Creek	685					
Ross Branch	137					
Rattrap Creek	1546					
Frogstool Branch	485					
Pungo Creek	416					
Coal Kiln	706					
Greens Creek	273					
Phillips Creek	92					
Machipongo	119					
Taylor Creek	152					
Cobb Mill Creek	568					
Lakewood Pond Drainage	158					

Conclusions drawn from the 1st iteration motivated selection of 4 streams for a more intensive investigation, which constituted the 2nd iteration. Since fieldwork was performed during the drier part of the year, late summer and fall, streams with relatively substantial flow were chosen. Only synoptic survey streams were chosen in order to provide complementary data to that dataset. An additional criterion was to select streams geographically distributed along the VAES from north to south. Parker Creek, Coal Kiln, Phillips Creek, and Machipongo streams were selected with watersheds ranging from 92-706 hectares (Figure 2-2).

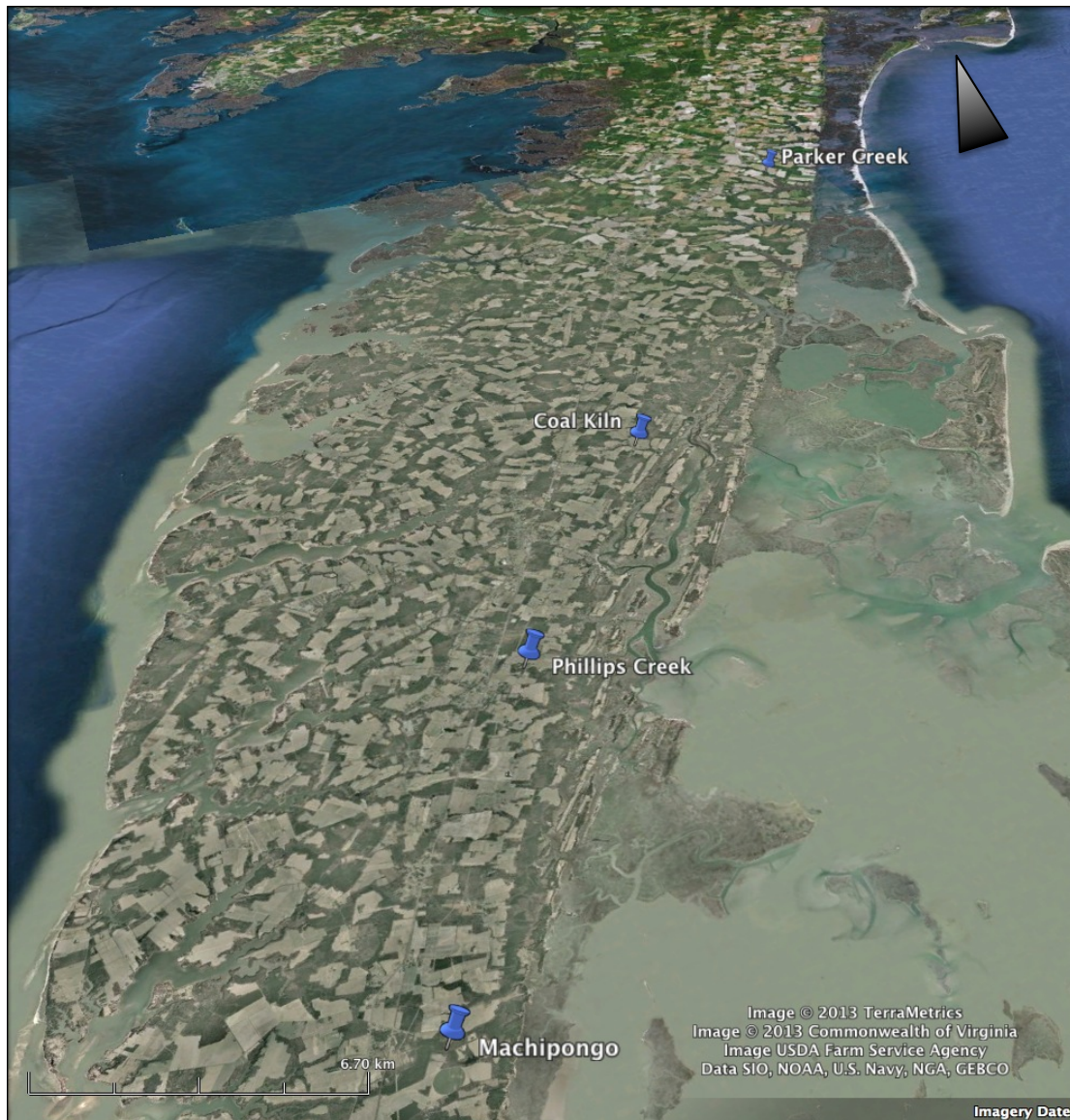


Figure 2-2. Location of the four streams selected for the 2nd iteration of fieldwork.

A suite of hydrological variables known to affect denitrification in streambed sediments was measured *in situ* using an oil-water piezomanometer drive-point. The oil-water piezomanometer drive-point was constructed following the schematics of *Kennedy et al.* [2007] with minor modifications. The device is designed to be easily portable and sample a range of depths. The device consists of three main parts: the groundwater arm, the manometer, and the surface-water arm

(Figure 2-3; Figure 2-4). (From hereon, when referring to the device in its entirety it is called the piezomanometer.)

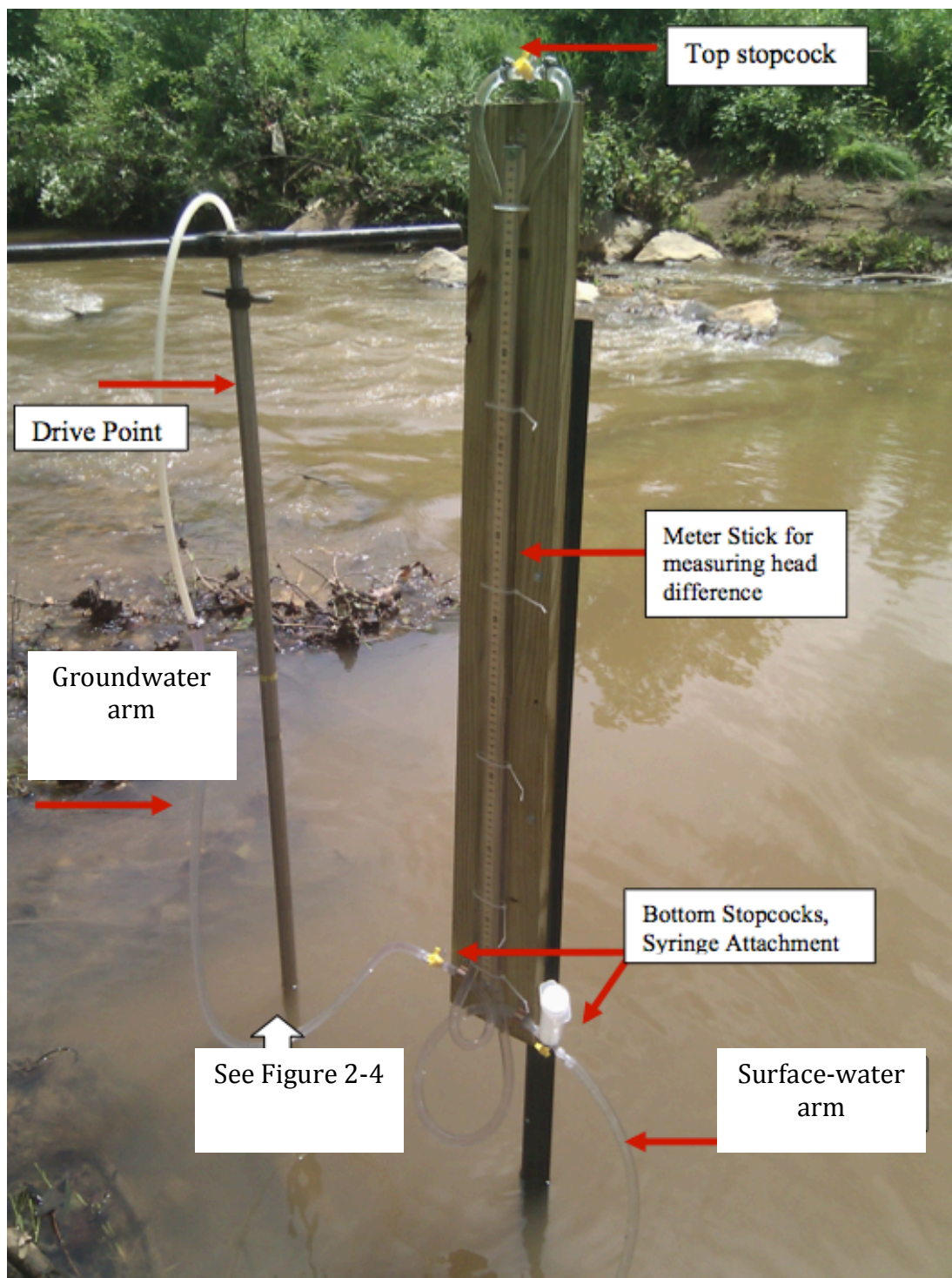


Figure 2-3. Picture of the oil-water piezomanometer drive-point inserted into a streambed.

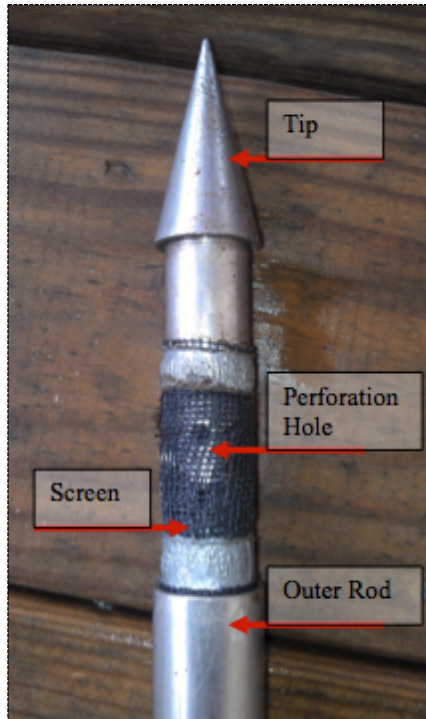


Figure 2-4. Tip of the drive-point.

2.1.1 Piezomanometer Construction

The groundwater arm consists of rigid polyethylene tubing that runs through a hollow stainless steel drive-point 2 m in length and connects to the manometer. The drive-point has a hollow metal sheath that encases an inner metal rod with a detachable tip. The tip has a cone-shaped head followed by a 10 cm perforated length. Attached to the perforated tip by a clamp is rigid polyethylene tubing of 3.2 mm inner diameter (ID) and 9.5 mm outer diameter (OD). The rigid tubing extends from the perforated length through the hollow drive-point and out the top. This end of the rigid tubing is attached to the manometer by sliding the manometer flexible Tygon® tubing over the rigid tubing and securing it with a worm gear hose clamp for an air/water tight fit. The sheath and inner rod are kept apart by rubber O-rings in machined slots of the inner rod, allowing for easy telescoping. At the top of the inner rod is a threaded bolt that keeps the sheath fully extended over the inner rod,

covering the perforated tip, for easier insertion into the streambed and protection of the tip. This bolt is unscrewed 10 cm when the drive-point reaches the desired depth. A threaded handlebar also screws onto the inner rod for plunging the drive-point.

The manometer and surface-water arm of the device use flexible Tygon® tubing with a 6.4 mm ID and 12.7 mm OD. The surface-water arm is a 1 m length of tubing attached to the manometer at one end and inserted into a stilling bottle at the other. To limit the effect of stream water velocity on the hydraulic head and cause variations in the manometer, a 250 mL polyethylene bottle protects the tube opening and acts as a stilling well. Small holes were cut out of the bottle for water infiltration, the bottle cap has a hole for the tube to be inserted, and a weight was placed in the bottom of the bottle.

The manometer consists of approximately 2.5 m of tubing that forms an inverted U-tube surrounding a meter stick screwed to a 1.1 m by 0.15 m treated board. The flexible tubing runs parallel to the meter stick and is held tightly in place by six zip ties. Excluding the connection of the groundwater tubing to the manometer, there are three tubing junctions completed by three-way stopcocks. Each end of the flexible tubing has a 6.4 mm luer fitting inserted into it, with silicone rubber sealant to ensure air- and water-tight connections.

An addition to the *Kennedy et al.* [2007] piezomanometer design was the insertion of a stopcock at the apex of the inverted U-tube, referred to as the top stopcock. The flexible tubing was cut and reconnected by a three-way Luer stopcock, with worm gear hose clamps on either side of the stopcock to help

maintain the connection since the curvature of the tubing exerts a constant stress on the connection. This top stopcock was added to the design for easy addition or removal of oil and for removal of air bubbles. It is essential to remove any air bubbles from the manometer because the compressibility of air will introduce error into pressure gradient readings. At the bottom of the manometer board, after running the length of the meter stick, both ends of tubing are looped (left-side counter-clockwise and right-side clockwise), go through a copper hold-down clamp, and face outwards. The loops create a local elevation maximum for both arms of the manometer to trap air bubbles and sediment. The manometer board is bolted onto a garden stake with variable height options, and the stake is inserted into the streambed.

In the laboratory, the manometer tubing was filled with deionized water. Using the top stopcock, light oil (corn oil) was injected with a 100 mL plastic syringe until the oil in the tubing reached the 50 cm mark on both sides of the meter stick. The manometer was then turned off to external influence by positioning the bottom stopcocks to off and the top stopcock only open to both sides of tubing. A thermometer was attached to the board for air-temperature readings during sampling.

2.1.2 Hydraulic Head Calculation

To measure the relative hydraulic head difference between the two manometer arms, the height of the oil-water interface on both arms was recorded and the manometer hydraulic head difference (Δh_m) was calculated using Equation 2-1:

$$\Delta h_m = GW - SW \quad \text{Equation 2-1}$$

where GW is the groundwater arm height (cm), and SW is the surface water arm height (cm). Compared to an air-water manometer, an oil-water manometer shows more sensitivity to head changes because oil is less compressible [Kelly and Murdoch, 2003]. The lesser density of oil than water amplifies the head difference between the two arms. A reduction factor is applied to the measurement to calculate the non-amplified hydraulic head difference (Δh_w) (Equation 2-2).

$$\Delta h_w = \frac{(\rho_w - \rho_m)\Delta h_m}{\rho_w} \quad \text{Equation 2-2}$$

where ρ_w is the density of water; ρ_m is the density of oil. Finally, the actual hydraulic head gradient $\left(\frac{dh}{dl}\right)$ between the two water bodies is calculated as:

$$\frac{dh}{dl} = \frac{\Delta h_w}{L} \quad \text{Equation 2-3}$$

where L is the length from the center of the perforated tip on the drive-point to the streambed sediment interface.

2.1.3 Manometer Equilibration, Accuracy, and Precision

In the laboratory, hydraulic head difference between two adjacent beakers of water was compared to readings from the manometer (excluding the steel drive-point attachment). Each arm of the manometer was placed into beakers equally filled with water. When the oil-water interfaces on both sides of the manometer equilibrated and equaled each other, water was added to one beaker, and manometer readings were taken over time. The reference hydraulic head difference was taken as the difference in water height between the beakers. Seven runs of varying head differences were performed and are graphed as hydraulic head

difference over time in Figure 2-5. The runs show logarithm-shaped curves that approach steady state at approximately 10 minutes.

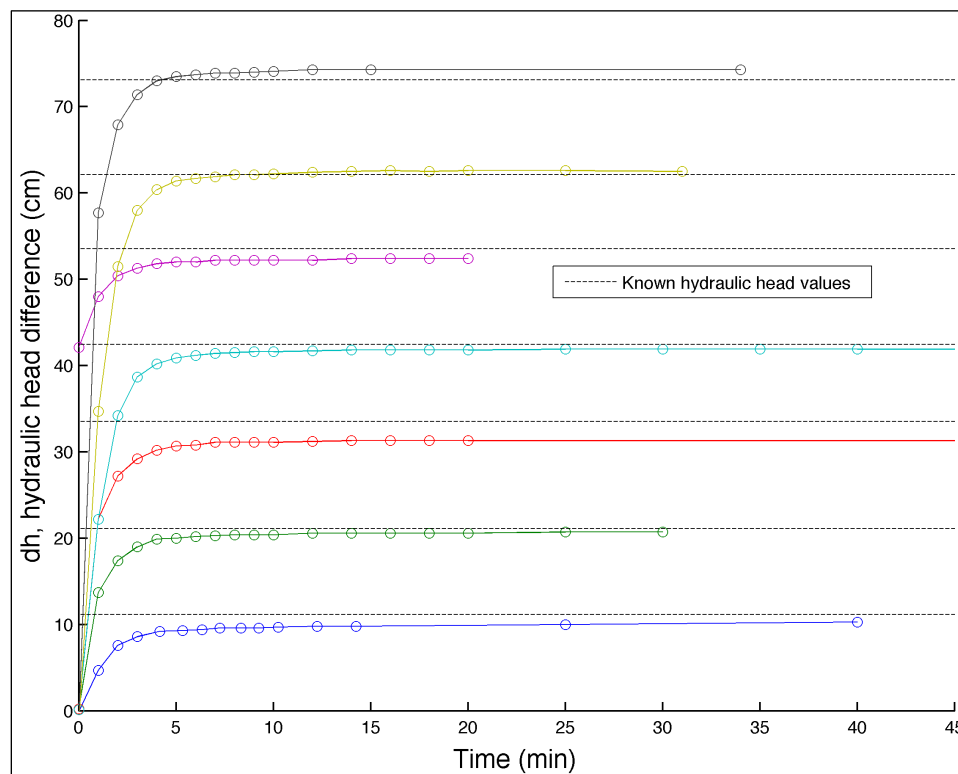


Figure 2-5. Comparison of known and manometer-measured hydraulic head differences in the laboratory.

2.1.4 Piezomanometer Use in the Field

In order to deploy the piezomanometer at a location, the drive-point was inserted into the streambed sediments and pushed down to the desired depth. The inner rod bolt was unscrewed 10 cm, and then the sheath was pulled up to the bolt to expose the screened perforated tip to the groundwater. The garden stake holding the manometer was inserted downstream of the drive-point to mitigate interference with groundwater streamlines. The groundwater and surface-water arms were connected to the manometer and the air in the tubing arms was displaced with water by withdrawing water from the stopcocks on both sides with a plastic syringe.

Approximately 100 mL of water was initially purged from each of the groundwater and surface-water arms. The volume of the groundwater arm tubing is approximately 80 mL, thus at least 1 tubing volume was flushed prior to equilibration. Groundwater was purged at a very slow rate to limit disturbance to the groundwater and to fill the tubing with representative water. Groundwater was withdrawn until minimal turbidity was achieved. The surface-water arm was easily filled with representative water, assuming stream stage was adequately deep.

When both arms were filled, the bottom stopcocks were opened allowing the manometer to equilibrate. The manometer was given at least 10 minutes to equilibrate to the opposing surface-water and groundwater pressures. After 10 minutes, if the oil-water interface was moving at ≥ 1 mm per minute then equilibration continued until the rate decreased to less than the 1 mm min^{-1} . After measuring the hydraulic head heights, a groundwater sample was collected. The manometer was turned off and a plastic syringe, washed with Alconox® and rinsed 10 times with deionized water, was attached to the valve of the groundwater-arm stopcock. Approximately 50-100 mL of groundwater was withdrawn from the drive-point and discharged into a vessel containing an YSI Pro-ODO® probe for a dissolved oxygen measurement. A groundwater sample of approximately 25-35 mL was injected into a sample bottle from the plastic syringe and placed in an ice-filled cooler for storage. Each day that fieldwork was conducted, a surface-water sample was collected as well; the timing of surface-water sample collection ranged from morning to late afternoon.

There were problems with the deployment of the piezomanometer to the 10 cm depth. The drive-point is about 2 m long and weighs approximately 25 lbs. Stabilizing the long and heavy drive-point at the 10 cm depth was difficult at some locations. Due to the comparatively lightweight sediment and the loose compaction of some sediment, the drive-point would sink to greater depths than 10 cm or would tip over. At the locations with drive-point problems, the drive-point required stabilization to maintain the 10 cm depth and to stay vertical. In addition, there is a general concern whether sediment surrounding the drive-point shaft when inserted to the 10 cm depth, formed a tight seal. At the next depth interval measured by the drive-point, 30 cm, a tight seal of sediment appeared likely because of the length of sediment surrounding the shaft, the difficulty of pushing the shaft to the greater depth, and more consistent measurements. The lack of a seal at 10 cm could have caused annular space around the shaft, and consequently interfered with the accuracy of measurements by the device.

2.2 Alternative Measurements of Pore-Water Velocity

In addition to piezomanometer measurements to calculate Darcy flow in streambed sediments, two other methods were employed to measure groundwater velocities for comparison. Seepage meters were deployed and temperature profiles measured.

Seepage meters were deployed adjacent to sample locations to measure specific discharge. Seepage meters were constructed and used following the methods detailed by *Lee* [1977]. Seepage meters were made from steel cylinders with a 10 cm diameter and cut to have a 10 cm length. A 1.27 cm diameter plastic

nozzle was inserted into a hole cut in the top of the cylinder and glued in place. Seepage meters were inserted into the streambed sediments, leaving about 2 cm of headspace between the sediment and the cylinder top. The seepage meters were given a few minutes for any gases trapped within the cylinder to escape, and then an empty and airless powder-coated latex condom was attached to the plastic nozzle with a cable-tie. The volume of water collected in the condom over a time interval provides a discharge rate.

Sediment temperature profiles were measured at all sample locations to estimate pore-water velocity using an analytical solution for the flow of heat and fluid in the 1-D vertical direction. A thermocouple was used to record temperatures at half of the stream stage, at the streambed sediment surface (0 cm), and 10, 20, 30, 40, 50 and 60 cm below the sediment surface. Pore-water velocity was calculated using two Matlab programs. One program was a non-linear curve-fitting algorithm developed by *Flewelling* [2009], which was based on the 1-D analytical solution for fluid flow by *Bredehoeft and Papadopoulos* [1965]. The other program used was *Ex-Stream* developed by *Swanson and Cardenas* [2011]. In *Ex-Stream*, the steady-state model of 1-D flow based on *Schmidt et al.* [2007] was selected.

2.3 Fieldwork and Sampling Design

Fieldwork was performed during base-flow conditions, daylight hours, and in seasonally stable conditions to limit temporal variability. At each stream, a study site was selected east of where the road (usually Route 600) intersected the stream. From the intersecting road, the nearest available area with a relatively straight reach and fluvial morphology unaffected by the road culvert was chosen. In the 1st

iteration of fieldwork, 12 streams were sampled and the piezomanometer was deployed at three sample locations, three m apart, located along the stream centerline. The distance of three m apart surpassed the minimum sampling density recommended in a sampling density study by *Kennedy et al.* [2008] in a similar low-order stream in the coastal plain of North Carolina. The objective was to take measurements at depths of 10 and 60 cm below the sediment surface at each sample location for construction of vertical profiles. Due to variable subsurface obstructions and sediment compaction the 60 cm depth was often not reached. A wooden plank was laid across the stream resting on the stream banks to avoid stepping in the stream and influencing it, particularly the hydraulic head gradient.

For the 2nd iteration of fieldwork, the four selected streams were more densely sampled and the data collected constitutes the bulk of this research. The 1st iteration sampling area was revisited at Parker Creek, Coal Kiln, Phillips Creek and Machipongo streams. The sampling scheme of the 2nd iteration was designed to investigate transverse patterns in streambeds, calculate reach-scale variables and make among stream comparisons. Sampling was performed in an aligned square-grid [*Gilbert, 1987*], with three transverse transects crossing the stream, transects were located approximately 3 m apart (Figure 2-6). Each transect consisted of five sample locations equally spaced across the stream, with the first and last sample locations located at the edge of the stream. At each sample location the objective was to insert the drive-point into streambed sediments to depths of 10, 30 and 60 cm below the sediment surface to perform a hydraulic head gradient reading, and withdraw a groundwater sample for *DO* measurement and laboratory analysis of

major anions. However, the objective depths were not always achieved because of sub-surface obstructions.

Within approximately 24 hours water samples were filtered with 0.45 μm glass fiber filters and stored in a refrigerator. Water samples were analyzed by ion chromatography for the major anions chloride, nitrate, and sulfate using a Dionex ICS-2100 and auto-sampler system. The system is calibrated by running a known standard solution. Sample ion chromatograms are compared to standard chromatograms to resolve ion type and concentration. A solution of potassium hydroxide is used to elute the system.

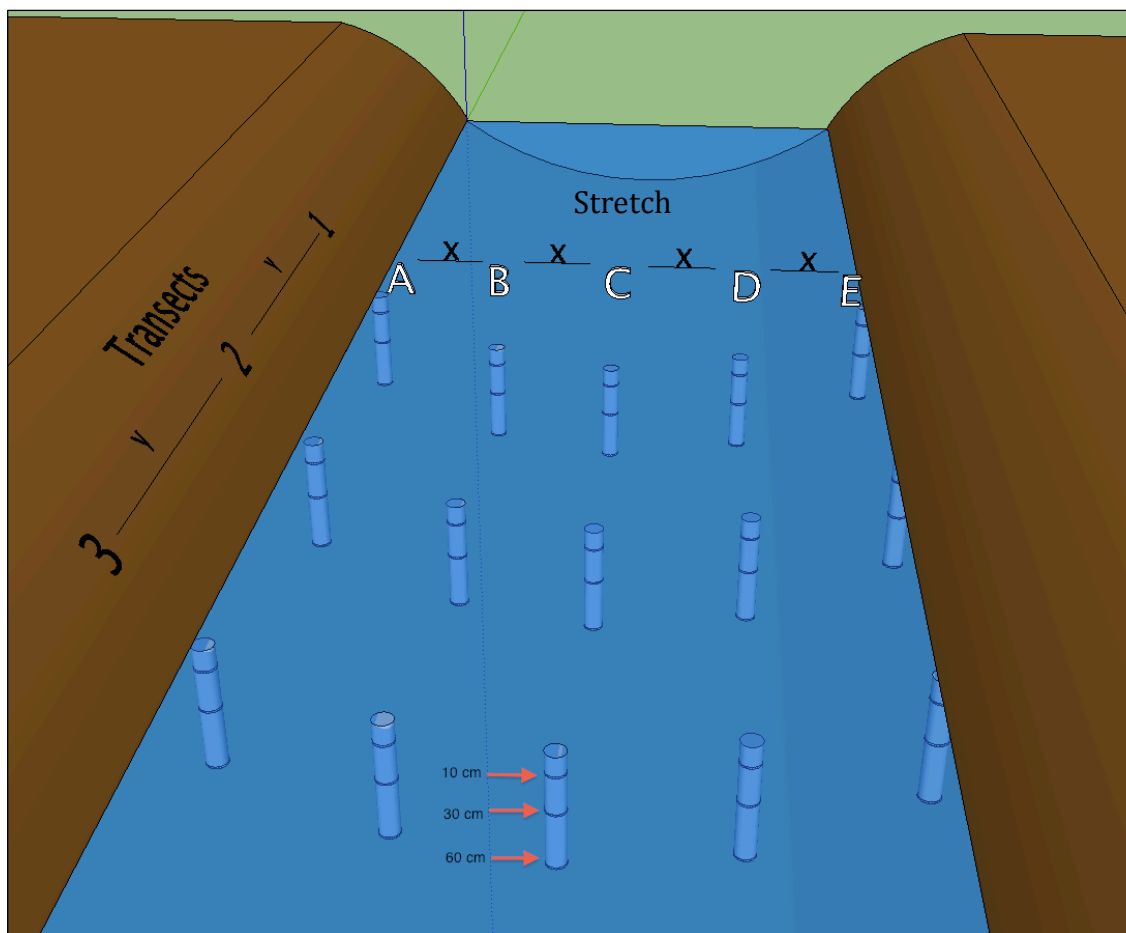


Figure 2-6. The aligned square grid sampling design performed in the 2nd iteration.

2.4 Streambed Sediment Analysis

Analysis of streambed sediments was performed for measurement of sediment organic matter and estimation of hydraulic conductivity. In February 2012, sediment cores were collected using PVC schedule 40 pipe of 100 cm length and 5 cm diameter. One end of each pipe was cut at a 30-degree angle across its width to sharpen the end for easier penetration into the streambed. Sediment cores were collected from the four streams of the 2nd iteration, at approximately the same transects of the groundwater investigation (Table 2-1; Figure 2-6). Three sediment cores were equally spaced across each of the three transects, with one in the center of the channel and the other two at the midpoint between the center and the stream bank. The pipe was driven with a sledgehammer until about 2-3 inches of pipe remained above the streambed. The headspace of the core was filled with stream water, either consequently from being submerged or manually, and a rubber stopper was pushed into the core. The core was slowly withdrawn from the streambed, using the vacuum to hold the contents, and a rubber stopper was pushed into the bottom. In the field, sediment recovery was recorded by measuring the distance from the top of the core to the sediment interface inside the core. Sediment cores were transported to the laboratory for analysis within 24 hours of collection.

Beginning at the top of the sediment cores, 10 cm sections were sliced and the contents put into individual pre-weighed aluminum dishes. The saturated sample was immediately weighed, placed in a 105°C drying oven for at least 24 hours, and then measured for the dry-weight of the sample. The dry-weight was subtracted from the saturated weight, which provided the water weight of the

sample. To find the void space of a sample a simple mass of water to volume conversion of 1 g equals 1 cm³ was used. The total volume of the sample was found by measuring the volume of the PVC section cut out. The sample porosity was calculated by dividing the void volume (given by measuring water loss) by the total volume of the sample.

After samples were dried, the total organic carbon (TOC) content was measured by loss on ignition in accordance with U.S. EPA methods [Schumacher, 2002]. Due to the large volume of sediments within each sample, a representative grab sample was collected for combustion. Samples were first homogenized by using a spoon to mix the contents. Some samples had very cohesive material and dried into aggregates. A pestle was used to break the aggregates apart. Pre-weighed aluminum dishes were filled with around 30 grams of homogenized sample and placed into a 500°C furnace for at least 24 hours for combustion. Combusted samples were removed from the furnace, left to cool for about 20 minutes, and then weighed. Subtracting the aluminum dish weight from both pre- and post-combustion weights, and then calculating the difference between pre- and post-combustion weights determined TOC.

A grain size analysis was performed for sediment characterization and estimation of hydraulic conductivity. The dried sediment remaining after combustion was used for the grain size analysis. A nest of sieves with opening sizes of 2.0, 1.0, 0.5, 0.25, 0.106, 0.045 mm and a sediment trap at the bottom were individually weighed before the sediment sample was poured into the top of the sieve nest. The sample was poured into the nest of sieves and then mechanically

shaken by a Rotap for 20 minutes to separate the sediments by size. After the mechanical shaking, each sieve was reweighed. The interval weights were used to construct a grain size distribution.

2.4.1 Estimation of Hydraulic Conductivity

Hydraulic conductivity (K) was estimated using the Kozeny-Carman equation adapted by *Carrier* [2003]. The equation is a function of grain size distribution, porosity and a grain shape factor. Kozeny [1927] empirically derived the equation and *Carman* [1938, 1956] later modified it by including a variable representing the weighted average of grain diameter [*Bear*, 1972]. The Kozeny-Carman equation is one of the most commonly used and recommended semi-empirical equations for estimating K from grain size distribution [*Vienken and Dietrich*, 2011; *Das*, 2006; *Odong*, 2007]. Comparisons between laboratory K measurements and K estimation by the Kozeny-Carman equation showed accurate estimation in a range of unconsolidated aquifer sediments and sandy soils [*Odong*, 2007; *Das*, 2006].

Hydraulic conductivity was calculated by the following equation:

$$K = 1.99 \times 10^4 \left(1 / \left\{ \sum [f_i / (D_{li}^{0.404} \times D_{si}^{0.595})] \right\} \right)^2 (1/SF^2) \times [e^3 / (1 + e)] \quad \text{Equation 2-4}$$

where f_i is the fraction of particles between two sieve sizes based on weight; D_{li} is the larger and D_{si} is the smaller sieve size, measured in centimeters; SF is the grain shape factor; and e is the void ratio. Grain particles from each of the streams were inspected and in general matched the characteristics of sub-angular [*Das*, 2006]. A shape factor of 7.5, which describes medium angularity, was used to describe all sediment samples [*Carrier*, 2003]. The void ratio is the volume of void space (gas or liquid), to the volume of solids. The void ratio, e , was calculated by:

$$e = \frac{\phi}{1 - \phi} \quad \text{Equation 2-5}$$

where ϕ is the porosity of the sediments. The accuracy of individual porosity measurements was questionable because water leaked while sediment cores were sliced into sections. In addition, some of the sediment cores dried out while stored in the laboratory, and were then rewetted. Rewetting of the sediment cores might not have reflected the *in situ* conditions. Therefore, the mean porosity value of each stream was used to calculate a void ratio for each stream. One void ratio for all the samples of a stream was used for calculation of K by Equation 2-4. The mean porosity values of each stream are presented in Table 2-2.

Table 2-2. Mean porosity value of each stream.

Stream	Porosity, ϕ
Coal Kiln	0.47
Machipongo	0.50
Parker Creek	0.47
Phillips Creek	0.50

The effective grain size (D_{10}) of samples was used to check the calculated K . D_{10} is the diameter at which 10% of the sample weight is finer [Fetter, 2001]. Particle size distribution curves of each sample were created with the points connected linearly. D_{10} values were calculated by finding the grain size where 10% weight intersected the particle size curve.

Filled contour maps of dh and chloride, DO , and nitrate concentrations were constructed for each depth interval of all streams using the Matlab program. For missing values of a stream reach interpolation by the *inpaint_nans* function was performed [D'Errico, 2004]. The density of data points in a stream reach was

increased by 10-fold in both horizontal and lengthwise directions by cubic spline interpolation for greater resolution.

2.5 Nitrogen Transport and Fate

The 1-dimensional vertical solute transport of nitrate in streambed sediments was calculated as an advective flux density. The advective flux density is the product of solute concentration and flow velocity (Equation 2-6).

$$J = C \times v \quad \text{Equation 2-6}$$

where C represents the solute concentration; and v represents the flow velocity.

The linear pore-water velocity was calculated by Equation 2-7.

$$v = \frac{K}{\phi} \frac{dh}{dl} \quad \text{Equation 2-7}$$

For calculating pore-water velocity at the three depths where hydraulic gradient was measured, K values of specific intervals were averaged according to the scheme presented in Table 2-3.

Table 2-3. K values from specific depth intervals were averaged to provide values for calculation of pore-water velocity.

Pore-water velocity depth (cm)	K depth intervals averaged (cm)
10	0-10 & 10-20
30	20-30 & 30-40
60	40-50, 50-60, & if available 60-70

The rate of nitrate removal along vertical flow paths was calculated by applying a nitrate mass balance to the vertical profiles. An equation of mass transport with reaction was used, disregarding dispersion, to determine the change in mass over time [Domenico and Schwartz, 1998]. The flow direction was

determined by comparing hydraulic heads along a vertical profile. The depth with larger hydraulic head provided the location of the inflow and the other depth was taken as the outflow. A decrease in mass along the flow path was interpreted as denitrification. Equation 2-8 represents the general relationship of change in mass over time.

$$v \frac{\partial N}{\partial x} = -R \quad \text{Equation 2-8}$$

where v is linear pore-water velocity, N is nitrate concentration, and x is a length. Specifically, the nitrate removal rate was calculated along the two depth intervals measured, between a shallow interval of 10-30 and a deeper interval of 30-60 cm. For each depth interval, hydraulic head values from the two locations were compared and flow direction determined to be towards the location with a lessor hydraulic head value. The length of the depth interval, L , was given by the absolute value of the difference between the two depths. The average pore-water velocity of both locations provided v . The nitrate removal rate was found by:

$$R = \frac{N_1 - N_2}{L/v} \quad \text{Equation 2-9}$$

where N_1 was the nitrate-nitrogen concentration at the location with a greater dh and N_2 was the nitrate-nitrogen concentrations at the location with a lessor dh .

2.6 Repeated Measures ANOVA

Transverse patterns of pore-water variables within a stream were tested by a repeated-measures analysis of variance (ANOVA). The sampling design at each stream resembles a center-aligned square grid, which was measured at three depths (Figure 2-6) [Gilbert, 1987]. All sampling areas were at a relatively straight stretch

of the channel and assumed to follow the theoretical riparian flow model of *Hornberger et al.* [1998]. The three transects were treated as blocks and each measurement had position and depth effects. Each position represented a plot and the depths represented subplots. For each position, the measurements at the three depths were not independent since they were located at the same stream position, and therefore were considered repeated measures of that position.

3 Results

3.1 Streambed Sediments

The majority of analyzed streambed sediment was fine or medium sand. Sediment sizes ranged from silt/clay to gravel (Figure 3-1). Fine and medium sands made up $\geq 85\%$ of the sediment sampled at each stream. Coal Kiln had the most homogenous sediments with only 1 sample of 53 not fine or medium sand. Phillips Creek was the only stream with sediments categorized smaller than fine sand. Six of the 47 sediment samples from Phillips Creek were silt/clay.

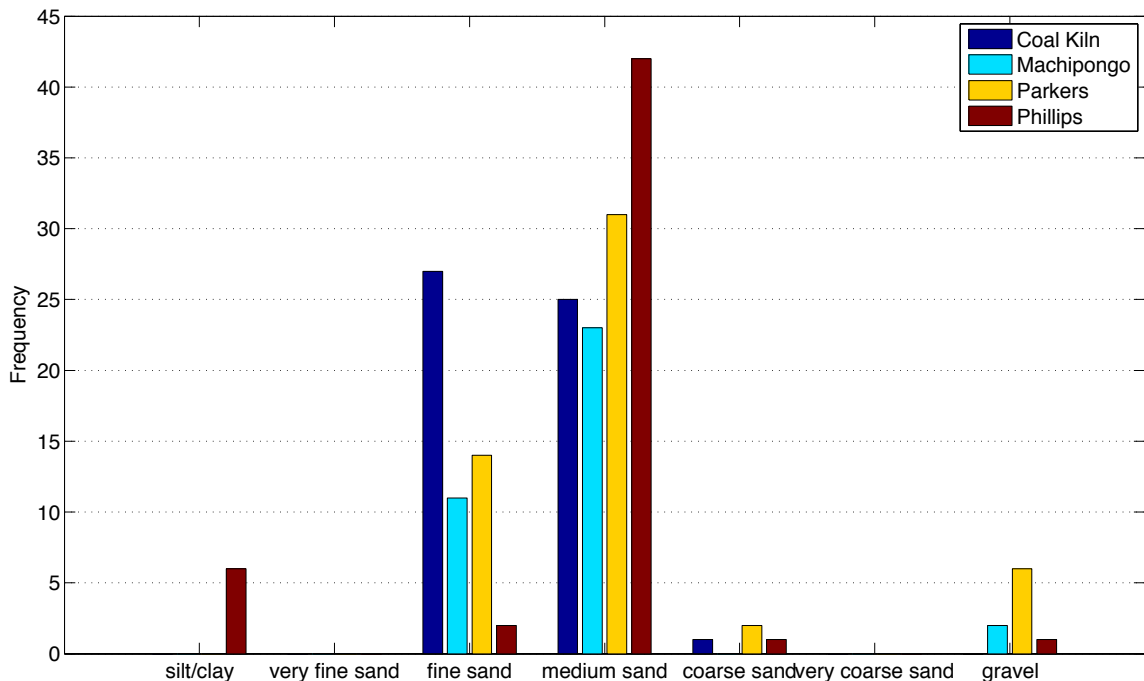


Figure 3-1. All streams: Histogram of sediment grain size.

Hydraulic conductivity (K) was calculated using Equation 2-4, a particle-size model. K varied little within or among streams (Figure 3-2). For all streams, K ranged from 6.75×10^{-5} to $5.11 \times 10^{-3} \text{ cm s}^{-1}$. This range is within textbook categories of silty sands and fine sands [Fetter, 2001; Freeze and Cherry, 1979]. At Coal Kiln, Machipongo and Phillips Creek, the mean K decreased along the vertical

profile from shallow to greater depths. At Parker Creek, K was constant from the surface to 60 cm and then decreased at the deepest interval of 60–70 cm. K was compared to the effective grain size (D_{10}) to determine whether Equation 2-3 provided a reasonable estimation of K . The comparison was made because D_{10} is regarded as a key variable for estimating K and is often included in grain size equations estimating K [MacDonald *et al.*, 2012]. Figure 3-3 shows D_{10} and K had a similar pattern. At each stream, mean effective grain size slightly decreased with greater depth. No definitive pattern of K with depth emerged due to the relatively large variances. Boxplots of K by depth and location in the stream channel showed limited variation within or among streams (See Appendix A, Figure 7-1; Figure 7-2). The range of K from all streams only spans three orders of magnitude.

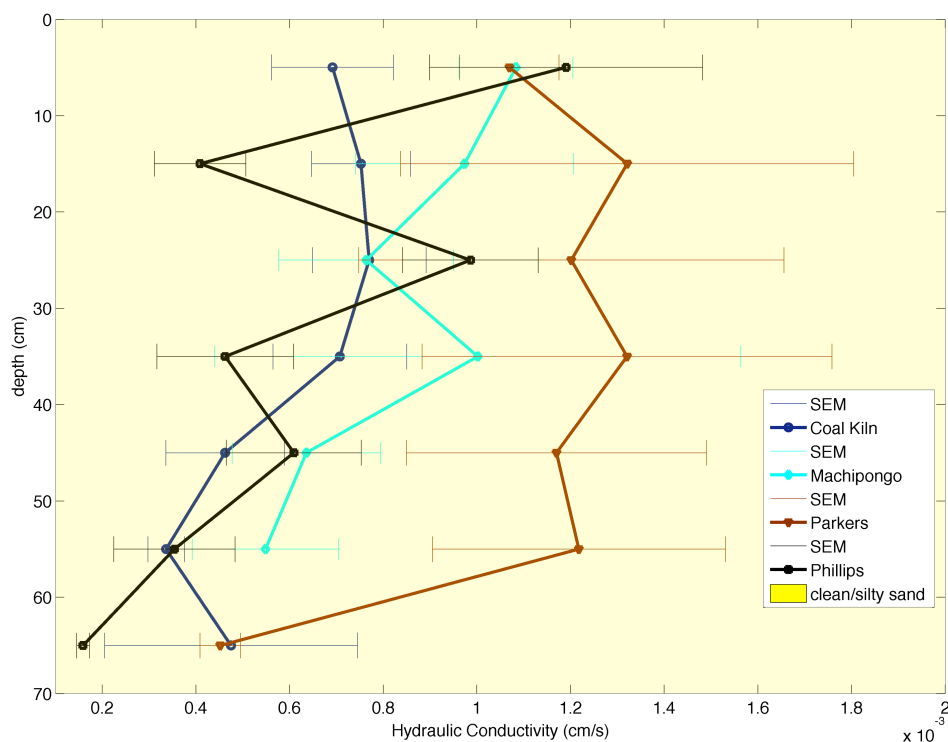


Figure 3-2. All streams: Mean K per depth interval of each stream, with Standard Error of the Mean (SEM) bars.

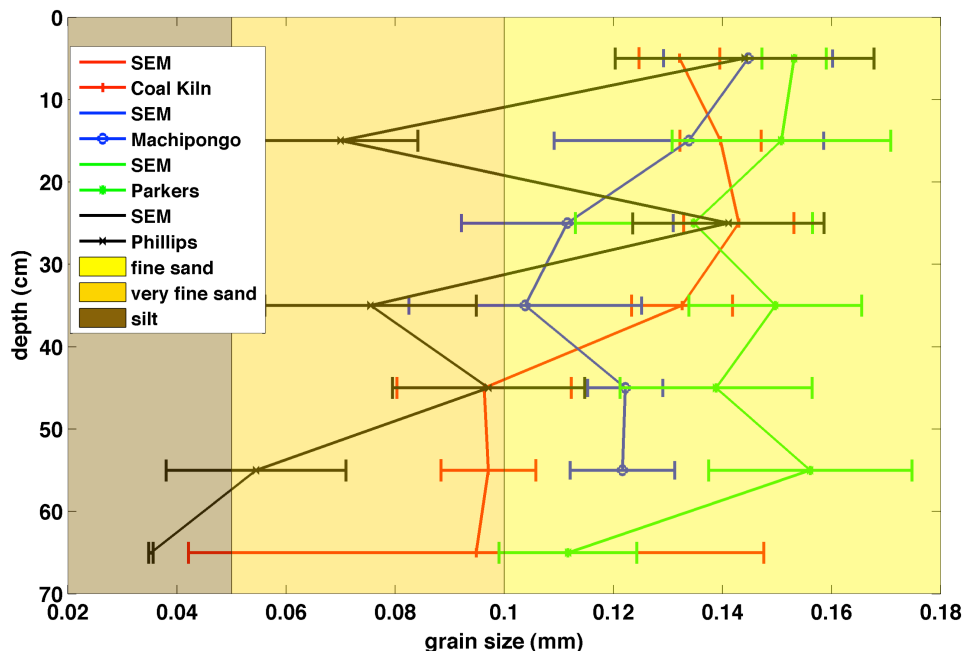


Figure 3-3. All streams: Mean effective grain size per depth interval of each stream, with SEM bars.

3.2 Flow Regime

The vertical flow regimes of the four sampled streams revealed a range of conditions and, in particular, a substantial amount of vertical flow in both directions. At each stream, the median dh per depth interval was always positive, thus the majority of groundwater was flowing upwards at each reach (Figure 3-4). The boxplots presented in this thesis show a box with the edges marking the 25th and 75th percentiles, the line in the box is the median, the whiskers extend to $\pm 2.7\sigma$ covering 99.3% of normally distributed data, and outliers are points beyond the whisker coverage marked by the “+” symbol. Unique to Coal Kiln, all 45 dh measurements were positive indicating no downward flow. Machipongo and Parker Creek each had a large span of negative and positive dh values at all depths (except the 60 cm depth interval of Parker Creek). At depth 60 cm of Parker Creek, the dh distribution was narrow and values were large compared to shallower depths, with

a mean value of 7.32 cm, and a standard deviation of 2.19 cm. The large positive dh at depth 60 cm indicated a strong upward flow of deeper groundwater into Parker Creek sediments. The dh values at Phillips Creek were approximately equal to zero at all depths, indicating limited vertical flow of groundwater. At Phillips Creek, the median dh per depth was 0.127, 0.0161 and 0.0239 cm at 60, 30 and 10 cm, respectively. The median values at Phillips Creek were 1-2 orders of magnitude less than the median at the respective depths of other streams. All streams showed a trend of decreasing dh as depth shallows, particularly Coal Kiln, Machipongo and Parker Creek.

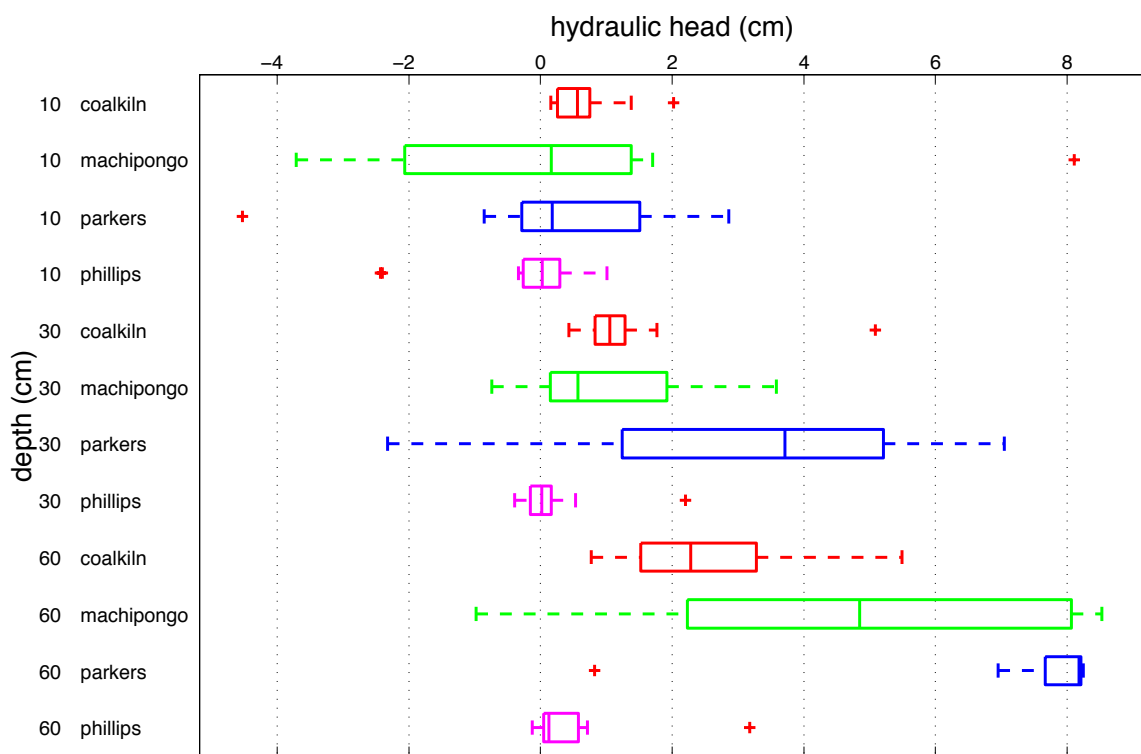
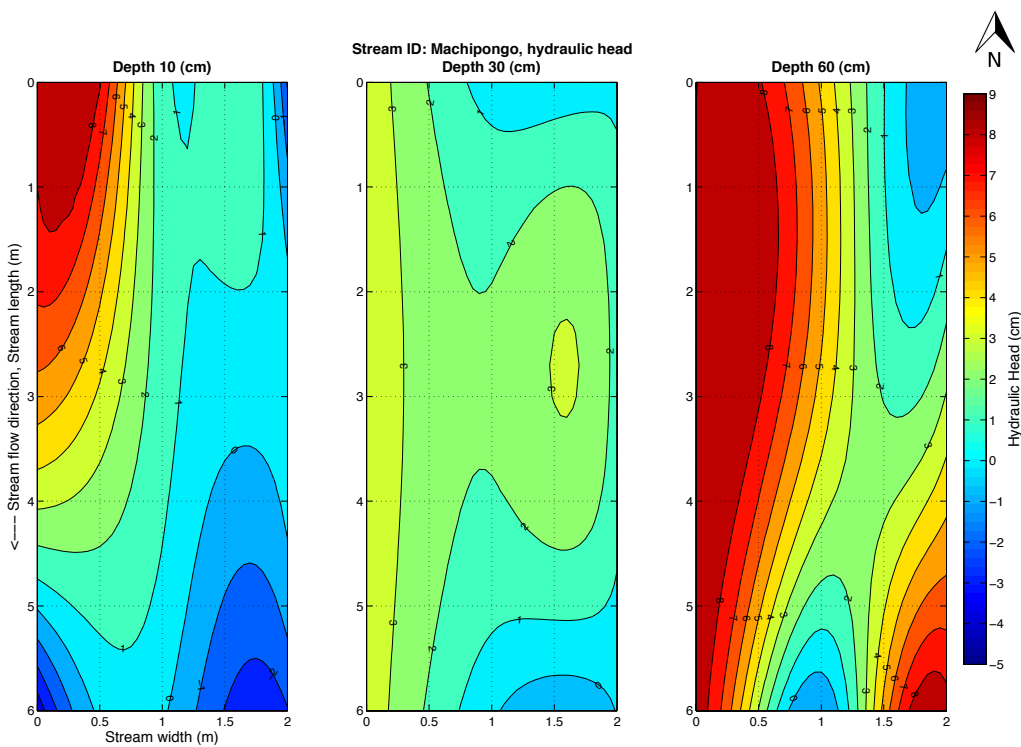
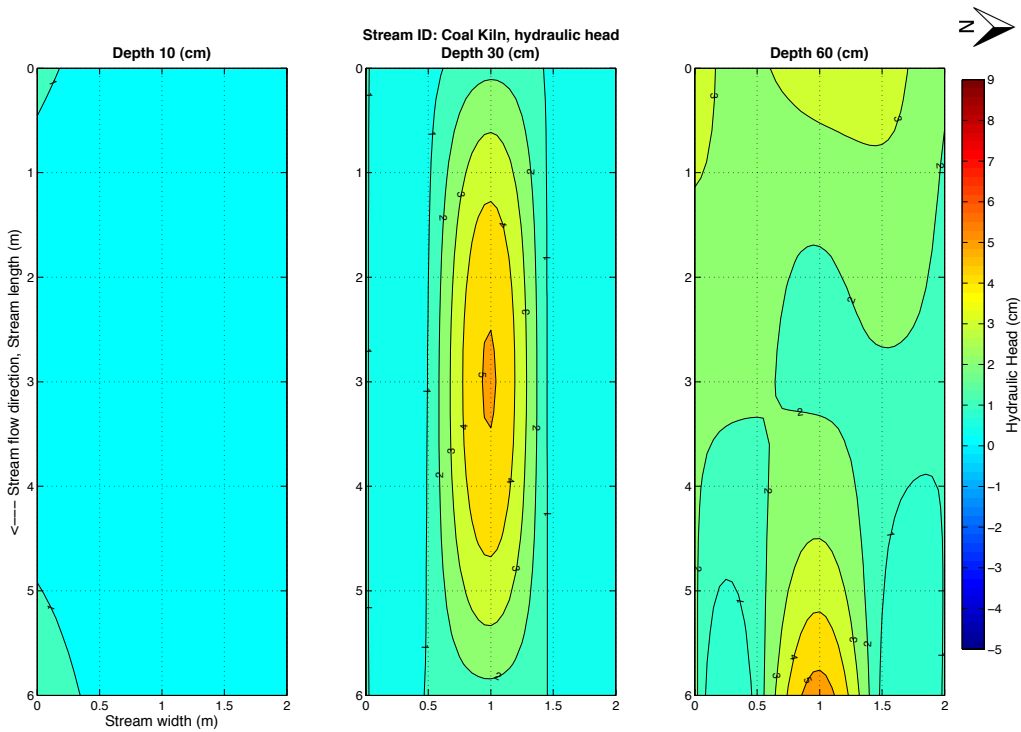


Figure 3-4. All streams: Boxplot of dh per depth interval of each stream.

Interpolated contour maps of dh by depth at each stream did not show any strong transverse or longitudinal patterns (Figure 3-5). At Machipongo and Parker Creek there were specific reach locations that consistently had relatively high or low

dh at all depths. Dh was greater along the western side of Machipongo, particularly the northwestern corner. The western side of the Machipongo's reach was bordered by a hillslope that presumably had a higher water table than the eastern side, which might have caused the elevated dh levels. The greatest difference between the western and eastern sides of the Machipongo reach occurred at depth 10 cm where the northwest corner dh was ~ 10 cm greater than the southeastern corner. At Parker Creek, low dh persisted in the northwestern corner of the reach. Coal Kiln and Phillips Creek were absent of any trends. Among the streams, negative dh was most abundant at the 10 cm depth interval.

At Machipongo, Parker Creek, and Phillips Creek, there were numerous locations with negative dh at the 10 cm depth. As explained in Section 2.1.4, the accuracy of some dh measurements at the 10 cm depth is questionable, particularly negative values. The percentage of dh measurements at 10 cm depth with a negative value was 0% at Coal Kiln, 40% at Machipongo, 27% at Parker Creek, and 50% at Phillips Creek.



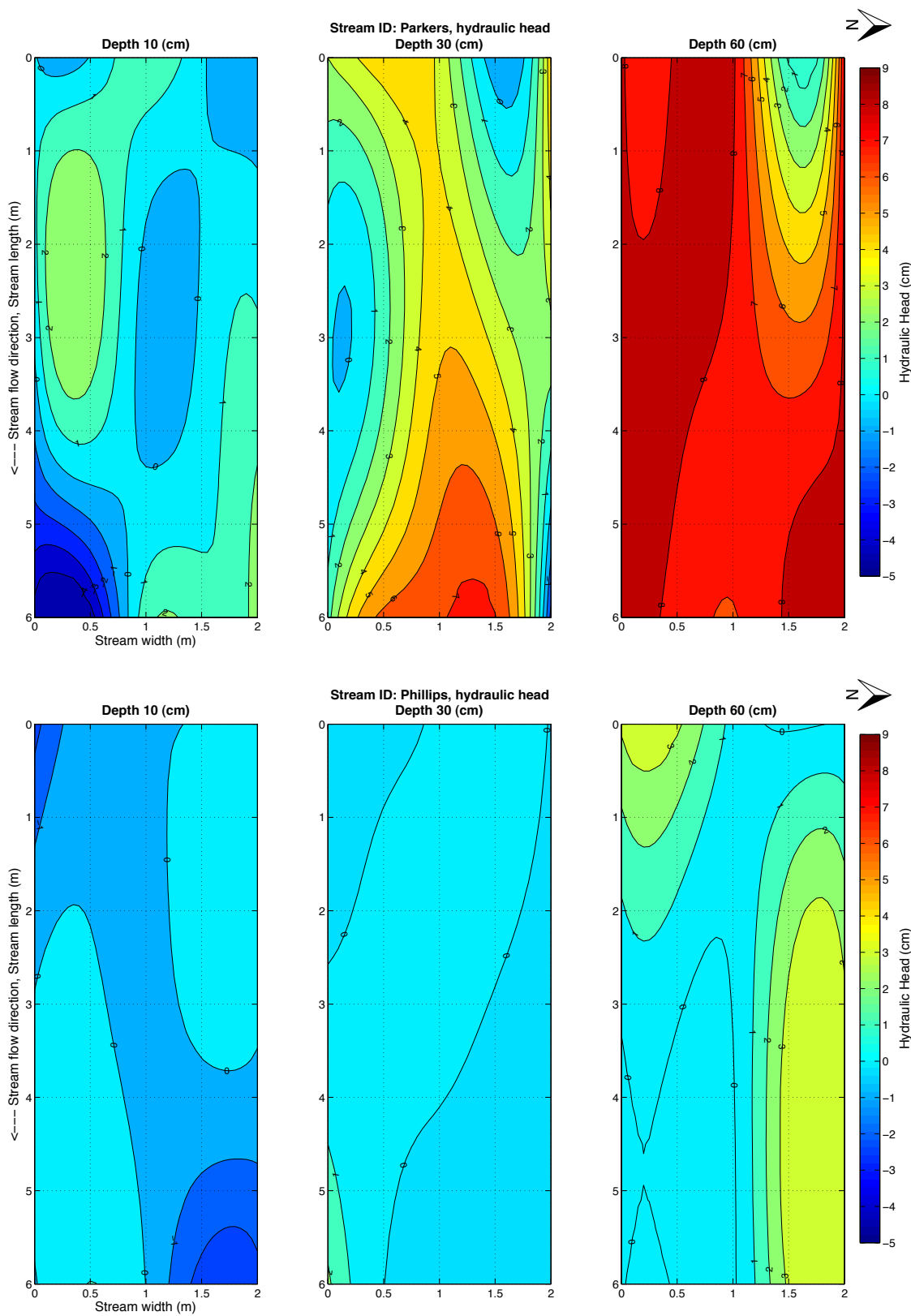


Figure 3-5. All streams: Cubic spline interpolated contour maps of hydraulic head per depth interval at each stream. Pore-water hydraulic head was measured relative to overlying surface water in the stream.

During the 1st iteration of fieldwork, a total of 27 seepage meter and 70 piezomanometer measurements were made. The average specific discharge from seepage meter measurements was 0.74 cm hr^{-1} and from piezomanometer measurements was 0.19 cm hr^{-1} ; within the same order of magnitude. (See Appendix B for details regarding the temperature method.)

The mean q per depth interval of each stream indicated q changed with depth within streams, and the mean q varied among streams particularly at the greatest depth (Figure 3-6). Coal Kiln and Machipongo had a similar range of mean q at depth 30 and 60 cm and differed at depth 10 cm. All q values at Coal Kiln were positive, whereas at Machipongo the mean q at 10 cm depth was negative with large error bars extending to positive values. The largest change in mean q within a stream was from -0.099 to 0.49 cm hr^{-1} at the 10 and 30 cm depth intervals, respectively, of Parker Creek. Among Coal Kiln, Machipongo, and Parker Creek, mean q rates per depth interval were the same order of magnitude. However, the mean rates at the 30 and 60 cm depths were about three times larger at Parker Creek than at Coal Kiln and Machipongo. The mean q values at Phillips Creek were an order of magnitude less than the other streams.

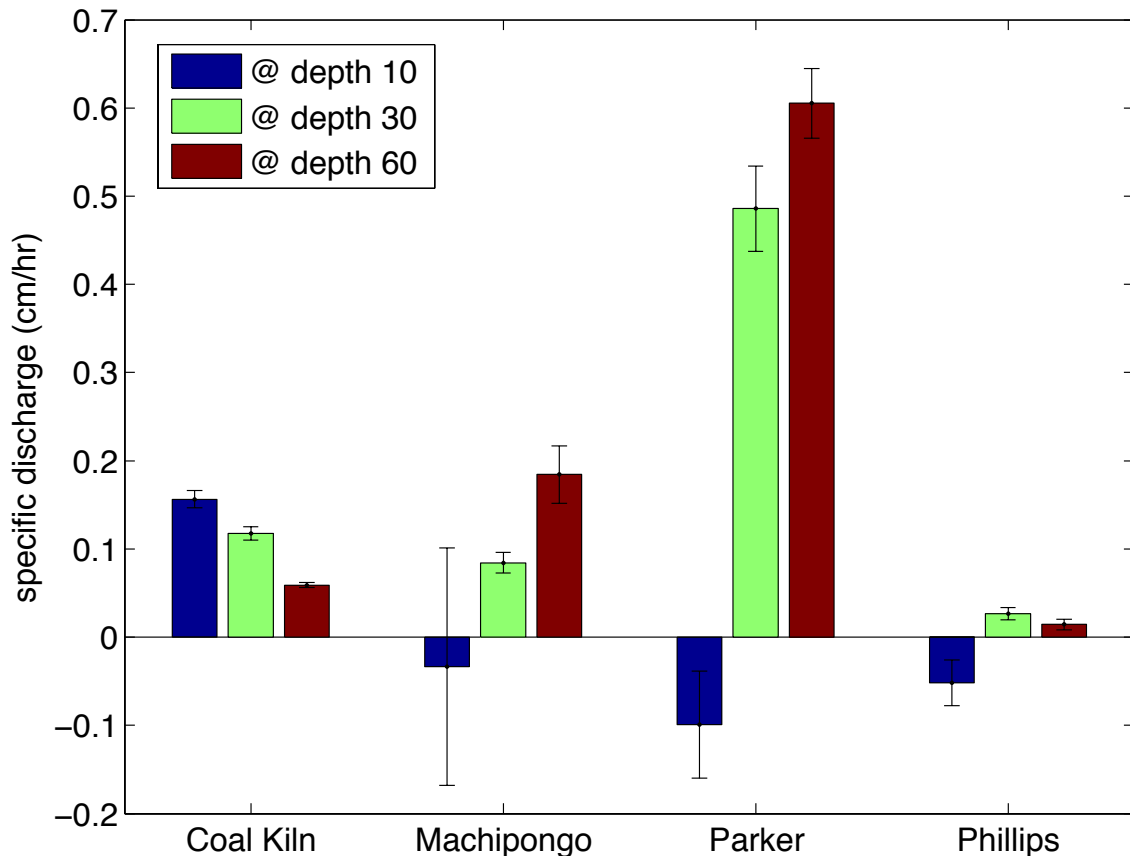


Figure 3-6. Mean q of each depth interval at each stream, with SEM bars.

Pore-water chloride concentrations were less than surface-water concentrations at Coal Kiln, Machipongo, and Parker Creek, suggesting in general little mixing between the two waters. At these three streams, pore-water chloride concentration profiles were constant over depth and always* less than their respective average surface water chloride concentration (See Appendix A, Figure 7-4). (*With the exception of one profile at Coal Kiln. Coal Kiln and Phillips Creek each had a profile with abnormally large chloride concentrations. The large values qualified as outliers to the chloride distribution at its stream's respective depth; the abnormal values were likely measurement errors). The boxplots of chloride concentration of each depth interval at Coal Kiln, Machipongo, and Parker Creek,

show pore-water chloride distributions were less than the average surface water concentration (Figure 3-7). The opposite was true at Phillips Creek. The pore-water chloride concentrations were almost always greater than the average surface-water value at Phillips Creek. In addition, Phillips Creek pore-water and surface-water chloride concentrations were closer in value than at the other streams. The proximity was not due to a lower surface water concentration at Phillips Creek; the average surface-water chloride concentration at each stream ranged from 18.55 to 24.58 mg L⁻¹, with a concentration of 20.40 mg L⁻¹ at Phillips Creek.

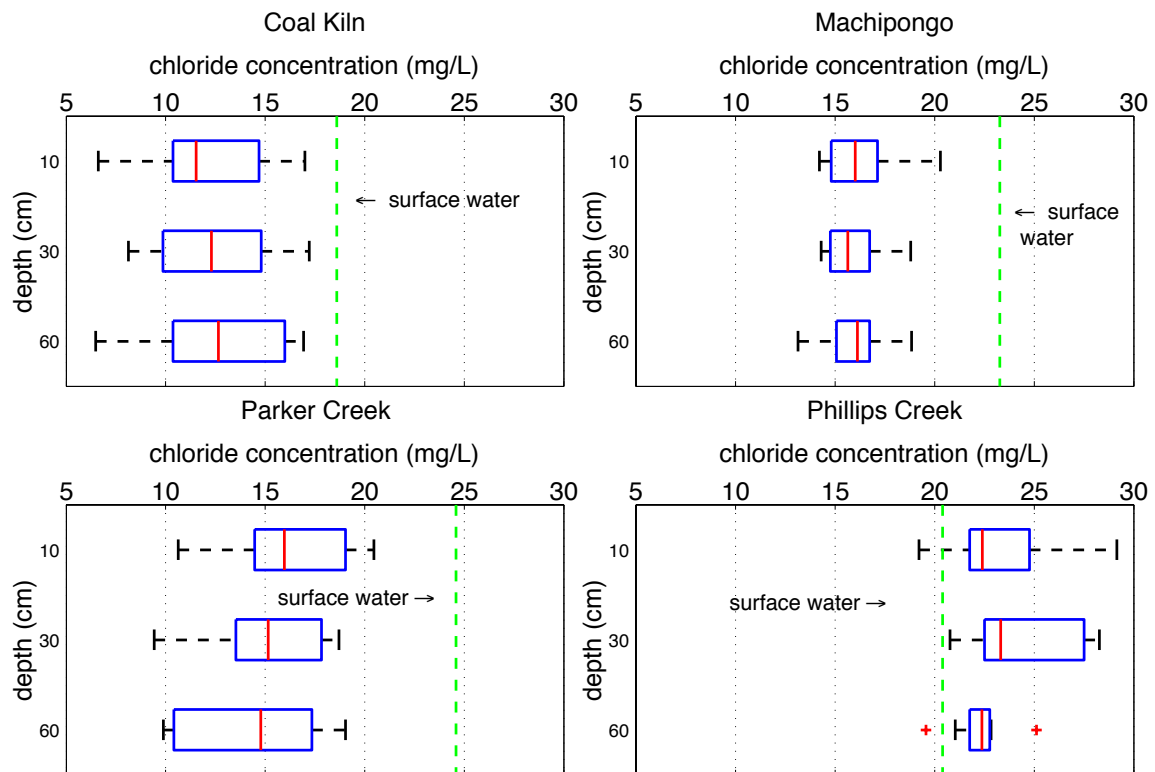
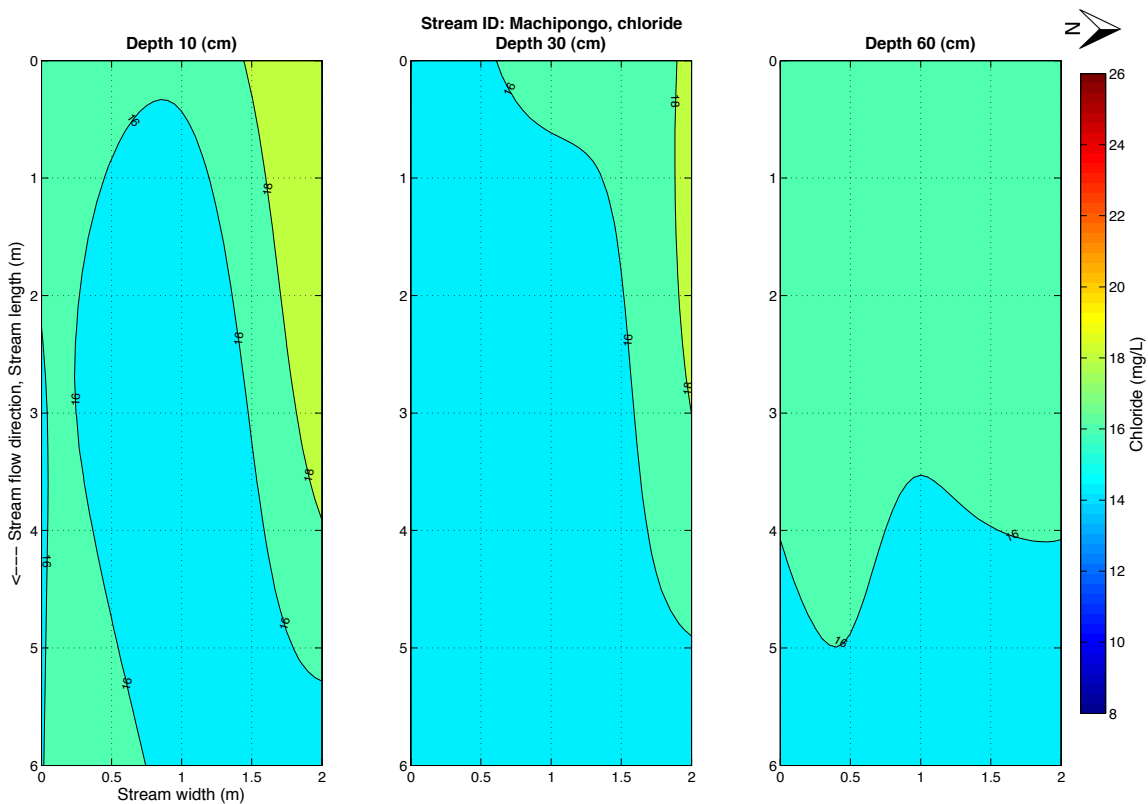
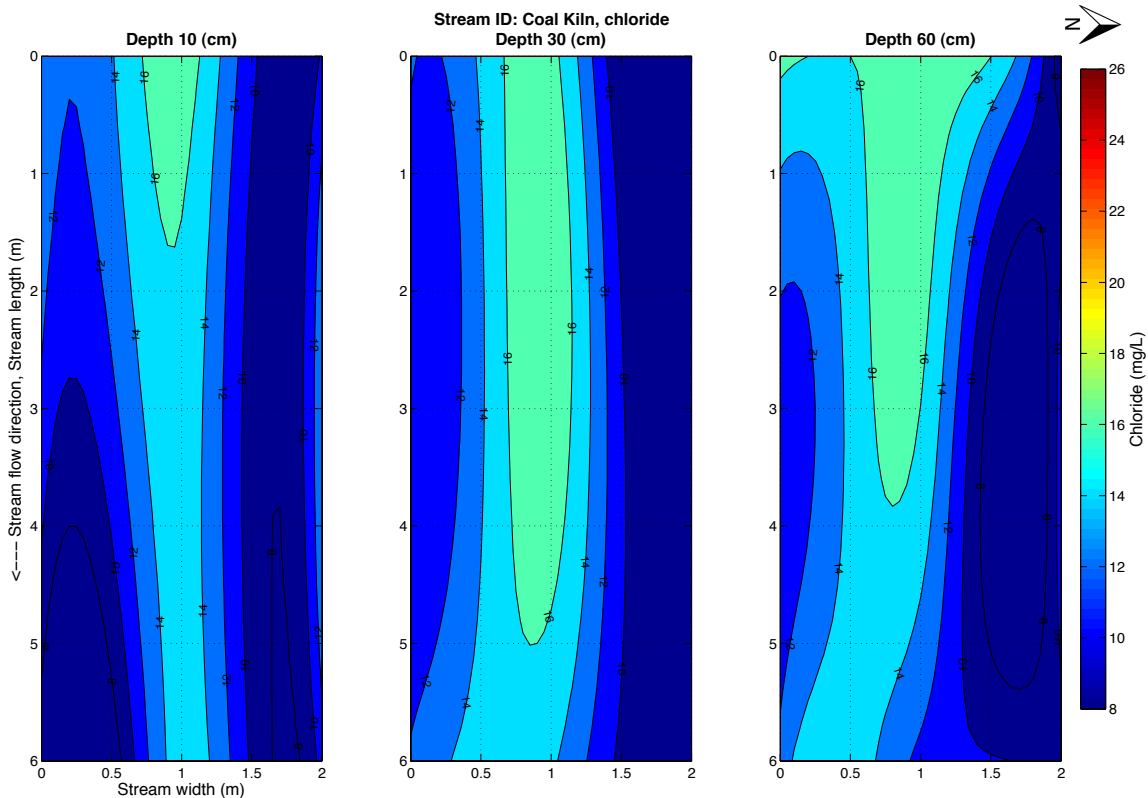


Figure 3-7. Boxplots of chloride concentration per depth interval of each stream. The vertical dashed green line represents the surface water chloride concentration.

The interpolated contour maps of chloride concentration with depth at Coal Kiln and Parker Creek illustrate a transverse pattern (Figure 3-8). At the two streams, pore-water chloride concentration was generally greater along the stream

sides compared to the center of the channel. The contour maps of Coal Kiln show pore-water chloride concentrations along the stream sides were generally 10 to 12 mg L⁻¹ and the center channel had a pocket of 16 mg L⁻¹. The transverse pattern was less pronounced at Parker Creek. The entire length of Parker Creek's north side had lower pore-water Cl⁻ concentration than the center channel at all depths; whereas only the eastern half of the south side had consistently lower pore-water concentrations than the center channel. The transverse pattern of pore-water chloride concentration was statistically tested at each stream. A repeated measures ANOVA revealed a significant difference of chloride values between stream positions (stretches), at Coal Kiln, $F(2,6) = 8.2, p < 0.05$. For Parker Creek, a repeated measures ANOVA also revealed a significant difference of pore-water chloride values between positions, $F(2,6) = 7.73, p < 0.05^*$. (*Levene's test of Equality of Error Variances was violated at depth 1 of Parker Creek, $F(2,6) = 7.99, p < 0.05$.) The descriptive statistics of Coal Kiln and Parker Creek are presented in Table 3-1.



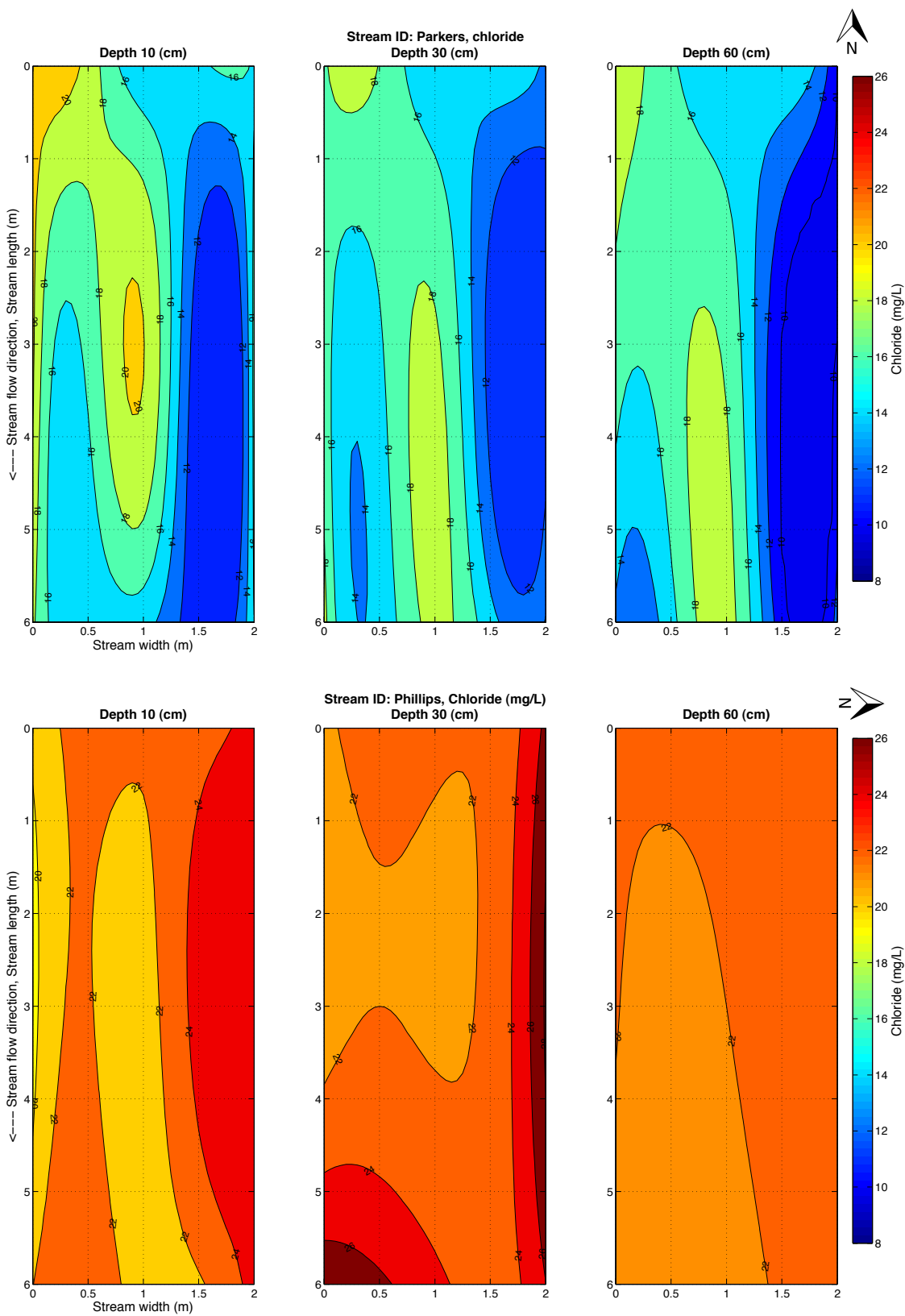


Figure 3-8. Interpolated contour maps of pore-water Cl⁻ mg L⁻¹ per depth interval at each stream.

Table 3-1. Descriptive statistics of repeated measures ANOVA between stream stretches A, C, and E, at Coal Kiln and Parker Creek.

Coal Kiln chloride descriptive statistics				
Measure: chloride mg L ⁻¹				
Stretch	Mean	Std. Error	95% Confidence Interval	
			Lower Bound	Upper Bound
A	11.906	0.968	9.537	14.275
C	15.517	0.968	13.148	17.886
E	10.066	0.968	7.697	12.435
Parker Creek chloride descriptive statistics				
Measure: chloride mg L ⁻¹				
Stretch	Mean	Std. Error	95% Confidence Interval	
			Lower Bound	Upper Bound
A	18.062	0.894	15.875	20.25
C	16.758	0.894	14.57	18.945
E	13.254	0.894	11.067	15.442

A groundwater chloride concentration discontinuity was determined using the descriptive statistics from the repeated measures ANOVA of pore-water chloride concentration between channel positions and by examining a histogram of pore-water chloride concentration (Table 3-1; Figure 3-9). From the descriptive statistics at Coal Kiln, the mid-point between the highest upper bound concentration of the two sides (stretches A and E) and the lower bound concentration of the center channel (stretch C), was 13.7 mg L⁻¹ Cl⁻. A histogram of all pore-water chloride concentrations at Coal Kiln showed that 13.7 mg L⁻¹ slightly overlapped a cluster of chloride values. The chloride concentration discontinuity was therefore decreased to 13.5 mg L⁻¹ so the value did not overlap any histogram bars at Coal Kiln (Figure 3-9, left panel). At Parker Creek, the descriptive statistics from only the north side (stretch E) was factored in to determining the chloride concentration discontinuity, since only the north side had consistently lower chloride values. The mid-point

between the concentration of the north side upper bound and the center channel lower bound values was $15 \text{ mg L}^{-1} \text{ Cl}^-$. A histogram of all pore-water chloride concentrations at Parker Creek showed two groups of concentrations. A value of 15 mg L^{-1} intersected the middle of one cluster of chloride concentrations. A discontinuity of $12.5 \text{ mg L}^{-1} \text{ Cl}^-$ was used instead, since 12.5 mg L^{-1} is between the two groups in the histogram (Figure 3-9).

The origin of pore water in streambed sediments was assessed according to the chloride concentration discontinuity. At Coal Kiln, 56% of pore water derived from riparian-influenced groundwater and 44% from riparian-bypass groundwater. At Parker Creek, 21% of pore water derived from riparian-influenced groundwater and 79% from riparian-bypass groundwater.

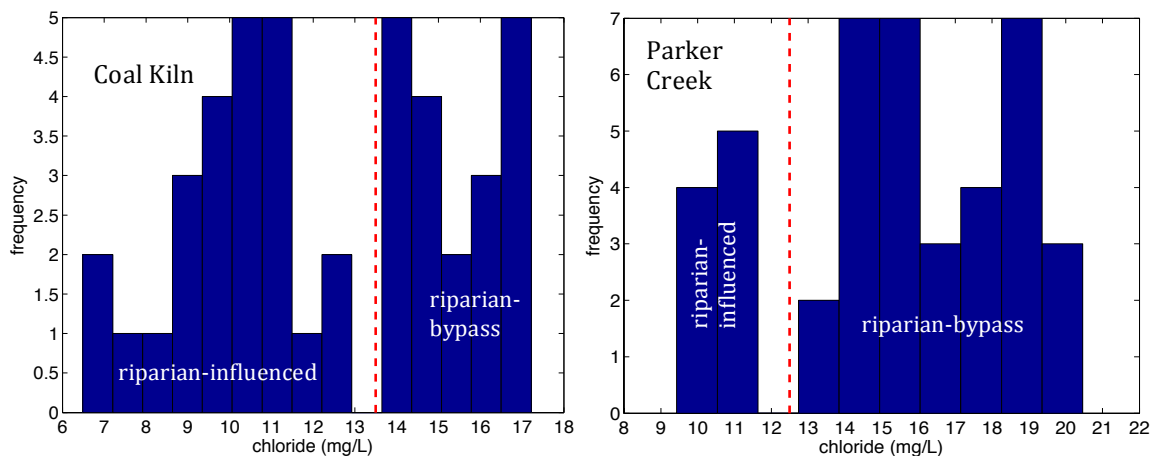


Figure 3-9. Histogram of all pore-water Cl^- concentrations at Coal Kiln in the left panel and Parker Creek in the right panel. The vertical dashed red line represents the Cl^- concentration discontinuity.

3.3 Chemical Conditions in Streambed Sediments

3.3.1 Total Organic Matter

A large portion of sediment cores had abundant total organic matter (TOM) content at all streams. TOM qualified as abundant if ($\text{TOM} \geq 0.5\%$). For each

stream, the maximum TOM of the 10 cm sediment sample intervals ranged from 4.12–36.47%, and the mean of the 10 cm intervals from each stream ranged from 1.3–7.3% (

Table 3-2). The mean length of sediment recovery in the sediment cores per stream ranged from 46–62 cm. The sediment cores of each stream had on average abundant TOM throughout 70-90% of the core. Coal Kiln and Parker Creek had similar amounts of TOM, and Machipongo and Phillips Creek had larger TOM values. Machipongo had the highest average TOM in sediment samples. For all streams the maximum TOM per profile was not distributed in a vertical pattern but the depths with the greatest frequency of maximum TOM occurred at depths \leq 40 cm (Figure 3-10).

Table 3-2. Descriptive statistics of TOM content of all depth intervals at each stream.

Stream	Sample size, n =	mean (g)	SEM (g)	median (g)	min (g)	max (g)
Coal Kiln	56	1.27	0.14	0.91	0.16	4.12
Machipongo	41	7.27	1.33	3.30	0.22	36.47
Parker Creek	54	1.61	0.23	0.95	0.00	7.98
Phillips Creek	52	3.46	0.48	2.37	0.12	18.27

The vertical distribution of TOM at streams occurred in two patterns (Figure 3-11). At Machipongo and Parker Creek, the boxplots by depth interval tapered off to low values at maximum depths. The bulk of TOM occurred from 20–40 cm at Machipongo and from 10–40 cm at Parker Creek. Conversely, at Coal Kiln and Phillips Creek the boxplots by depth interval increased near the maximum depth. Within Coal Kiln, TOM values were generally higher at depths ranging from 40–70

cm. Among streams, Phillips Creek had the most scattered vertical distribution of TOM. A higher load of TOM occurred at 50–70 cm of Phillips Creek. Each stream had TOM evenly distributed in the transverse direction (Appendix A, Figure 7-3).

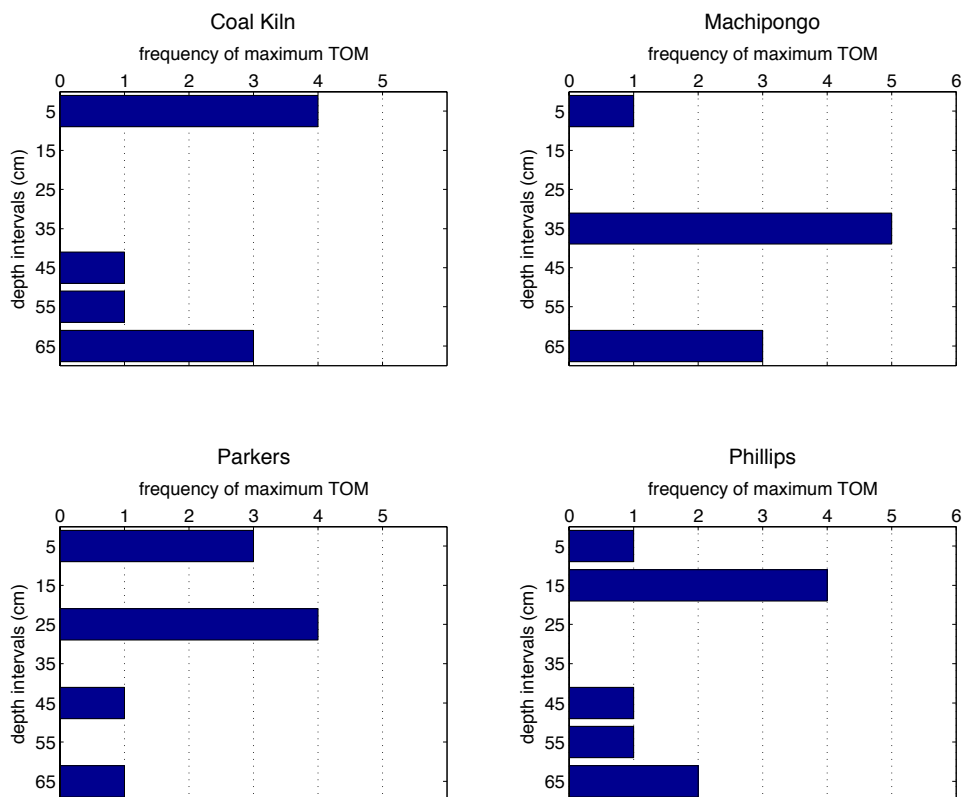


Figure 3-10. Histogram showing the frequency of maximum TOM per sediment core for each depth interval.

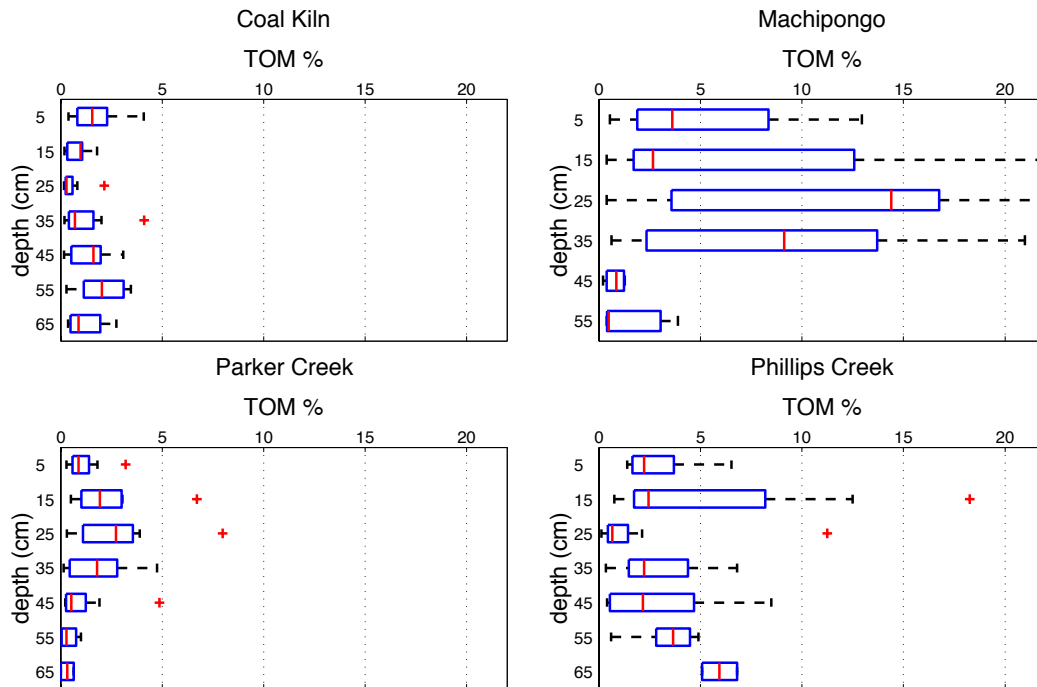


Figure 3-11. Boxplots of TOM% per depth interval of each stream.

3.3.2 Pore-Water Dissolved Oxygen

Hypoxic pore waters persisted throughout most sample depths at Coal Kiln, Machipongo, and Phillips Creek (Figure 3-12). At the 60 cm depth interval the median dissolved oxygen (*DO*) concentration in the pore waters of these three streams ranged from 0.82–1.30 mg L⁻¹ and slightly increased at depth 10 cm to 1.04–1.80 mg L⁻¹. Comparatively, Parker Creek had higher average *DO* concentrations in streambed sediments at depths 30 and 60 cm. Median *DO* steadily decreased with shallower depths at Parker Creek, dropping to a hypoxic level at the 10 cm interval. A repeated measures ANOVA of *DO* concentrations at Parker Creek yielded a significant main effect of depth, $F(2, 12) = 4.12$, $p < 0.05$. Depth 10 cm had significantly lower *DO* (2.25 ± 0.58 mg L⁻¹) than at depth 60 cm (4.48 ± 0.62 mg L⁻¹) (Table 3-3). Limited *DO* persisted throughout Coal Kiln, Machipongo, and Phillips

Creek and was eventually reached at the shallowest interval of streambed sediment underlying Parker Creek stream water.

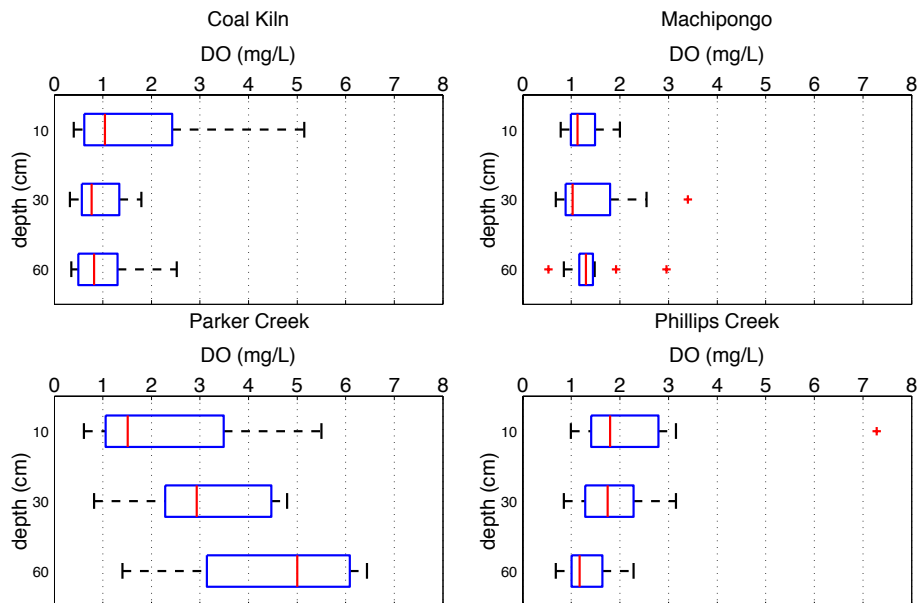


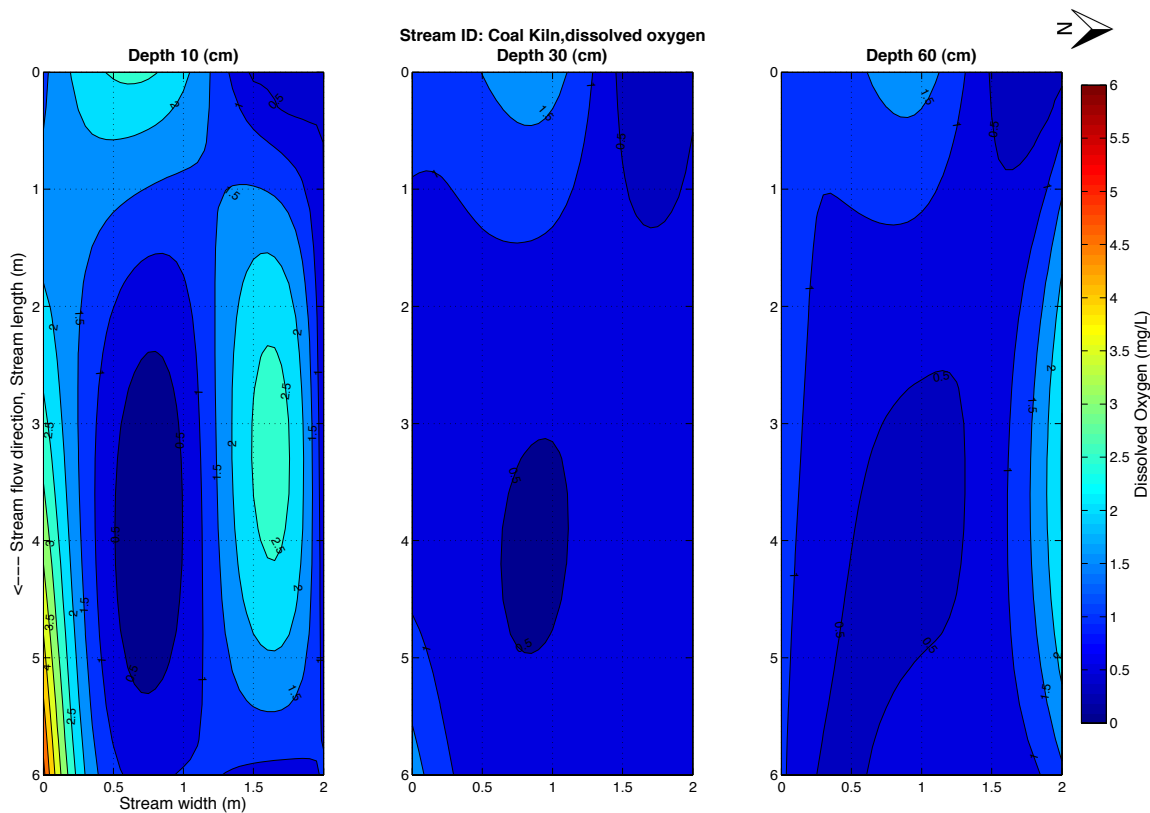
Figure 3-12. Boxplots of *DO* per depth interval of each stream.

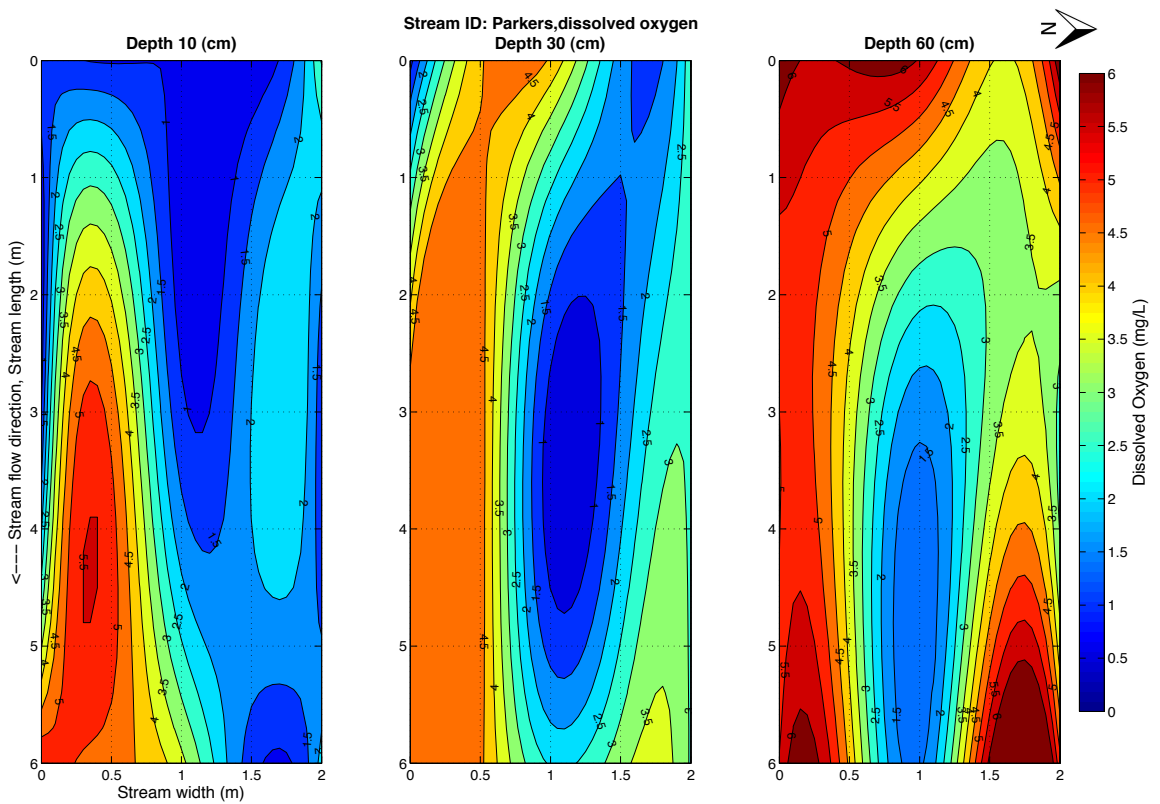
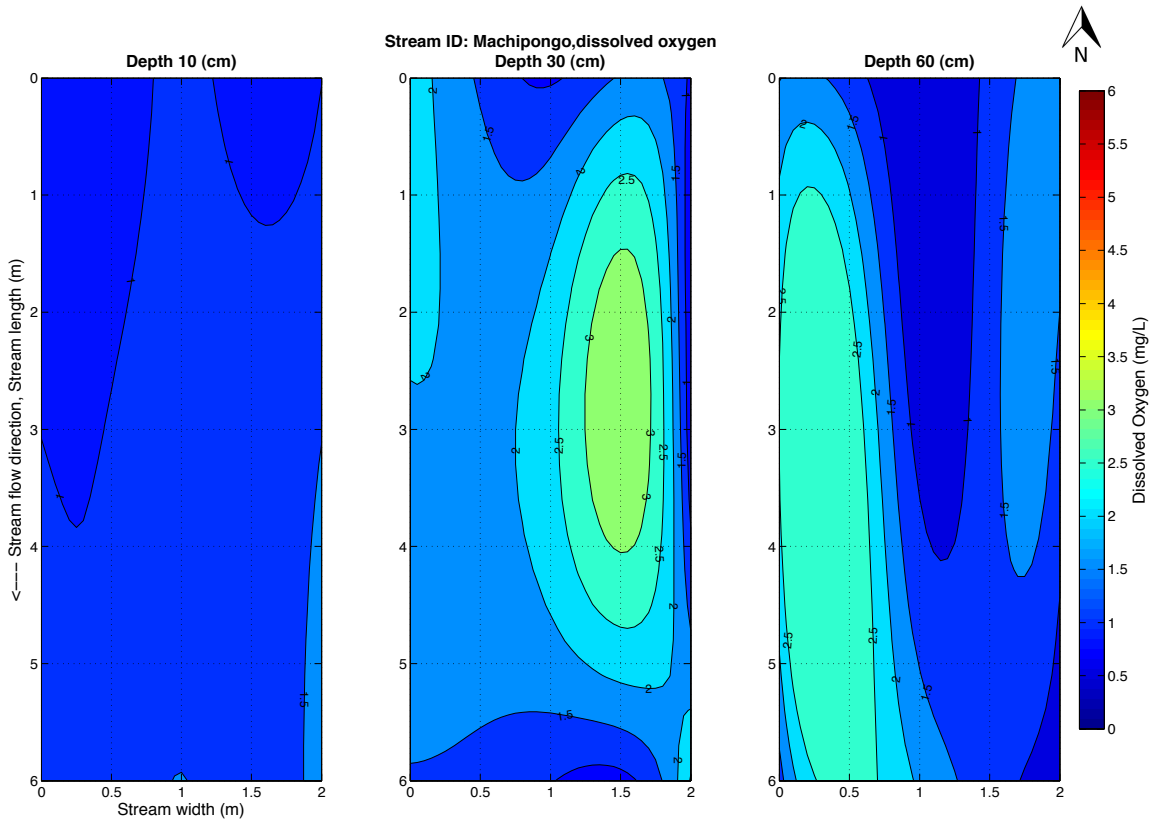
Table 3-3. Descriptive statistics of *DO* per depth interval from repeated measures ANOVA between stream stretches A, C, and E, at Parker Creek.

Parkers <i>DO</i> descriptive statistics				
Measure: <i>DO</i>				
Depth (cm)	Mean (mg L ⁻¹)	Std. Error	95% Confidence Interval	
			Lower Bound	Upper Bound
10	2.24	0.58	0.81	3.67
30	2.98	0.56	1.61	4.35
60	4.48	0.62	2.97	5.99

There was a transverse pattern of higher *DO* in pore waters along the stream sides versus the center channel at Coal Kiln, Machipongo, and Parker Creek. The difference between sides and center occurred at all depths of Coal Kiln and Parker Creek, and at depths 30 and 60 cm of Machipongo. Contour maps of *DO* per depth interval at each stream are shown in Figure 3-13. The trend was most pronounced at Parker Creek where a pocket of hypoxic pore water persisted in the center

channel with DO of $\sim 2 \text{ mg L}^{-1}$, whereas the stream sides of Parker Creek, at maximum depth, had a median DO of 5 mg L^{-1} . A repeated measures ANOVA, however, indicated no significant difference in DO between stream positions at Parker Creek, $F(2, 6) = 1.16, p > 0.05$. Thus, a qualitative transverse DO pattern can be seen in the contour maps of these three streams, but the pattern was weak.





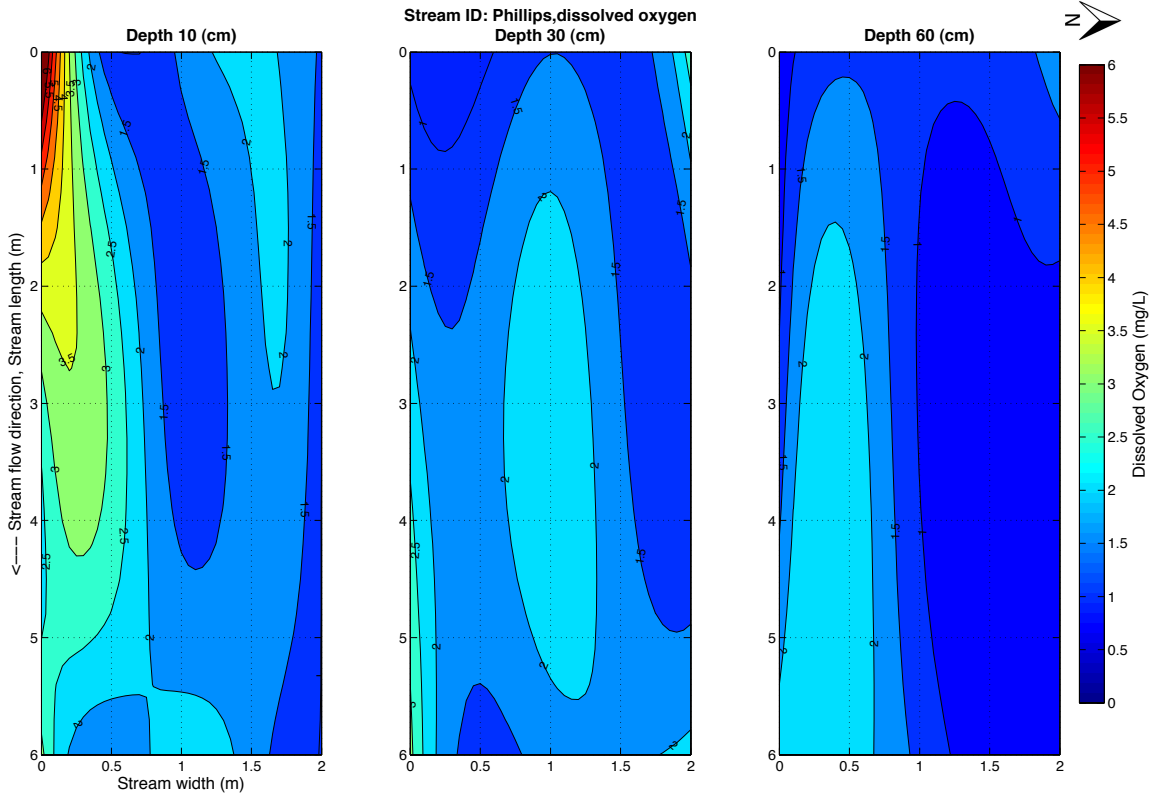


Figure 3-13. Interpolated contour maps of pore-water *DO* per depth interval at each stream.

3.3.3 Pore-Water Nitrate

The pore waters of the four streams can be grouped in to those with higher versus lower nitrate concentrations. Coal Kiln and Parker Creek had the higher nitrate concentrations. Boxplots of nitrate concentration per depth interval at each stream are presented in Figure 3-14. At the maximum sample depth of Coal Kiln and Parker Creek, nitrate concentrations ranged from ~ 0 –7.65 and 1.26–8.08 mg $\text{NO}_3\text{-N L}^{-1}$, respectively. Whereas, nitrate concentrations at maximum depth of Machipongo and Phillips Creek ranged from 0.01–3.46 and 0.01–0.39 mg $\text{NO}_3\text{-N L}^{-1}$, respectively. Nitrate concentrations remained low in all directions of reach sediments at Machipongo and Phillips Creek. Moving up the vertical profile at Phillips Creek, the median nitrate concentrations per depth interval were 0.06, 0.04

and $0.055 \text{ mg NO}_3\text{-N L}^{-1}$. Values were similarly low at Machipongo, moving up Machipongo's vertical profile, median nitrate concentrations per depth of 0.16 , 0.075 and $0.1 \text{ mg NO}_3\text{-N L}^{-1}$.

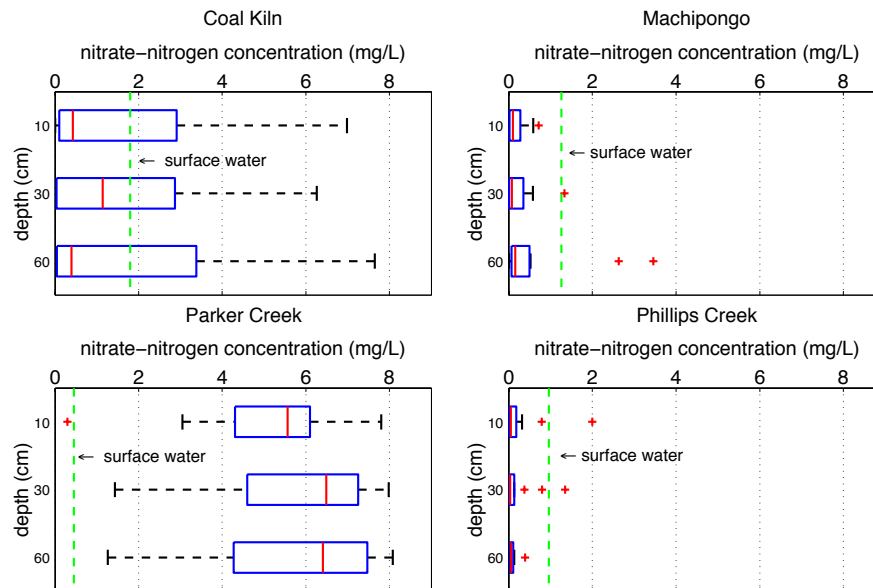
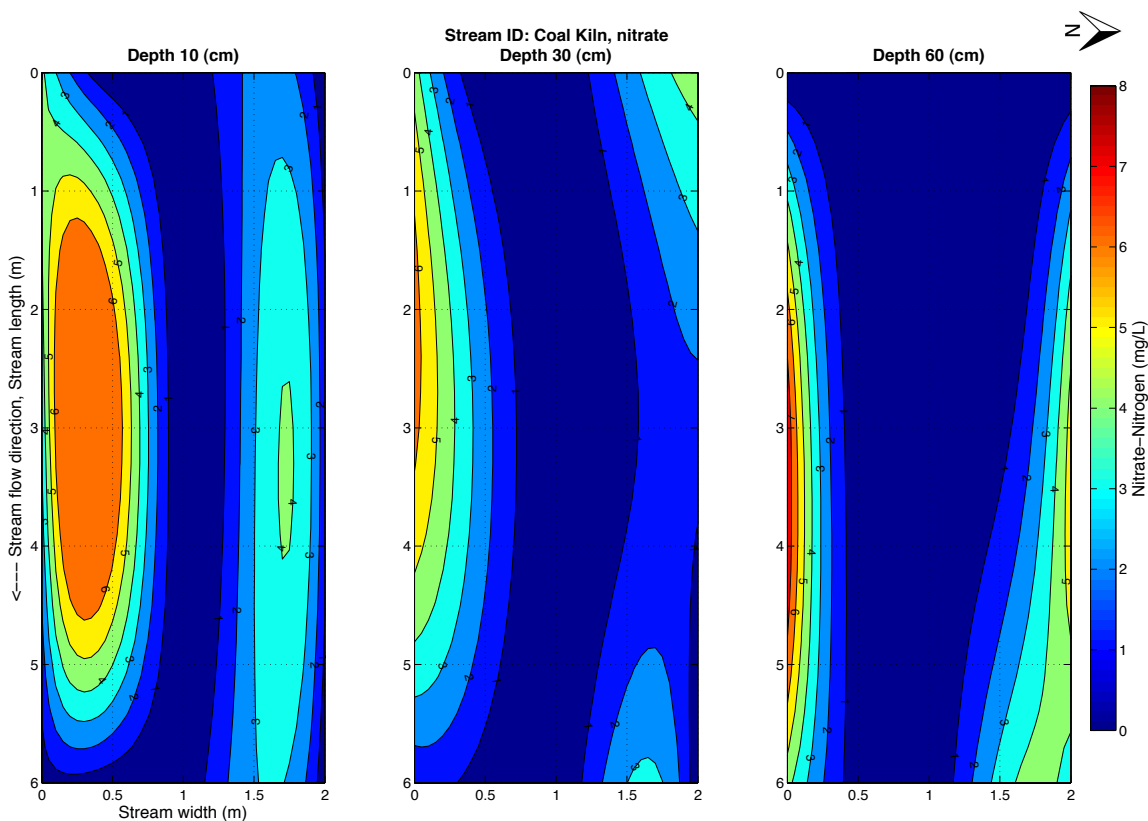
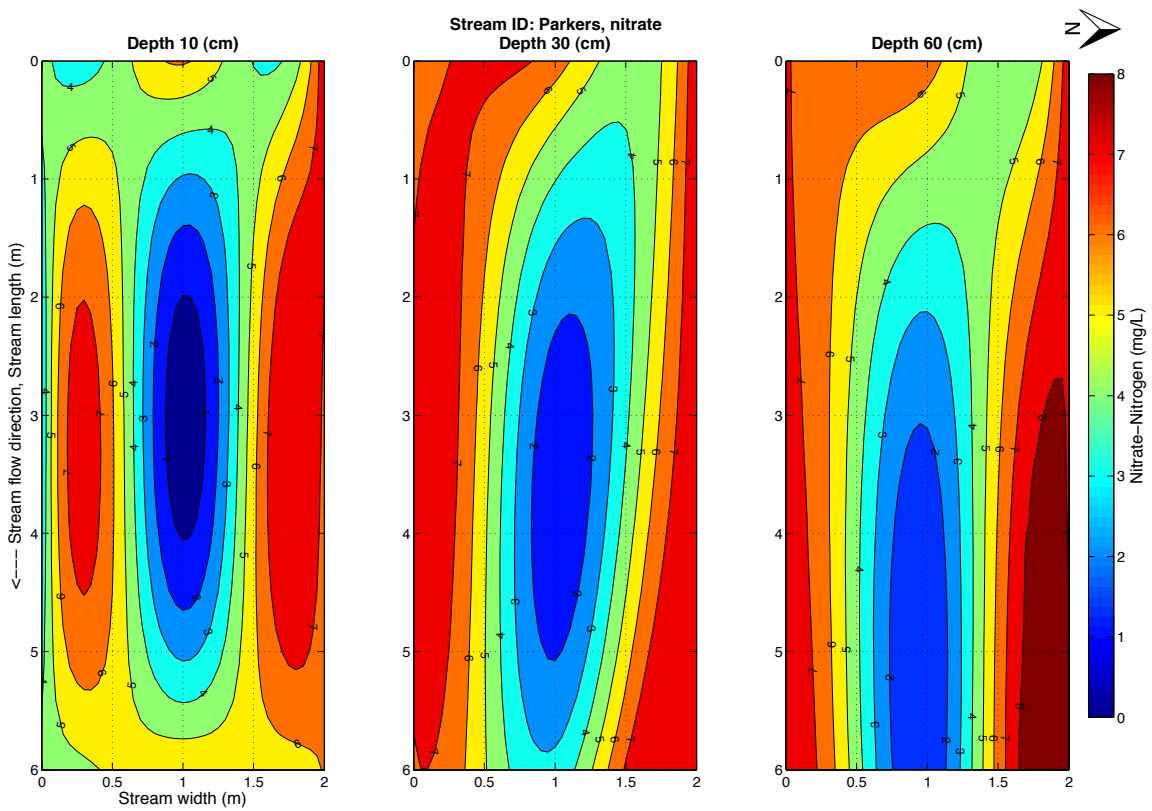
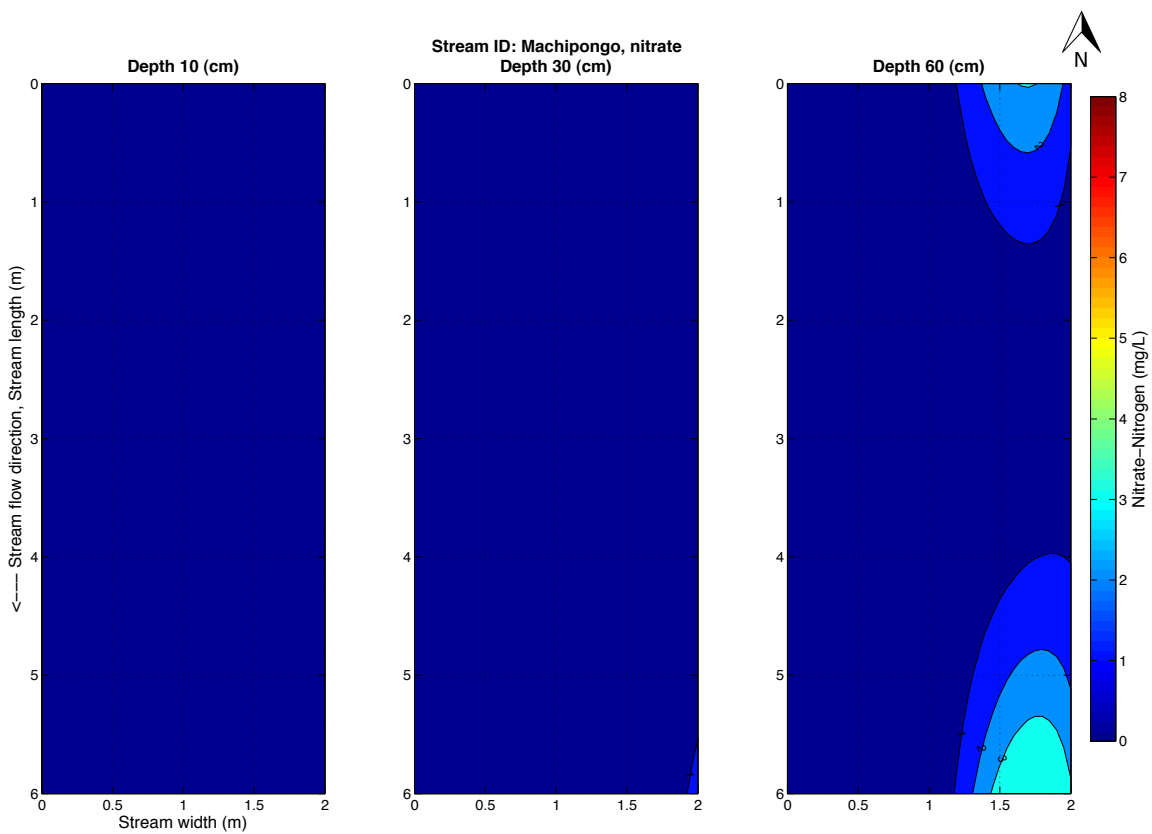


Figure 3-14. Boxplots of nitrate concentration per depth interval of each stream. The vertical dashed green line represents the surface water nitrate concentration.

The low nitrate concentrations and narrow concentration range at Machipongo and Phillips Creek are illustrated by dark blue contour maps (Figure 3-15) at all depth intervals with the exception of a few locations. The nitrate concentration contour maps of Coal Kiln and Parker Creek (Figure 3-15) illustrate a wide range of values and a transverse pattern of high to low to high nitrate across the stream. This transverse pattern was sharpest at Coal Kiln. The center channel of Coal Kiln was consistently $0\text{--}1 \text{ mg NO}_3\text{-N L}^{-1}$ for the entire length of the reach and at all depths. Nitrate difference between positions at Coal Kiln was statistically significant, $F(2,6) = 5.92$, $p < 0.05^*$. (* Levene's test of Equality of Error Variances was violated at depth 1 of Coal Kiln, $F(2,6) = 5.93$, $p < 0.05$.) The descriptive statistics of the above test are presented in Table 3-4. At Parker Creek, the

transverse pattern was strongest at depth intervals 30 and 60 cm. The pattern existed at the 10 cm depth interval as well, but only at transect 2, and not along the entire reach length. A repeated measures ANOVA of nitrate at Parker Creek indicated no significant difference between positions, $F(2,6) = 4.86$, $p > 0.05$ (Table 3-4). The transverse pattern of higher nitrate loads along the sides is the opposite pattern of chloride concentration at Coal Kiln and Parker Creek. The nitrate and chloride contour maps of the respective streams are imperfect inverse images of each other.





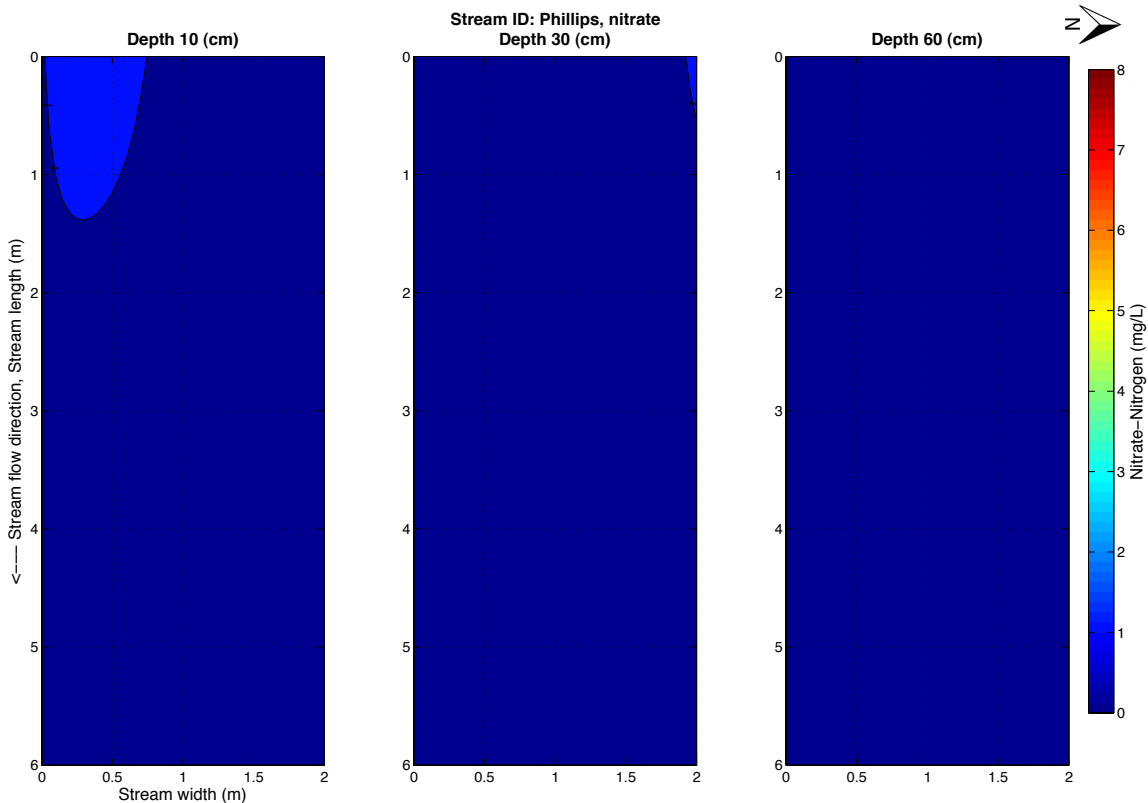


Figure 3-15. Interpolated contour maps of pore-water nitrate mg L^{-1} per depth interval at each stream.

Table 3-4. Descriptive statistics of nitrate-nitrogen mg L^{-1} per depth interval from repeated measures ANOVA between stream stretches A, C, and E, at Coal Kiln and Parker Creek.

Coal Kiln nitrate-nitrogen descriptive statistics				
Measure: Nitrate-nitrogen mg L^{-1}				
Stretch	Mean	Std. Error	95% Confidence Interval	
			Lower Bound	Upper Bound
A	3.52	0.71	1.79	5.25
C	0.08	0.71	-1.65	1.81
E	1.80	0.71	0.07	3.53
Parkers nitrate-nitrogen descriptive statistics				
Measure: Nitrate-nitrogen mg L^{-1}				
Stretch	Mean	Std. Error	95% Confidence Interval	
			Lower Bound	Upper Bound
A	6.05	0.86	3.94	8.15
C	3.71	0.86	1.60	5.82
E	7.47	0.86	5.36	9.58

The contour maps of Coal Kiln and Parker Creek suggest high nitrate values were coincident with low chloride values, which occurred along the stream sides.

Figure 3-16 shows plots of chloride to nitrate concentrations at Coal Kiln and Parker Creek. The relationship between nitrate and chloride concentrations in the pore waters of Coal Kiln and Parker Creek was tested using the Pearson correlation coefficient, r , and indicated moderate to strong correlations, with a greater correlation at Parker Creek than Coal Kiln (Table 3-5). For all depths of Coal Kiln, nitrate and chloride had a moderate negative correlation, $r = -0.31$, $n = 45$, $p = 0.035$. Data from only the 30 and 60 cm depths of Coal Kiln had a stronger correlation of [$r = -0.42$, $n = 29$, $p = 0.024$]. For all depths of Parker Creek, there was a moderate negative correlation between nitrate and chloride of [$r = -0.48$, $n = 42$, $p = 0.001$]. The correlation between nitrate and chloride at Parker was greatest for data from just the 60 cm depth, [$r = -0.60$, $n = 11$, $p = 0.05$]. Although the relationship between nitrate and chloride concentrations was not as robust as expected, the contour maps present a general pattern of low chloride and high nitrate concentrations along the channel sides of Coal Kiln and Parker Creek.

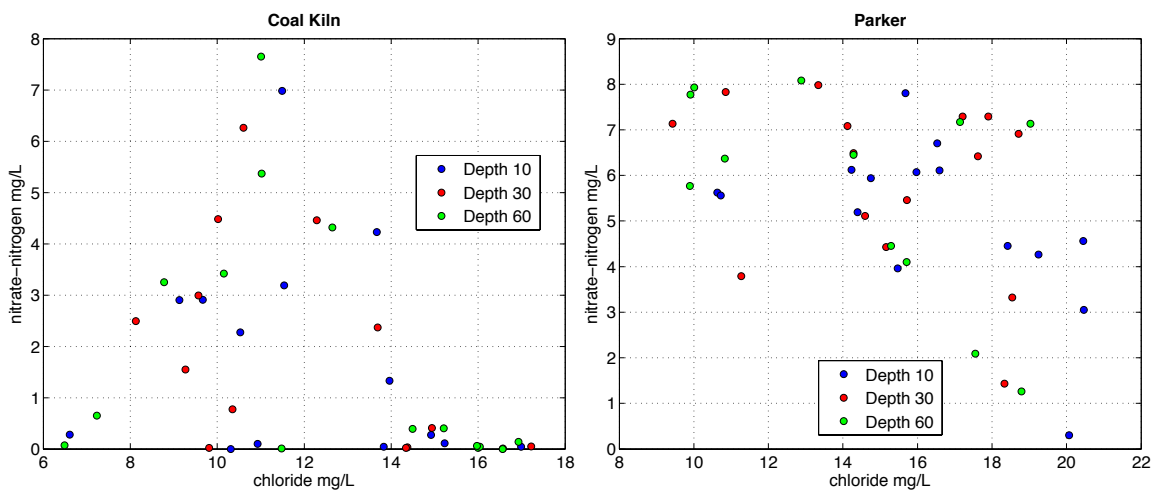


Figure 3-16. Scatter plot of Cl⁻ to nitrate-nitrogen at Coal Kiln and Parker Creek, left panel and right panel respectively.

Table 3-5. Pearson correlation coefficient of chloride and nitrate of specific depth intervals at Coal Kiln and Parker Creek.

Stream	Depth (cm)	Relationship	Correlation Coefficient, r	p
Coal Kiln	10,30,60	Cl^{-1} to N	-0.31	0.035
Coal Kiln	30,60	Cl^{-1} to N	-0.42	0.024
Parker Creek	10,30,60	Cl^{-1} to N	-0.48	0.001
Parker Creek	60	Cl^{-1} to N	-0.60	0.050

3.4 Nitrate Transport

The mean advection of nitrate (J) per streambed sediment depth reveal two stream reaches with stable fluxes and 2 reaches where J substantially changed from depth 30 to 10 cm. The mean J per depth interval of each stream is presented in Figure 3-17. Mean J values at Coal Kiln and Machipongo were small and stable along the vertical profile. The largest changes of mean J per depth occurred at Parker Creek and Phillips Creek; at these two streams mean J decreased with shallower depth along the vertical profile. Mean J transitioned from positive values at depth 30 cm to a negative value at 10 cm. The negative flux indicates a mean nitrate advection down into the streambed sediments; however, the accuracy of negative dh values at the 10 cm depth is questionable (See 2.1.4). The error bars of mean J at Parker Creek's 10 cm depth, span relatively small negative and positive values. Regardless whether the true mean J at depth 10 cm was positive or negative, the absolute value of J decreased from deeper sediments to shallow. Phillips Creek had a large negative J at depth 10 cm compared to small positive J values at depths 30 and 60 cm.

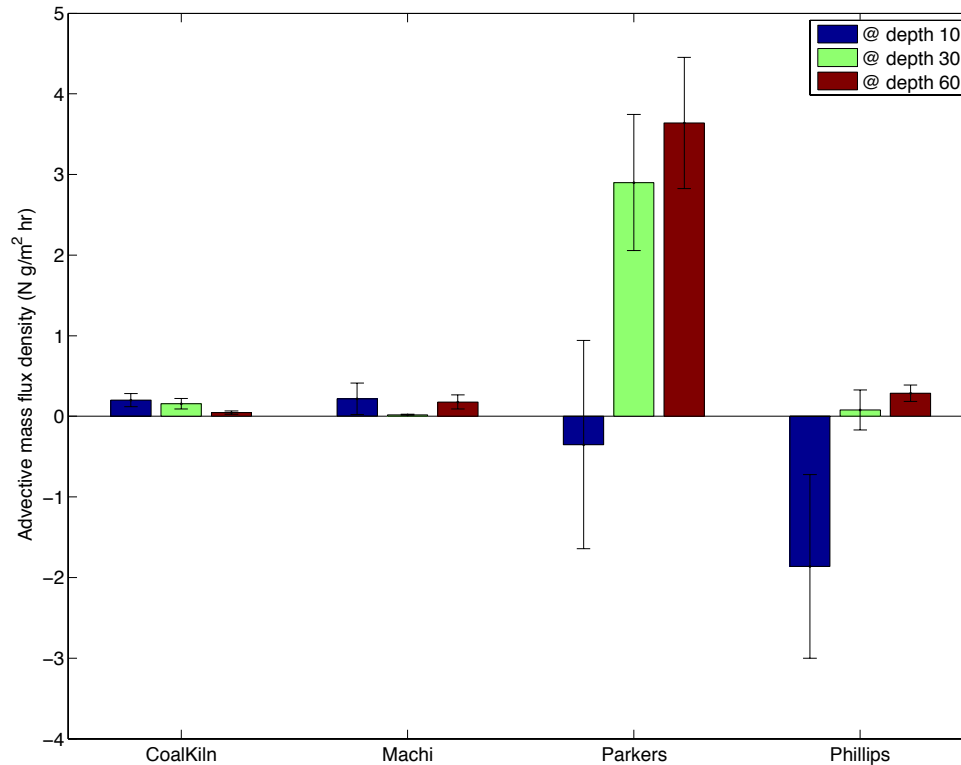


Figure 3-17. Mean J per depth interval of each stream, with SEM bars.

3.5 Nitrate Fate

Individual vertical profiles of nitrate concentration at each stream showed large concentration changes along profiles at Coal Kiln and Parker Creek, whereas at Machipongo and Phillips Creek profiles were relatively stable (Figure 3-18). The vertical profiles are complicated by vertical flow paths in both directions, except at Coal Kiln (pore-water dh at Coal Kiln was always greater than dh of stream water). (The direction of vertical pore-water flow is not considered in the vertical profiles of Machipongo, Parker Creek, and Phillips Creek presented in Figure 3-19 for simplicity.) At Coal Kiln, there were about an equal number of profiles with increasing nitrate concentration, as there were profiles with decreasing nitrate concentration, as depth shallows. From depth 60 to 10 cm of profiles at Coal Kiln, the largest nitrate increase was from 0.39 to 6.98 mg NO₃-N L⁻¹ and the largest

nitrate decrease was from 7.65 to 3.19 mg NO₃-N L⁻¹. At Parker Creek, many of the profiles had stable concentrations from 60 to 30 cm depth, and then slightly decreased from 30 to 10 cm depth. From depth 60 to 10 cm of Parker Creek profiles, the largest nitrate increase was from 1.26 to 5.94 mg NO₃-N L⁻¹ and the largest nitrate decrease was from 7.17 to 3.05 mg NO₃-N L⁻¹. The profiles of Machipongo and Phillips Creek were almost all less than the mean surface water nitrate concentration of the respective streams. Most of the profiles at Machipongo and Phillips Creek were vertically straight, indicating that nitrate concentrations did not vary much.

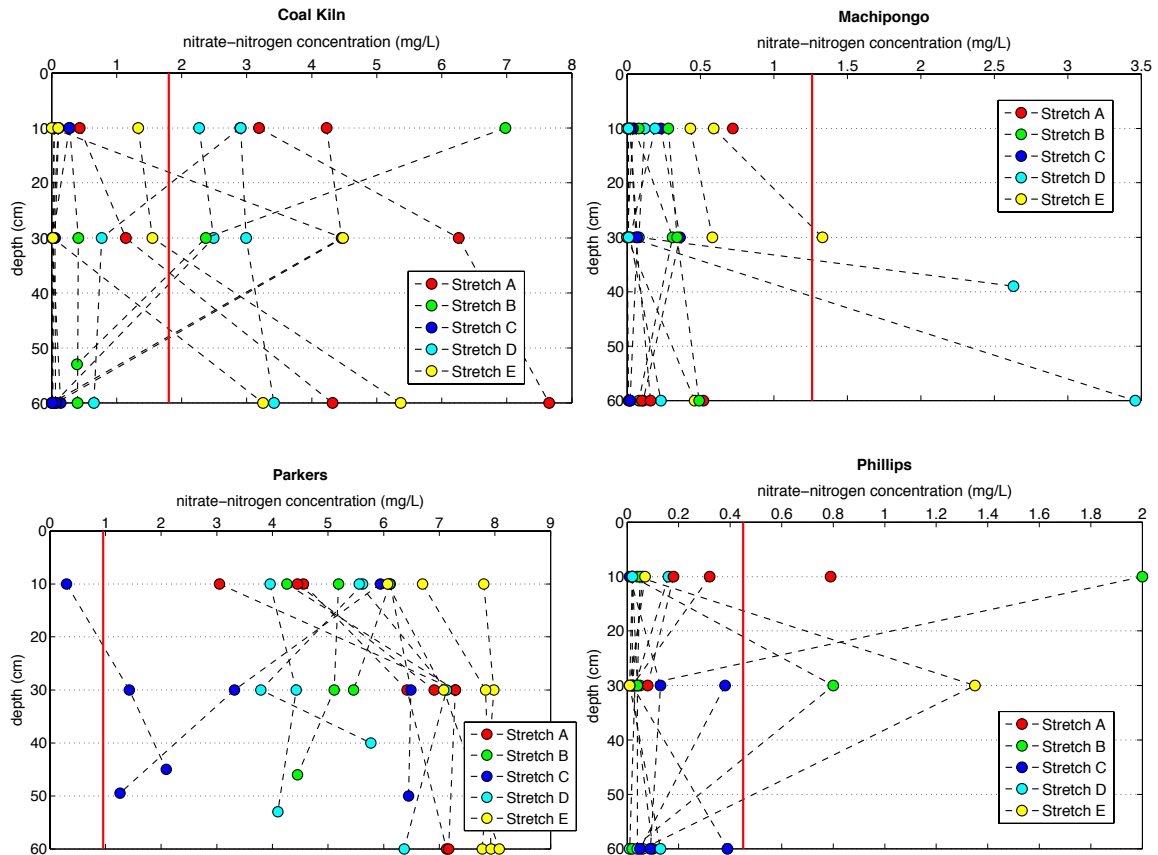


Figure 3-18. Vertical profiles of nitrate mg L⁻¹ at each stream. The vertical red line represents stream water nitrate concentration.

For all streams, the mean nitrate removal rate (R) along vertical flow paths ranged from negative to positive. The nitrate removal rate was calculated along the depth intervals of 10–30 and 30–60 cm and rates were separated according to vertical flow direction, up or down (Figure 3-19). A negative rate indicates a nitrate gain along the flow path and a positive rate indicates nitrate removal along the flow path. Comparisons of R between upwards to downwards flow directions is complicated by unequal sample sizes. At the deeper interval of Coal Kiln, the magnitude of the rate was greatest in the upward flowing water with a negative value. In other words, pore water flowing upwards from depth 60 to 30 cm at Coal Kiln, had a mean nitrate removal rate of $\sim 0.005 \text{ mg NO}_3\text{-N L}^{-1} \text{ hr}^{-1}$. On average,

there was a larger nitrate increase than decrease at the deeper interval. The largest average R , considering both depth intervals at Coal Kiln, was a positive value at interval 10–30 cm, flowing downwards. Therefore on average for downward flowing water at the shallower interval, there was nitrate removal. At Machipongo, on average there was nitrate removal for all flow directions at both intervals, except in downward flowing waters of the shallower interval. The only substantial R values at Parker Creek were positive, indicating nitrate removal, and both had upward flow paths. R was minimal at Phillips Creek with only the shallower interval having substantial values. The shallow interval at Phillips Creek had opposing rates of approximately equal size.

Flow direction was disregarded to calculate the mean R per depth interval of each stream (Figure 3-20). At Coal Kiln the deeper interval had a nitrate gain on average whereas the shallower interval had a nitrate removal of about the same size. The rates are of approximately equal magnitude, suggesting a neutral nitrate rate of removal and gain in the sediments. Compared to Coal Kiln, Machipongo's rates were reversed per depth interval. However, R at the deeper interval was greater than at the shallower interval and thus there was more nitrate being removed than gained. Both intervals at Parker Creek experienced nitrate removal. The largest magnitude of mean rate (including both negative and positive values) was $0.004 \text{ mg NO}_3\text{-N L}^{-1} \text{ hr}^{-1}$ and occurred at the shallower interval of Parker Creek. The average rate at Phillips Creek was approximately $0 \text{ mg NO}_3\text{-N L}^{-1} \text{ hr}^{-1}$ for both intervals.

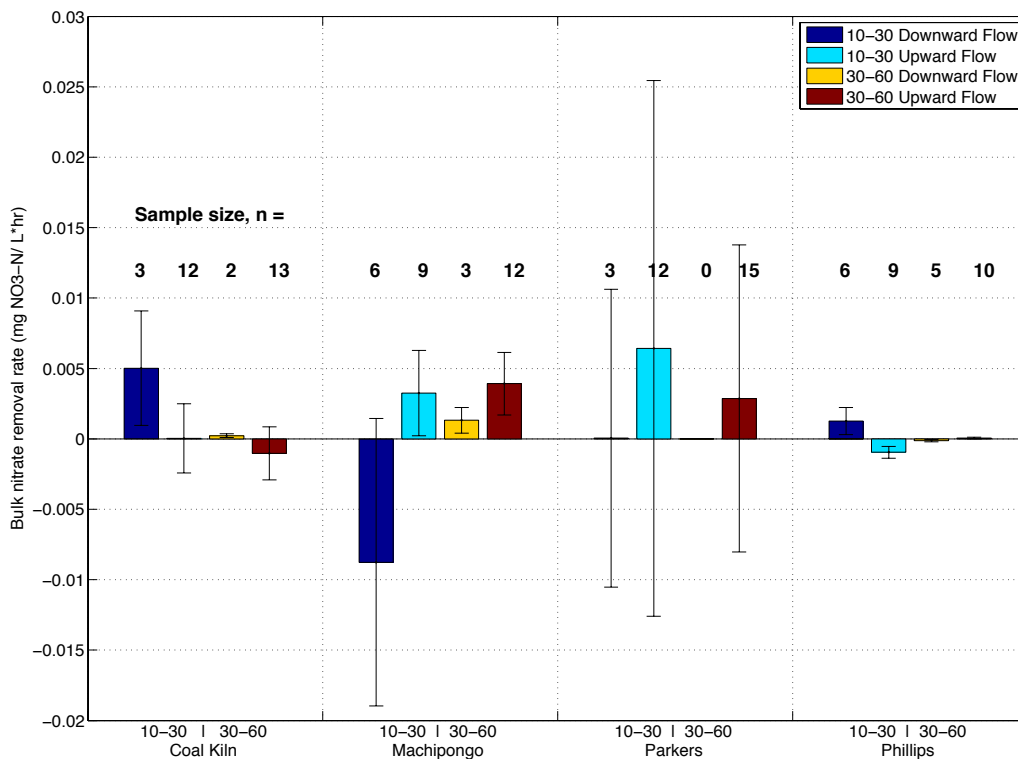


Figure 3-19. Mean nitrate removal rate between depth intervals (between 10 and 30 cm and between 30 and 60 cm) organized by vertical flow direction at each stream, with SEM bars. The sample size of each bar is featured directly above the bar.

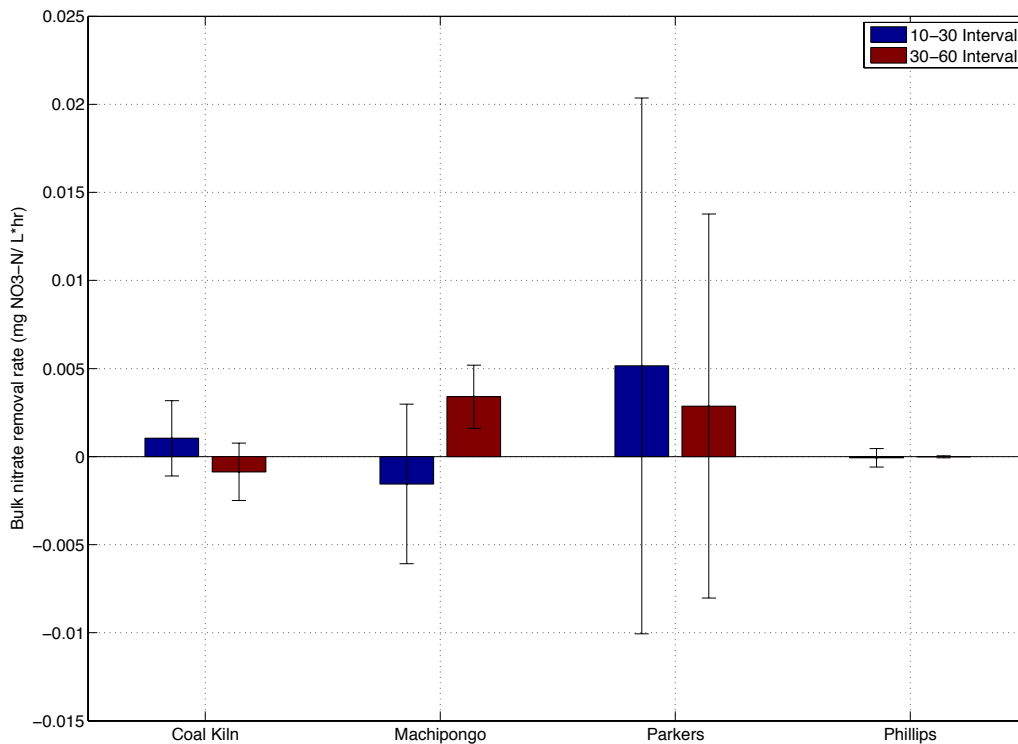


Figure 3-20. Mean nitrate removal rate between depth intervals (between 10 and 30 cm and between 30 and 60 cm) for each stream, with SEM bars.

Streambed sediment conditions appeared poised for denitrification, but high oxygen levels persisted or were replenished along the sides of Coal Kiln and Parker Creek and likely inhibited denitrification. At depth 10 cm of Coal Kiln, the *DO* range increased to larger concentrations than at greater depth. *DO* concentrations were as high as 5 mg L⁻¹ at the 10 cm depth of both Coal Kiln and Parker Creek. A scatter plot of *DO* and nitrate concentration from all depths at Coal Kiln does not show a strong relationship; whereas, the relationship between *DO* and nitrate at Parker Creek appears stronger (Figure 3-21). *DO* and nitrate concentrations at Coal Kiln were moderately correlated in pore-water samples from the 60 cm depth interval [$r=0.50$, $n=15$, $p=0.06$], and in pore-water samples from all depths of Parker Creek were strongly correlated [$r=0.74$, $n=11$, $p=0.009$] (Table 3-6). Based on a least squares linear regression, *DO* concentration explained 31% of the variation in nitrate at Parker Creek, $R^2=0.313$, and the following formula could be used to predict nitrate concentration: $\text{nitrate} = 0.54 \cdot \text{DO} + 3.8$ [$n=40$, $p=0.0016$] (Figure 3-22).

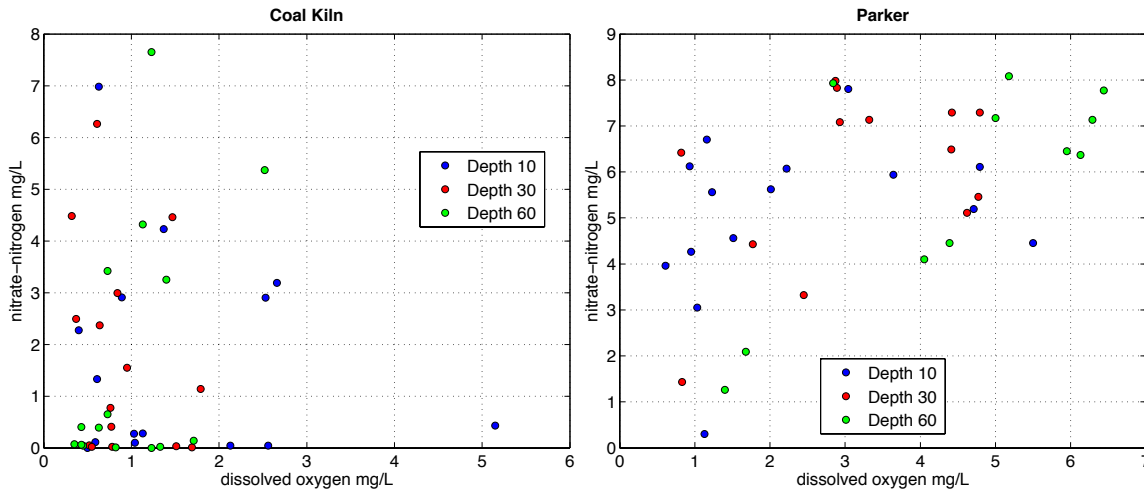


Figure 3-21. Scatter plot of *DO* to nitrate-nitrogen of pore-water at Coal Kiln and Parker Creek, left panel and right panel respectively.

Table 3-6. Pearson's correlation coefficient, r , of DO to NO_3^- and Cl^- to NO_3^- for specific depth intervals of Coal Kiln and Parker Creek.

Stream	Depths	Relationship	Correlation coefficient, r	p
Coal Kiln	60	DO to NO_3^-	0.50	0.060
Parker Creek	10,30,60	DO to NO_3^-	0.49	0.002
Parker Creek	10,30,60	Cl^- to NO_3^-	-0.48	0.001
Parker Creek	30,60	DO to NO_3^-	0.54	0.006
Parker Creek	60	DO to NO_3^-	0.74	0.009
Parker Creek	30,60	Cl^- to NO_3^-	-0.57	0.004
Parker Creek	60	Cl^- to NO_3^-	-0.60	0.050

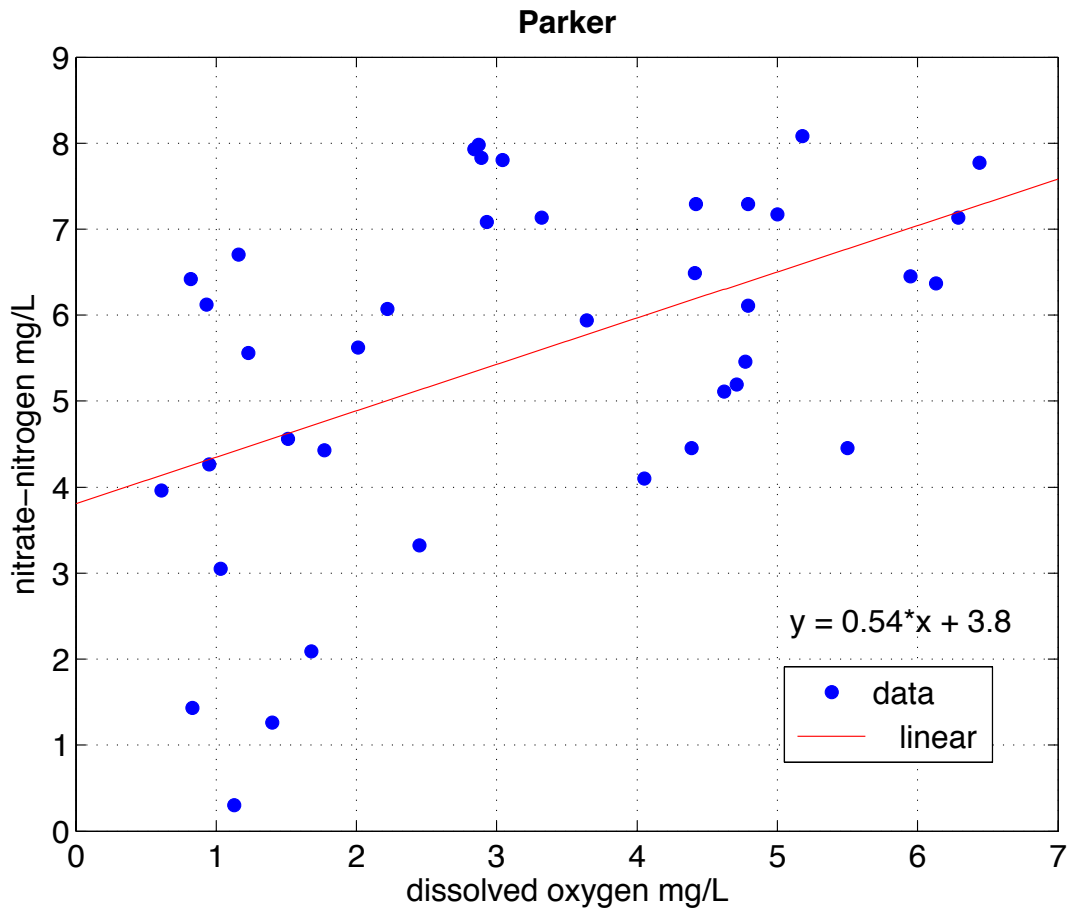


Figure 3-22. Scatter plot of DO to nitrate-nitrogen and a least squares linear regression trendline of pore-water at all depths of Parker Creek.

The nitrate removal rate was relatively unaffected by *DO* and TOM gradients at Coal Kiln and Parker Creek, no relationship emerged. The nitrate removal rate at Coal Kiln and Parker Creek had a narrow distribution that straddled zero. Changes in *DO* and TOM at Coal Kiln and Parker Creek did not offer any insight to the controlling processes of the nitrate removal rate in the streambed sediments (See Appendix A, Figure 7-5; Figure 7-6).

4 Discussion

The streambed sediments of VAES streams appear favorable for microbial activity, including denitrification. Carbon was ubiquitous in the sediments and pore-water velocity was generally slow enough that residence time of nutrients was sufficient for microbial activity. At Machipongo and Phillips Creek, low *DO* and nitrate concentrations in pore water suggest nitrate was removed earlier along the flow path, perhaps deeper. Similar pore water conditions existed in the center channel sediments at Coal Kiln and Parker Creek, but the pore water along the streams sides had a different aqueous chemistry, higher *DO* and nitrate, and lower chloride concentrations. The pore water along the streams sides of Coal Kiln and Parker Creek is expected to have taken a flow path with different influences compared to the center channel pore water, resulting in different aqueous chemistries. *DO* at Coal Kiln and in particular Parker Creek, probably inhibited denitrification in sediments along the stream sides. At three of the streams, discharging groundwater diluted the stream-water nitrate concentration.

4.1 Streambed Sediment Architecture and Effects of Fluvial Processes

The Kozeny-Carman particle size model for estimating *K* provided values within the expected range and stream averages in close proximity to past hydraulic conductivities found on the VAES. The grain-size analysis of sediment samples indicated fine and medium sand at the four streams, which matches a description of the underlying Columbia aquifer as mainly consisting of sandy surficial sediments [Richardson, 1994]. The homogeneity of grain-size analysis results was reflected in the narrow range of *K* values among streams, which only spanned three orders of

magnitude. In this study, the mean K of Coal Kiln sediments was $6.23 \times 10^{-4} \text{ cm s}^{-1}$, which falls between the results of two slug tests at Coal Kiln by *Probasco* [2010] of 7.4×10^{-5} and $2.6 \times 10^{-3} \text{ cm s}^{-1}$. A mean K of $1.7 \times 10^{-3} \text{ cm s}^{-1}$ from falling head measurements on an intact core extracted from Cobb Mill Creek on the VAES [*Gu*, 2007], was one order of magnitude greater than the mean K of $8.39 \times 10^{-4} \text{ cm s}^{-1}$ from all samples of the four streams sampled here. The calculated K values from the four streams fall within the expected range of silty sands and fine sands as listed by *Freeze and Cherry* [1979]. In general, the streambed sediments on the VAES are conducive to high flow-through rates.

Transverse and vertical patterns of sediment architecture shaped by fluvial processes were expected but did not emerge at the four streams [*Chamley*, 1990; *Genereux et al.*, 2008]. A decrease in surface-water velocity results in the deposition of materials that can no longer remain suspended in the water column. A relatively straight section of channel was selected at each stream and theoretically there should be a transverse gradient of surface water velocity [*Hornberger et al.*, 1998]. Based on fluvial sedimentology, greater deposition of fines and materials with less mass will occur along the sides than the center of the straight channel sections [*Chamley*, 1990; *Genereux et al.*, 2008]. A substantial supply of fines and organic matter debris to the streams is expected to derive from the densely vegetated stream borders observed in the field and the adjacent agricultural fields. In addition, a vertical trend of higher organic matter content in shallow sediment depths could occur from deposition of allochthonous materials to the sediment surface. However, there were no strong trends in sediment TOM distribution

(Figure 3-11; Figure 7-3). A slight pattern of decreasing TOM with depth occurred at Machipongo and Parker Creek, but not at Coal Kiln or Phillips Creek. Even though finer sediments and organic matter debris typically decrease K [Freeze and Cherry, 1979], no transverse or vertical trends in K were observed.

The small range of K at the four streams is probably due to the shortfalls of using a particle-size model to estimate K . Grain-size analysis destroys the original sedimentary structure; consequently, important factors such as compaction, packing, and permeability are not included in estimation of K [Chen, 2000; Song, 2009; Vienken *et al.*, 2011; MacDonald, 2012]. The extracted sediment cores contained debris ranging in size, such as organic matter particulates, twigs, a pinecone, and cobbles. The small to large debris deposited in VAES streams form heterogeneous sediments, which make prediction of K by particle-size models difficult [MacDonald, 2012]. In agreement with the conclusions of Vienken *et al.* [2011], using a grain-size model for estimation of average K was reliable, but did not provide precise K values at a high spatial resolution.

TOM abundance and distribution was used as a surrogate for carbon availability, which is an important factor for microbial activity [Brunke, 1997]. Streambed sediments of the Delmarva Peninsula have been characterized as having low organic matter content [Böhlke and Denver, 1995; Speiran, 1996]. Past research at Cobb Mill Creek found TOM peaked in the top 20 cm and then decreased with depth [Galavotti, 2004; Gu, 2007]. Galavotti [2004] and Gu [2007] reported maximum TOM values of 5.2 and ~25%, respectively, both of which occurred in the top 20 cm of sediments. Scarce organic matter, particularly as depth increases in

soils and sediments, has repeatedly been reported as a limiting factor to denitrification [Bradley *et al.*, 1992; Willems, 1997; Hedin *et al.*, 1998; Hoffman, 2000; Inwood *et al.*, 2007; Stelzer *et al.*, 2011]. At the four streams sampled, the vast majority of streambed sediments had abundant (> 0.5%) organic matter content. At the maximum depth sampled (Coal Kiln 60-70 cm; Machipongo 50-60 cm; Parker Creek 60-70 cm; Phillips Creek 60-70 cm), mean TOM concentration remained abundant, at all streams except Parker Creek. High TOM values at the maximum sample depths of Coal Kiln, Machipongo, and Phillips Creek suggest an abundant carbon supply could extend to greater depths in VAES streams than previously reported.

The large stock of organic matter in the sediments of the study streams could be the result of both powerful and weak fluvial forces. Flood events can input organic debris to the channel; the debris can obstruct surface water flow, and cause local sites of deposition [Harmon *et al.*, 1986; Hyatt and Naiman, 2001; Naiman *et al.*, 2002]. Organic inputs to the stream could also come from forest deadfall directly falling into the channel. At the sample areas of Machipongo, Parker Creek, and Phillips Creek, forest bordered the streams and the forest canopies extended over the streams. In addition, autochthonous organic matter from autotrophic and heterotrophic activity in the stream could contribute to the sediment organic matter content. Naiman [2002] states that small channels normally cannot move debris and consequently large woody debris has a random distribution in the channel. The streams of VAES are low-order and low gradient, with slow stream-water velocities. Possibly, the slow velocities of VAES streams cannot easily move large debris in the

channel, debris forms persistent structures or debris dams that trap sediment, and deposition buries the debris over time [Bilby and Likens, 1980; Hassan et al., 2005]. The longevity of large woody debris in sediments is dependent on a host of factors, and can remain in sediments for decades to centuries [Hyatt and Naiman, 2001]. Insufficient energy to organize channel material might explain the lack of a transverse trend of TOM or *K*. Additionally, slow surface water velocities allow accumulation of organic matter in the sediments because of the limited scouring forces and ability to transport materials downstream.

4.2 Flow Regime

The streams of VAES are small gaining streams fed by the unconfined Columbia aquifer. The four streams visited have an average gradient of 2.9 m km^{-1} . Whether a stream reach is gaining or losing overall, surface water can enter the sediments as a result of localized head differences from bedforms, streambed roughness, and debris [Garcia-Gil, 1993; Woessner, 2000]. Hydraulic gradients ranged from negative to positive at all depth intervals of Machipongo, Phillips Creek, and Parker Creek (except the 60 cm depth interval of Parker Creek). A negative hydraulic gradient does not definitively identify hyporheic exchange. Debris buried in the channel or a small lens of impermeable material can create lateral and downward flow paths in gaining reaches. Based on an unpublished tracer experiment and other fieldwork, hyporheic exchange is expected to be minimal on the VAES [Gu et al., 2007]. Negative dh values observed at the 10 cm depth are likely erroneous due to issues with the piezomanometer (See 2.1.4). However, negative dh values at greater depths are more likely accurate and reflect tortuous flow paths.

Hydraulic gradients at each stream visited varied by orders of magnitude on a spatial scale of tens of centimeters in all dimensions. The heterogeneous flow regimes represent the varied and random influences of streambed sediment architecture such as riparian zone effects of tree roots and bank stabilization, hillslopes, and debris.

Hydraulic head values agree with field observations of stream conditions such as stream stage, surface water velocity, streambed sediment topography, channel geometry, and landscape features. All 45 dh measurements at Coal Kiln reach were positive. The study area at Coal Kiln was a narrow channel with steep banks, no woody vegetation along the stream banks or upstream for ~ 10 m, and a smooth streambed topography. The dh measurements suggest the reach was strictly gaining. The study area at Machipongo is bordered on the west by a hillslope with higher elevation than the floodplain on the east. The uneven topography presumably caused the higher dh values on the western side. The maximum depth interval at Parker Creek had a narrow dh distribution with a mean value of 7.32 cm, indicating a roughly constant equipotential under the reach. The homogenous dh values at maximum depth of Parker Creek matches the symmetrical topography of the wide, flat floodplain that borders either side of the stream. No obvious landscape features were present at Parker Creek to influence dh along a transverse or longitudinal direction. During the sampling period at Phillips Creek, there was almost no surface-water flow, just ponded water. The extremely low stream stage at Phillips Creek is reflected by the narrow dh distributions straddling

zero at all depths. Observation of the riparian landscape and channel morphology helped check the reliability of *in situ* measurements and explain the results.

The flow regime of a single stream reach studied here does not offer much insight to the flow regime of a VAES stream along its entire length of ~2 km. Instead, the pooled dh/dl data from the 4 streams presents a good estimate of the range of conditions expected along VAES stream lengths. *Phillips* [2003] estimated a general dh/dl of 0.2 in near surface areas of concentrated discharge on the Delmarva Peninsula. The mean of all hydraulic gradient measurements at the four streams was 0.044, a magnitude of order less than the *Phillips* [2003] estimate. The difference between the average dh/dl measurement and the estimate can partly be explained by a substantial number of erroneous negative dh/dl measurements. Of the four streams, the mean dh/dl of 0.079 at Parker Creek was the closest to the *Phillips* [2003] estimate. Temporal changes in the aquifer by the annual water budget are not accounted for by one estimate of dh/dl . Fieldwork was performed from late summer to mid-fall, typically the driest part of the year, which could explain the overestimation of dh/dl by *Phillips* [2003]. Generalization of a stream's flow regime overlooks local flow regimes that are typically responsible for tortuous flow paths.

4.3 Chloride as a Chemical Marker of Water Bodies

The mechanisms affecting chloride concentration in groundwater and surface water at VAES streams appear unique to the groundwater and surface water. Chloride transport in groundwater can be affected by an array of mechanisms, which make chloride not a reliable conservative tracer [*Flewelling et*

al., 2011; *Korom and Seaman*, 2012]. The groundwater and stream water of sampled streams each had uniform chloride concentrations respectively, and the distinct chloride signature was used to distinguish the two water bodies. At Coal Kiln, Machipongo, and Parker Creek, surface-water chloride concentration was always greater than that of pore water (Figure 3-7; Figure 4-1). (*At Coal Kiln, one profile had greater values than the stream water at depths 10 and 30 cm. The two samples qualified as outliers to the distribution of the respective depth interval.) Lower chloride values in pore water than in stream water was previously observed on the Delmarva by *Böhlke and Denver* [1995], *Galavotti* [2004], *Flewelling* [2009] (Figure 4-2). Presuming stream-water and pore-water chloride concentrations were stable during the sampling period, the vertical profiles of chloride concentration should show any mixing of the two water bodies. Vertical profiles with negative hydraulic head values at depth 10 cm were expected to reflect hyporheic mixing, and consequently, have increasing chloride concentrations with shallower depths along the vertical profile. However, the relationship was not true. The sediments with negative hydraulic head could receive surrounding pore water of a greater head gradient than surface water, consequently not altering the chloride concentration.

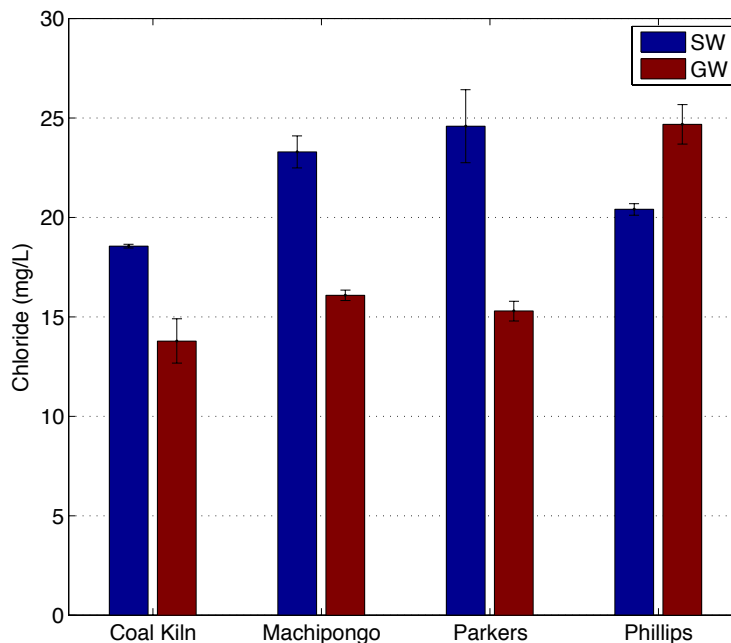


Figure 4-1. Mean chloride concentration of stream water and groundwater at each stream, with SEM bars.

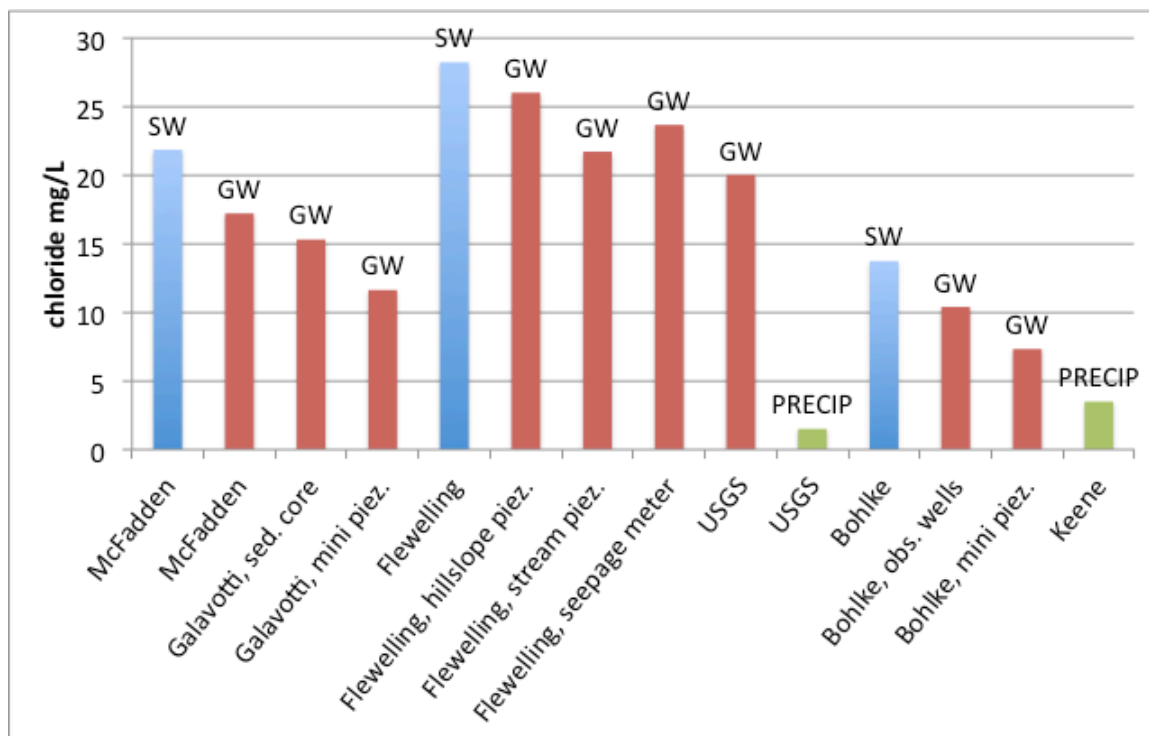


Figure 4-2. Chloride concentration of surface water, groundwater, and precipitation on the Delmarva Peninsula from numerous studies.

A transverse pattern of chloride concentration in groundwater, most pronounced at Coal Kiln and Parker Creek, was identified as a chemical marker for differently sourced groundwater. The theoretical hillslope groundwater flow model

described by *Hornberger et al.* [1998] was used to determine groundwater origins. Lower chloride values represented riparian-influenced groundwater and higher chloride values represented riparian-bypass groundwater. The opposite gradient of groundwater chloride concentration was observed at Cobb Mill Creek; shallow hillslope groundwater had higher chloride concentrations than in groundwater under the stream channel [*Flewelling et al.*, 2011]. *Flewelling et al.* [2011] noted that there could be a number of reasons causing the concentration gradient, and speculated that evapotranspiration by riparian vegetation could be one process leading to higher chloride concentrations in the shallow hillslope groundwater. Likewise, the mechanisms that contributed to more dilute chloride concentrations in riparian-influenced groundwater at Coal Kiln and Parker Creek are unknown and could be manifold. Some of the processes could be chloride adsorption by a highly weathered soil [*Korom and Seaman*, 2012], microbial uptake or chlorination of organic compounds [*Bastviken*, 2007], or dry deposition of chloride from seasalt spray. Perhaps contributing to the different concentrations is chloride from fertilizers, which elevate the riparian-bypass concentration. Regardless, the processes influencing chloride concentration appear to be systematic to a specific riparian area, resulting in relatively homogenous concentrations in a specific riparian area.

The distinct chloride concentrations were used to identify source components. At Coal Kiln, riparian-influenced and riparian-bypass groundwater inputs to the surface water were about equal, whereas at Parker Creek, there was a lot greater input of riparian-bypass groundwater. The contribution of riparian-

influenced versus riparian-bypass groundwater is likely to change as water table elevation changes. Riparian-influenced groundwater should contribute less to total groundwater discharge when water table elevation decreases because there is less groundwater in contact with riparian soil horizons and the root zone. Pore-water samples were collected from the streams during the driest part of the year, late summer and fall. During other seasons, riparian-influenced groundwater should contribute a greater amount to total groundwater discharge than observed here. The groundwater source is important because it typically influences the magnitude of nitrate load to the stream [Flewelling *et al.*, 2011]. Using chloride as a chemical marker to identify differently sourced riparian waters should be done cautiously, because the controlling processes may vary temporally and be nuanced to the respective site.

4.4 Streambed Sediment Denitrification and Nitrate Loads

The three main controls of denitrification in streambed sediments of the VAES are carbon supply, dissolved oxygen level, and pore-water velocity. Nitrate availability and denitrifier presence in the streambed environment are also major controls of denitrification, but both are considered to be abundant at the VAES [Hamilton *et al.*, 1993]. Nitrate concentrations in the surficial aquifer are elevated above background levels and frequently surpass the Primary Maximum Contaminant Level of $10 \text{ mg L}^{-1} \text{ N}$ set by the EPA [Hamilton *et al.*, 1993; Speiran, 1996; Denver *et al.*, 2004; US EPA]. Microbial abundance typically depends on habitat substrate sites, and electron acceptor and donor availability [Hedin *et al.*, 1998]; thus microorganisms are presumed prevalent in VAES streambed sediments.

There is contradiction in the literature whether *DO* or organic matter is the most significant control of denitrification in streambed sediments [Hill *et al.*, 2000].

However, the argument becomes moot for the streams sampled by this study since organic matter was abundant.

The hydrological conditions and carbon availability of the four streams studied were conducive to microbial activity. Previous research on the Delmarva Peninsula reported low concentrations of organic matter in streambed sediments [Böhlke and Denver, 1995; Speiran, 1996]. At the four streams studied, the mean percent of sediment core with abundant TOM ranged from 70 – 90%. TOM was prevalent in the transverse, longitudinal, and vertical directions of streambed sediments. Prior studies on the VAES reported streambed sediment organic matter did not limit denitrification, but the amount of organic matter rapidly decreased past the top 20 cm of streambed sediments [Galavotti, 2004; Gu, 2007]. At Coal Kiln, Machipongo, and Phillips Creek, an abundant amount of TOM extended beyond the 20 cm depth to the greatest depth sampled, which ranged from 60-70 cm. The high TOM content to greater depths than previously reported suggests larger biologically active zones in near-stream sediments than delineated on the VAES before. A larger biologically active zone makes pore-water dissolved oxygen depletion more likely, and in-turn denitrification more likely. Extrapolating TOM concentrations with depth suggests abundant TOM extends to greater depths than sampled.

As pore-water velocity increases, two mechanisms can limit the amount of denitrification. In quickly advecting water, less oxygen is depleted by respiration and relatively slower rates of diffusion limit transport of nitrate to denitrification

sites [Willems, 1997]. From laboratory experiments on streambed sediment cores, Willems [1997] and Gu [2007] reported that at a pore-water velocity of 1.36 and 1.6 cm hr⁻¹, respectively, the nitrate removal rate began to decrease. The relationship found by Willems [1997] and Gu [2007] was used as a guideline for the streams studied here since stream characteristics of the studies are similar. All of the study streams had average pore-water velocities less than the velocity reported by Willems [1997] and Gu [2007] that decreased the amount of denitrification. Pore-water velocities of the streams appeared generally favorable to allow extensive nitrate removal by denitrification.

At two streams, the main factor limiting denitrification was *DO* concentration. As groundwater travels through the Columbia aquifer, groundwater often remains aerobic because of low concentrations of organic matter and reduced species in the aquifer [Denver, 1989; Hamilton et al., 1993]. Aerobic groundwater is expected to enter the biologically active zone in sediments beneath streams, and have *DO* levels decrease due to microbial respiration. Coal Kiln and Parker Creek were the only streams with high *DO* and nitrate in the pore water within streambed sediments, which occurred along the sides of both streams. The increase in the *DO* concentration from depth 30 to 10 cm at Coal Kiln was most likely not from seepage of oxygen-saturated stream water since all hydraulic head measurements were positive (Figure 3-12). At Coal Kiln, the increase in the *DO* distribution at depth 10 cm when microbial respiration is expected to deplete *DO* could be explained by oxygen-rich riparian groundwater entering the sediments at the 10 cm depth and in-stream autotrophic respiration. At Parker Creek, average *DO* decreased with

shallower depths, following the expected trend, however *DO* values remained as high as 5 mg L⁻¹ at the 10 cm depth along the sides of the channel. The persistently high *DO* along stream sides of Parker Creek could have occurred from riparian groundwater entering the sediments, which had not experienced much microbial activity and thus oxygen depletion.

The hypoxic conditions and low nitrate values of groundwater at the maximum depth intervals of Machipongo and Phillips Creek, as well as the center channels of Coal Kiln and Parker Creek, are contrary to reported regional aquifer conditions [Hamilton *et al.*, 1993; Denver *et al.*, 2004]. Based on observed TOM values, it is suspected that microbial activity depleted oxygen and nitrate loads at locations beyond the sampled area, in vertically downward or transverse directions. The low *DO* and nitrate concentrations in pore water in the center channel of Coal Kiln and Parker Creek was identified as riparian-bypass groundwater based on chloride concentration. At Coal Kiln and Parker Creek, microbial activity probably occurred earlier along the riparian-bypass flow path than sampled. Abundant organic matter and low *DO* existed in streambed sediments to a much greater depth than expected.

At the four streams visited, denitrification in the streambed sediments was extremely minimal (Figure 3-20). At Phillips Creek, denitrification was hardly observed because there was no nitrate in the pore water. Machipongo, Coal Kiln, and Parker Creek had larger denitrification rates. Like Phillips Creek, pore-water nitrate concentrations at Machipongo were generally low, so there was not a large mass of nitrate to be removed. However, relatively fast pore-water velocities

increased the nitrate removal rates at Machipongo, and on average there was denitrification at the greater depth segment (30-60 cm). At Coal Kiln, the nitrate removal rates were more subdued. At Parker Creek, on average there was denitrification at both depth segments, although the relatively large error bars of both depth intervals overlap zero, indicating the rates are not statistically different than zero. The mean nitrate removal rates of the four streams were 1-2 orders of magnitude less than the values reported by *Gu* [2007].

Groundwater discharge at three of the four streams diluted the surface water nitrate concentration. The nitrogen concentration of the total groundwater discharge of each stream was calculated using the estimated streambed area per point value described in Section 3.2. The nitrate concentration for all groundwater discharge from the sample area was lower than the surface water at Coal Kiln, Machipongo, and Phillips Creek. Whereas at Parker Creek, groundwater discharge from the sample area increased the nitrate concentration of surface water. The groundwater discharge at Parker Creek contributed a nitrate concentration of 5.9 mg L⁻¹ N, greater than the surface water concentration of 0.45 mg L⁻¹ N. A national study of headwater streams during base flow conditions by *Clark et al.* [2003], determined a general background nitrate concentration of 0.6 mg L⁻¹ N in stream water. Coal Kiln, Machipongo, and Phillips Creek had surface water nitrate concentrations exceeding 0.6 mg L⁻¹ N, but not by much.

5 Conclusion

Temporal effects on the water budget of the VAES likely impact many of the hydrological observations made in this study. Besides sediment core collection, fieldwork was performed during the summer and early fall of 2010, the driest part of the year on the VAES [Denver *et al.*, 2004]. A lower water table on the VAES during summer results in a decreased contribution of shallow groundwater with higher nitrate concentrations than deeper groundwater, to stream base flow [Denver *et al.*, 2004]. The low pore-water nitrate concentrations at Machipongo and Phillips Creek might be due to limited shallow groundwater flow to the streams. However, another explanation is denitrification earlier along flow paths than observed. A low water table might explain the large portion of riparian-bypass groundwater discharging at Parker Creek. A temporal study at VAES streams would clarify how hydrological variables change with the annual water budget and provide a better understanding of annual nitrate fluxes to receiving waters.

The large stock of sediment carbon in the streams sampled in this study conflicts with prior reports of the VAES [Denver *et al.*, 2004; Galavotti, 2004; Gu, 2007]. The methods quantifying sediment TOM content by Denver *et al.* [2004] are unknown, but the methods by Galavotti [2004] and Gu [2007] are identical to the methods used by this study. Galavotti [2004] extracted 29 and Gu [2007] extracted 3 sediments cores from Cobb Mill Creek. Landscape features of Cobb Mill Creek and the four streams of this study are similar. There is not a clear reason why TOM content differed so much between Cobb Mill Creek and the other streams. An objective of this Thesis was to delineate the biologically active zone of streambed

sediments. To my surprise, both TOM and *DO* observations indicate the biologically active zone extends to greater depths than measured. Future research should measure deeper into the sediments to map the vertical extent of the biologically active zone beneath streams. If the nitrate concentrations of the Columbia aquifer reported by *Hamilton et al.* [1993] and *Denver et al.* [2004] are widespread on the VAES, which is expected, then there is a large amount of denitrification occurring earlier along the flow paths and like at greater depths in the sediments than observed here.

6 References

- Anderson, M. P. (2005) Heat as a ground water tracer. *Ground water*, 43(6), 951–968.
- Bastviken, D., Ejlertsson, J., and Tranvik, L. (2001) Similar bacterial growth on dissolved organic matter in anoxic and oxic lake water. *Aquatic Microbial Ecology*, 24(1), 41–49.
- Battin, T. J. (2000) Hydrodynamics is a major determinant of streambed biofilm activity: from the sediment to the reach scale. *American Society of Limnology Oceanography*, 45(6), 1308–1319.
- Bear, J. (1972) *Dynamics of Fluids in Porous Media*, Elsevier, New York, New York.
- Bilby, R. E. and Likens, G. E. (1980) Importance of organic debris dams in the structure and function of stream ecosystems. *Ecology*, 61(5), 1107–1113.
- Birgand, F., Skaggs, R. W., Chescheir, G. M., and Gilliam, J. Wendell (2007) Nitrogen removal in streams of agricultural catchments—a literature review. *Critical Reviews in Environmental Science and Technology*, 37(5), 381–487.
- Böhlke, J. K. and Denver, J. M. (1995) Combined use of groundwater dating, chemical, and isotopic analyses to resolve the history and fate of nitrate contamination in two agricultural watersheds, Atlantic coastal plain, Maryland. *Water Resources Research*, 31(9), 2319–2339.
- Bradley, P. M., Fernandez, M. J., and Chapelle, F. H. (1992) Carbon limitation of denitrification rates in an anaerobic groundwater system. *Environmental Science & Technology*, 26(12), 2377–2381.
- Bredehoeft, J. D. and Papadopulos, I. S. (1965) Rates of vertical groundwater movement estimated from the Earth's thermal profile. *Water Resources Research*, 1(2), 325–328.
- Bricker, S. B., Clement, C. G., Pirhalla, D. E., Orlando, S. P., and Farrow, D. R. G. (1999) National estuarine eutrophication assessment: effects of nutrient enrichment in the Nation's estuaries, 71 pp., NOAA, National Ocean Service, Special Projects Office and the National Centers for Coastal Ocean Science. Silver Spring, MD.
- Brunke, M. and Fischer, H. (1999) Hyporheic bacteria - relationships to environmental gradients and invertebrates in a prealpine stream. *Archiv Fur Hydrobiologie*, 146(2), 189–217.
- Brunke, M. and Gonser, T. (1997) The ecological significance of exchange processes between rivers and groundwater. *Freshwater Biology*, 37(1), 1–33.
- Cardenas, M. B. (2009) Stream-aquifer interactions and hyporheic exchange in gaining and losing sinuous streams. *Water Resources Research*, 45(6), 1–13.
- Cardenas, M. B., Wilson, J. L., and Zlotnik, V. A. (2004) Impact of heterogeneity, bed forms, and stream curvature on subchannel hyporheic exchange. *Water Resources Research*, 40(8), 1–14.
- Carman, P. C. (1937) Fluid Flow through Granular Beds. *Trans.Inst.Chem. Eng.*, 15,150.
- Carman, P.C. (1956) *Flow of Gases through Porous Media*. Butterworths Scientific Publications, London, England.

- Carrier, W. D. I. (2003) Goodbye, Hazen; Hello, Kozeny-Carman. *Journal of Geotechnical and Geoenvironmental Engineering*, (November), 1054–1056.
- Chamley, H. (1990) *Sedimentology*, Springer-Verlag, Berlin, Germany.
- Chen, X. (2000) Measurement of streambed hydraulic conductivity and its anisotropy. *Environmental Geology*, 39(12), 1317–1324.
- Clark, G. M., Mueller, D. K., and Mast, M. A. (2000) Nutrient concentrations and yields in undeveloped stream basins of the United States. *Journal of the American Water Resources Association*, 36(4), 849–860.
- Cooper, A. B. (1990) Nitrate depletion in the riparian zone and stream channel of a small headwater catchment. *Hydrobiologia*, 202, 13–26.
- Das, B. M. (2006) *Principles of geotechnical engineering*, 6th ed., Thomson, United States.
- Denver, J. M. (1989) Effects of agricultural practices and septic-system effluent on the quality of water in the unconfined aquifer in parts of eastern Sussex County, Delaware, Geological Survey Report of Investigations, Newark.
- Denver, J. M., Ator, S. W., Debrewer, L. M., Ferrari, M. J., Barbaro, J. R., Hancock, T. C., et al. (2004) Water quality in the Delmarva Peninsula, Delaware, Maryland, Virginia, 1999-2001, *Circular 1228*, 40 pp., US Geological Survey, Reston, Virginia.
- Fetter, C W, J. (2000) *Applied Hydrogeology*, 4th ed., Prentice Hall, Upper Saddle River, New Jersey.
- Fischer, H., Kloep, F., Wilzcek, S., and Pusch, M. T. (2005) A River's Liver – Microbial processes within the hyporheic zone of a large lowland river. *Biogeochemistry*, 76(2), 349–371.
- Fischer, H. and Pusch, M. (2001) Comparison of bacterial production in sediments , epiphyton and the pelagic zone of a lowland river. *Freshwater Biology*, 46(10), 1335–1348.
- Flewelling, S. A. (2009) Nitrogen storage and removal in catchments on the Eastern Shore of Virginia, Ph.D. Thesis, 144 pp., University of Virginia, Charlottesville, VA.
- Flewelling, S. A., Herman, J. S., Hornberger, G. M., and Mills, A. L. (2011) Travel time controls the magnitude of nitrate discharge in groundwater bypassing the riparian zone to a stream on Virginia's coastal plain. *Hydrological Processes*, doi: 10.1002/hyp.8219.
- Freeze, R. A. and Cherry, J. A. (1979) *Groundwater*, Prentice-Hall, Englewood Cliffs, New Jersey.
- Galavotti, H. S. (2004) Spatial profiles of sediment denitrification at the ground water – surface water interface in Cobb Mill Creek on the Eastern Shore of Virginia, Masters Thesis, 94 pp., University of Virginia, Charlottesville, VA.
- Galloway, J. N., Aber, J. D., Erisman, J. A. N. W., P, S., Howarth, Robert W., Cowling, E. B., et al. (2003) The nitrogen cascade. *BioScience*, 53(4), 341–356.
- Garcia-Gil, S. (1993) The fluvial architecture of the upper Buntsandstein in the Iberian Basin, central Spain. *Sedimentology*, 40, 125–143.

- Genereux, D. P., Leahy, S., Mitasova, H., Kennedy, C. D., and Corbett, D. R. (2008) Spatial and temporal variability of streambed hydraulic conductivity in West Bear Creek, North Carolina, USA. *Journal of Hydrology*, 358(3-4), 332–353.
- Gilbert, R. O. (1987) *Statistical Methods for Environmental Pollution Monitoring*, Van Norstrand Reinhold Co., New York, New York.
- Gold, A. J., Groffman, P. M., Addy, K., Kellogg, D. Q., Stolt, M., and Rosenblatt, A. E. (2001) Landscape attributes as controls on ground water nitrate removal capacity of riparian zones. *Journal Of The American Water Resources Association*, 37(6), 1457–1464.
- Gregory, S. V., Swanson, F. J., McKee, W. A., and Cummins, K. W. (1991) An ecosystem perspective of riparian zones. *BioScience*, 41(8), 540–551.
- Groffman, P. M., Howard, G., Gold, A., and Nelson, W. (1996) Microbial nitrate processing in shallow groundwater in a riparian forest. *Journal of Environmental Quality*, 25, 1309–1316.
- Gu, C. (2007) Hydrological control on nitrate delivery through the groundwater-surface interface, Ph.D. Thesis, 250 pp., University of Virginia, Charlottesville, VA.
- Gu, C., Hornberger, G. M., Herman, J. S., and Mills, A. L. (2008) Influence of stream-groundwater interactions in the streambed sediments on NO₃ – flux to a low-relief coastal stream. *Water Resources Research*, 44(11), 1–13.
- Gu, C., Hornberger, G. M., Mills, A. L., Herman, J. S., and Flewelling, S. A. (2007) Nitrate reduction in streambed sediments: effects of flow and biogeochemical kinetics. *Water Resources Research*, 43(12), 1–10.
- Hamilton, B. P. A., Denver, J. M., Phillips, P. J., and Shedlock, R. J. (1993) Water-quality assessment of the Delmarva Peninsula, Delaware, Maryland, and Virginia-Effects of agricultural activities on, and distribution of, nitrate and other inorganic constituents in the surficial aquifer, *Open-File Report 93-40*, 87 pp., US Geological Survey, Towson, Maryland.
- Harmon, M., Franklin, J., Swanson, F., Sollins, P., Gregory, SV, Lattin, J., et al. (1986) Ecology of coarse woody debris in temperate ecosystems. *Advances in Ecological Research*, 15, 133-276.
- Harvey, Judson W. and Bencala, K. E. (1993) The effect of streambed topography on surface-subsurface water exchange in mountain catchments. *Water Resources Research*, 29(1), 89–93.
- Hassan, M. A., Church, M., Lisle, T. E., Brardinoni, F., Benda, L., and Grant, G. E. (2005) Sediment transport and channel morphology of small, forested streams. *Journal Of The American Water Resources Association*, (August), 853–876.
- Haycock, N. E. and Pinay, G. (1993) Groundwater nitrate dynamics in grass and poplar vegetated riparian buffer strips during the winter. *Journal of Environmental Quality*, 22, 273-278.
- Hedin, L. O., Fischer, J. C. Von, Ostrom, N. E., Kennedy, B. P., Brown, G., Robertson, G. P., et al. (1998) Thermodynamic constraints on nitrogen transformations and other biogeochemical processes at soil-stream interfaces. *Ecology*, 79(2), 684–703.
- Hill, A. R. (1996) Nitrate removal in stream riparian zones. *Journal of Environmental Quality*, 25, 743–755.

- Hill, A. R., Devito, K. J., Campagnolo, S., and Sanmugadas, K. (2000) Subsurface denitrification in a forest riparian zone : Interactions between hydrology and supplies of nitrate and organic carbon. *Biogeochemistry*, 51, 193–223.
- Hoffman, C. C., Rysgaard, S., and Berg, P. (2000) Denitrification rates predicted by nitrogen-15 labeled nitrate microcosm studies, in situ measurements, and modeling. *Journal of Environmental Quality*, 29(6).
- Hornberger, G. M., Raffensperger, J. P., Wiberg, P. L., and Eshleman, K. N. (1998) *Elements of Physical Hydrology*, John Hopkins University Press, Baltimore, Maryland.
- Howarth, R. W., Anderson, D., Cloern, J., Elfring, C., Hopkinson, C., and Lapointe, B. (2000) Nutrient pollution of coastal rivers, bays and seas, *Issues in Ecology*, 7, 1–40.
- Hyatt, T. L. and Naiman, R. J. (2001) The residence time of large woody debris in the Queets River, Washington , USA. *Ecological Applications*, 11(1), 191–202.
- Inwood S.E., Tank J.L. & Bernot M.J. (2007) Factors controlling sediment denitrification in Midwestern streams of varying land use, *Microbial Ecology*, 53, 247–258.
- Jacobs, T. and Gilliam, J. W. (1985) Riparian losses of nitrate from agricultural drainage waters. *Journal of Environmental Quality*, 14, 472–478.
- Justic, D., Rabalais, N. N., and Turner, R. E. (1995) Stoichiometric nutrient balance and origin of coastal eutrophication. *Marine Pollution Bulletin*, 30: 41–46.
- Kelly, S. E. and Murdoch, L. C. (2003) Measuring the hydraulic conductivity of shallow submerged sediments. *Ground water*, 41(4), 431–439.
- Kennedy, C. D., Genereux, D. P., Corbett, D. R., and Mitsova, H. (2007) Design of a light-oil piezomanometer for measurement of hydraulic head differences and collection of groundwater samples. *Water Resources Research*, 43(9), 1–9.
- Kennedy, C. D., Genereux, D. P., Corbett, D. R., and Mitsova, H. (2009) Spatial and temporal dynamics of coupled groundwater and nitrogen fluxes through a streambed in an agricultural watershed. *Water Resources Research*, 45(9), 1–18.
- Kennedy, C. D., Genereux, D. P., Mitsova, H., Corbett, D. R., and Leahy, S. (2008) Effect of sampling density and design on estimation of streambed attributes. *Journal of Hydrology*, 355(1-4), 164–180.
- Korom, S. F. and Seaman, J. C. (2012) When “conservative” anionic tracers aren’t. *Ground water*, 50(6), 820–4.
- Kozeny, J. (1927) Uber Kapillare Leitung Des Wassers in Boden. Sitzungsber Akad. Wiss.Wien Math.Naturwiss.Kl, Abt.2a, 136,271-306 (In German).
- Kristensen, E., Devol, A. H., and Ahmed, S. I. (1995) Aerobic and anaerobic of organic decomposition matter marine sediment: Which is fastest ? *American Society of Limnology Oceanography*, 40(8), 1430–1437.
- Lee, D. R. (1977) A device for measuring seepage flux in lakes and estuaries. *American Society of Limnology Oceanography*, 22(1), 140–147.

- Lowrance, R., Altier, L., Newbold, J., Schnabel, R., Groffman, P. M., Denver, J. M., et al. (1997) Water quality functions of riparian forest buffers in Chesapeake Bay watersheds. *Environmental Management*, 21(5), 687–712.
- MacDonald, A. M., Maurice, L., Dobbs, M. R., Reeves, H. J., and Auton, C. A. (2012) Relating in situ hydraulic conductivity, particle size and relative density of superficial deposits in a heterogeneous catchment. *Journal of Hydrology*, 434-435, 130–141.
- Maier, R. M., Pepper, I., and Gerba, C. (2009) *Environmental Microbiology*, Elsevier, New York, New York.
- Marion, A., Bellinello, M., Guymer, I., and Packman, A. (2002) Effect of bed form geometry on the penetration of nonreactive solutes into a streambed. *Water Resources Research*, 38(10), 27-1–27-12.
- Meek, J. (1996) Do changing attitudes mean changing practices? *Nonpoint Source*, (44), 1-32.
- Meng, A A, III, and Harsh, J. F. (1988) Hydrogeologic framework of the Virginia Coastal Plain, *Survey Professional Paper 1404-C*, 82 pp., U.S. Geological Survey, Washington, D.C.
- Mills, A. L., Hornberger, G. M., and Herman, J. S. (2008) Sediments in low-relief coastal streams as effective filters of agricultural nitrate, in *American Water Resources Association*, Virginia Beach, VA.
- Mixon, R. B. (1985) Stratigraphic and geomorphic framework of uppermost cenozoic deposits in the southern Delmarva Peninsula, Virginia and Maryland, *Professional Paper 1067-G*, 58 pp., U.S. Geological Survey, Washington, D.C.
- Naiman, R. J., Balian, E. V., Bartz, K. K., Robert, E., and Latterell, J. J. (2002) Dead wood dynamics in stream, 26 pp., USDA Forest Service Gen. Tech. Rep PSW-GTR-181.
- Nixon, S. W., Ammerman, J. W., Atkinson, L. P., Berounsky, V. M., Billen, G., Boicourt, W. C., et al. (1996) The fate of nitrogen and phosphorus at the land-sea margin of the North Atlantic Ocean. *Biogeochemistry*, 35(1), 141–180.
- O'Neill, G. J. and Gordon, A. M. (1994) The nitrogen filtering capacity of Carolina poplar in an artificial riparian zone. *Journal of Environmental Quality*, 23, 1218–1223.
- Odong, J. (2007) Evaluation of empirical formulae for determination of hydraulic conductivity based on grain-size analysis. *Journal of American Science*, 3(3), 54–60.
- Peterjohn, W. T. and Correll, D. L. (1984) Nutrient dynamics in an agricultural watershed : observations on the role of a riparian forest. *Ecology*, 65(5), 1466–1475.
- Phillips, O. M. (2003) Groundwater flow patterns in extensive shallow aquifers with gentle relief: theory and application to the Galena/Locust Grove region of eastern Maryland. *Water Resources Research*, 39(6), 1–13.
- Phillips, P. J., Denver, J. M., Shedlock, R. J., and Hamilton, P. A. (1993) Effect of forested wetlands on nitrate concentrations in ground water and surface water on the Delmarva Peninsula. *Wetlands*, 13(2), 75–83.

- Prasad, R. and Power, J. F. (1995) Nitrification inhibitors for agriculture, health, and the environment. *Advances in Agronomy*, 54, 233–281.
- Probasco, P. G. (2010) Riparian buffer landscape effects on groundwater flow paths and nitrate occurrences in groundwater near streams of the Eastern Shore of Virginia, Masters Thesis, 147 pp., University of Virginia, Charlottesville, VA.
- Pusch, M. (1996) The metabolism of organic matter in the hyporheic zone of a mountain stream, and its spatial distribution. *Hydrobiologia*, 323(2), 107–118.
- Rabalais, N. N., Turner, R. E., and Scavia, D. (2002) Beyond science into policy : Gulf of Mexico hypoxia and the Mississippi River. *BioScience*, 52(2), 129–142.
- Richardson, D. L. (1994) Hydrogeology and analysis of the ground-water-flow system of the Eastern Shore, Virginia, *Water-Supply Paper 2401*, 117 pp., U.S. Geological Survey, Reston, Virginia.
- Schmidt, C., Conant Jr., B., Bayerraich, M., and Schirmer, M. (2007) Evaluation and field-scale application of an analytical method to quantify groundwater discharge using mapped streambed temperatures. *Journal of Hydrology*, 347(3-4), 292–307.
- Schumacher, B. A. (2002) Methods for the Determination of Total Organic Carbon in Soils and Sediments, 25 pp., U.S. Environmental Protection Agency, Las Vegas, Nevada.
- Sheibley, R. W., Duff, J. H., Jackman, A. P., Triska, F. J., Survey, U. S. G., and Park, M. (2003) Inorganic nitrogen transformations in the bed of the Shingobee River , Minnesota : Integrating hydrologic and biological processes using sediment perfusion cores. *American Society of Limnology Oceanography*, 48(3), 1129–1140.
- Sinnott, A. and Tibbitts, G. C., Jr., (1968) Ground-water resources of Accomack and Northampton Counties Virginia, *Mineral Resources Report 9*, Department of Conservation and Economic Development, Charlottesville, Virginia.
- Song, J., Chen, X., Cheng, C., Wang, D., Lackey, S., and Xu, Z. (2009) Feasibility of grain-size analysis methods for determination of vertical hydraulic conductivity of streambeds. *Journal of Hydrology*, 375(3-4), 428–437.
- Spalding, R. F. and Exner, M. E. (1993) Occurrence of Nitrate in Groundwater—A Review. *Journal of Environmental Quality*, 22(3), 392–402.
- Speiran, G. K. (1996) Geohydrology and geochemistry near coastal ground-water-discharge areas of the Eastern Shore, Virginia, *U.S. Geological Survey Water-Supply Paper 2479*, 81 pp., Washington, D.C.
- Stelzer, R.S., Bartsch, L. A., Richardson, W.B., and Strauss, E.A. (2011) The Dark Side of the Hyporheic Zone: Depth Profiles of Nitrogen and its Processing in Stream Sediments. *Freshwater Biology*, 56, 2021–2033.
- Storey, R. G., Fulthorpe, R. R., and Williams, D. D. (1999) Perspectives and predictions on the microbial ecology of the hyporheic zone. *Freshwater Biology*, 41(1), 119–130.
- Swanson, T. E. and Cardenas, M. B. (2011) Ex-Stream: A MATLAB program for calculating fluid flux through sediment–water interfaces based on steady and transient temperature profiles. *Computers & Geosciences*, 37(10), 1664–1669.

- Triska, F. J., Kennedy, V. C., Avanzino, R. J., Zellweger, G. W., and Bencala, K. E. (1989) Retention and transport of nutrients in a third-order stream in northwestern California : hyporheic processes. *Ecology*, 70(6).
- US EPA data are available at <http://water.epa.gov/drink/contaminants/basicinformation/nitrate.cfm>.
- USDA, (2009) 2007 Census of Agriculture, USDA National Agricultural Statistics Service, pp. 739.
- Vidon, P. G. F. and Hill, A. R. (2004) Denitrification and patterns of electron donors and acceptors in eight riparian zones with contrasting hydrogeology. *Biogeochemistry*, 71(2), 259–283.
- Vienken, T. and Dietrich, P. (2011) Field evaluation of methods for determining hydraulic conductivity from grain size data. *Journal of Hydrology*, 400(1-2), 58–71.
- Wagner-Riddle, C., Thurtell, G. W., King, K. M., Kidd, G. E., and Beauchamp, E. G. (1996) Nitrous oxide and carbon dioxide fluxes from a bare soil using a micrometeorological approach. *Journal of Environmental Quality*, 25(4), 898–907.
- Willems, H. P. L., Rotelli, M. D., Berry, D. F., Smith, E. P., Reneau, R. B., and Mostaghimi, S. (1997) Nitrate removal in riparian wetland soils : effects of flow rate , temperature , nitrate concentration and soil depth. *Water Resources Research*, 31(4), 841–849.
- Winter, T. C., Harvey, J. W., Franke, O. L., and Alley, W. M. (1998) Ground water and surface water, a single resource, *Circular 1139*, 87 pp., U.S. Geological Survey, Denver, Colorado.
- Woessner, W. W. (2000) Stream and fluvial plain ground water interactions: rescaling hydrogeologic thought. *Ground water*, 38(3), 423-429.
- Wondzell, S. M. and Swanson, Frederick J. (1999) Floods, channel change, and the hyporheic zone. *Water Resources Research*, 35(2), 555–567.
- Wroblicky, G. J., Campana, M. E., Valett, H. M., and Dahm, N. (1998) Seasonal variation in surface-subsurface water exchange and lateral hyporheic area of two stream-aquifer system. *Water Resources Research*, 34(3), 317–328.
- Young, E. O. and Briggs, R. D. (2005) Shallow ground water nitrate-N and ammonium-N in cropland and riparian buffers. *Agriculture, Ecosystems & Environment*, 109, 297–309.
- Zarnetske, J. P., Gooseff, M. N., Brosten, T. R., Bradford, J. H., McNamara, J. P., and Bowden, W. B. (2007) Transient storage as a function of geomorphology, discharge, and permafrost active layer conditions in Arctic tundra streams. *Water Resources Research*, 43(7), doi:10.1029/2005WR004816.

7 Appendix A

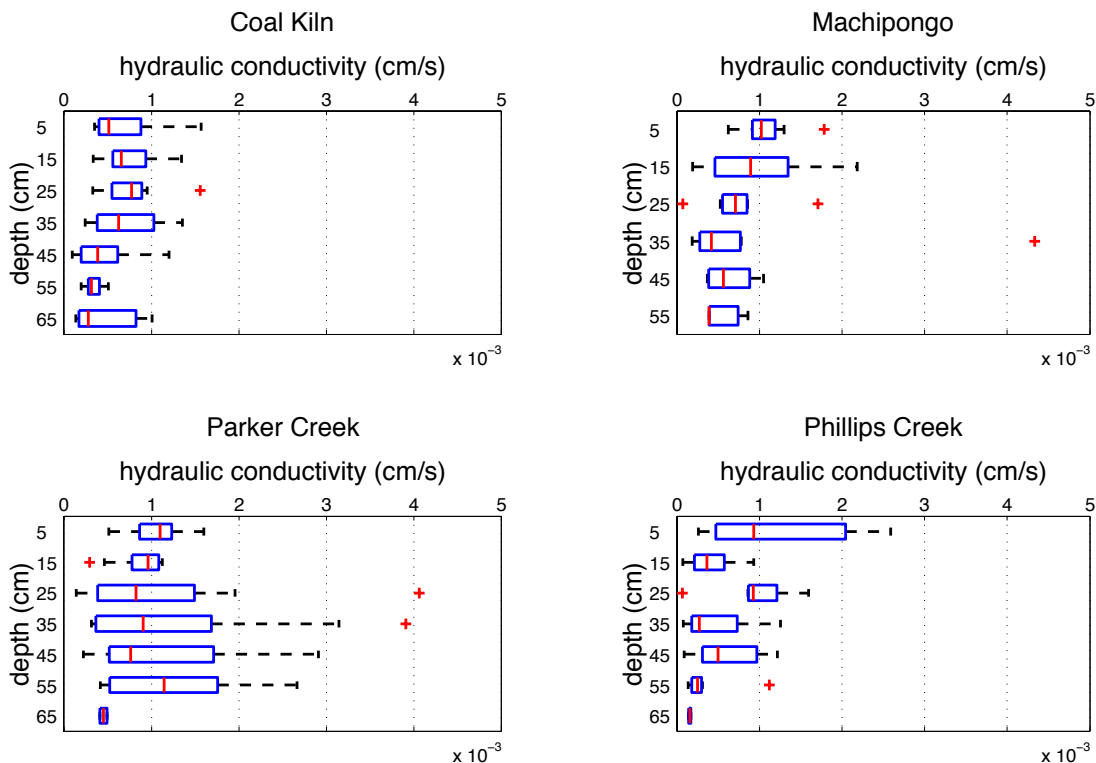


Figure 7-1. Boxplots of K by depth interval at each stream.

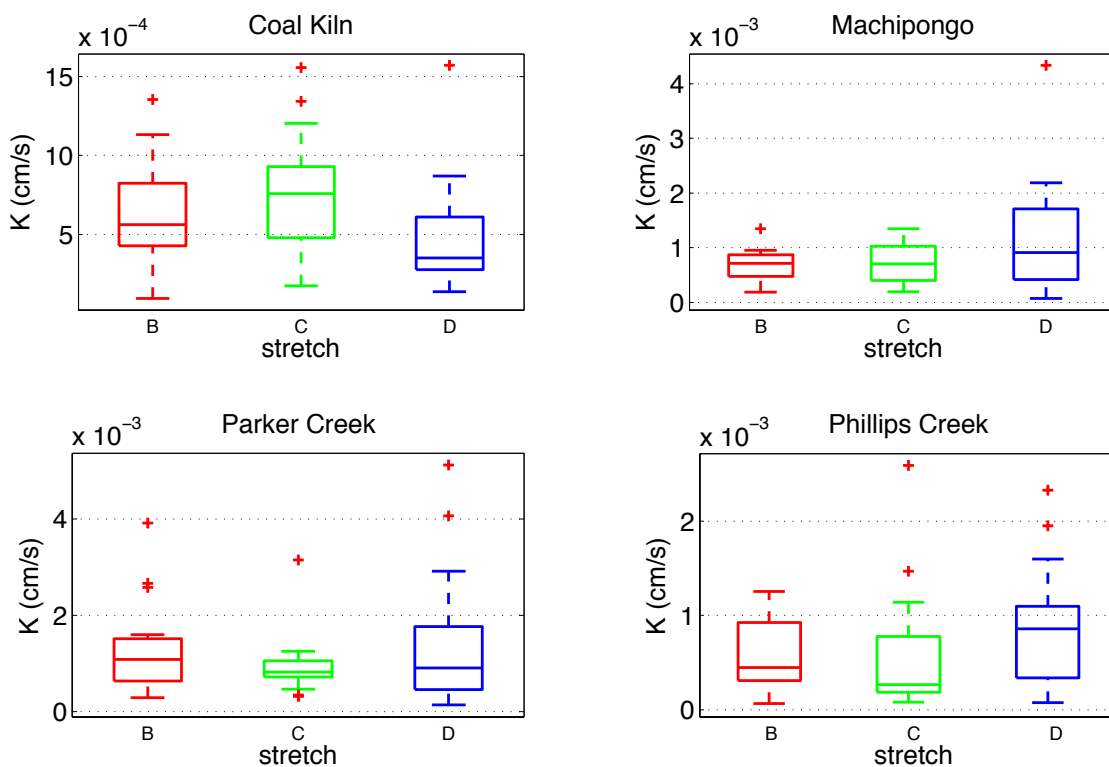


Figure 7-2. Boxplots of K by location in channel, the stream stretch, at each stream.

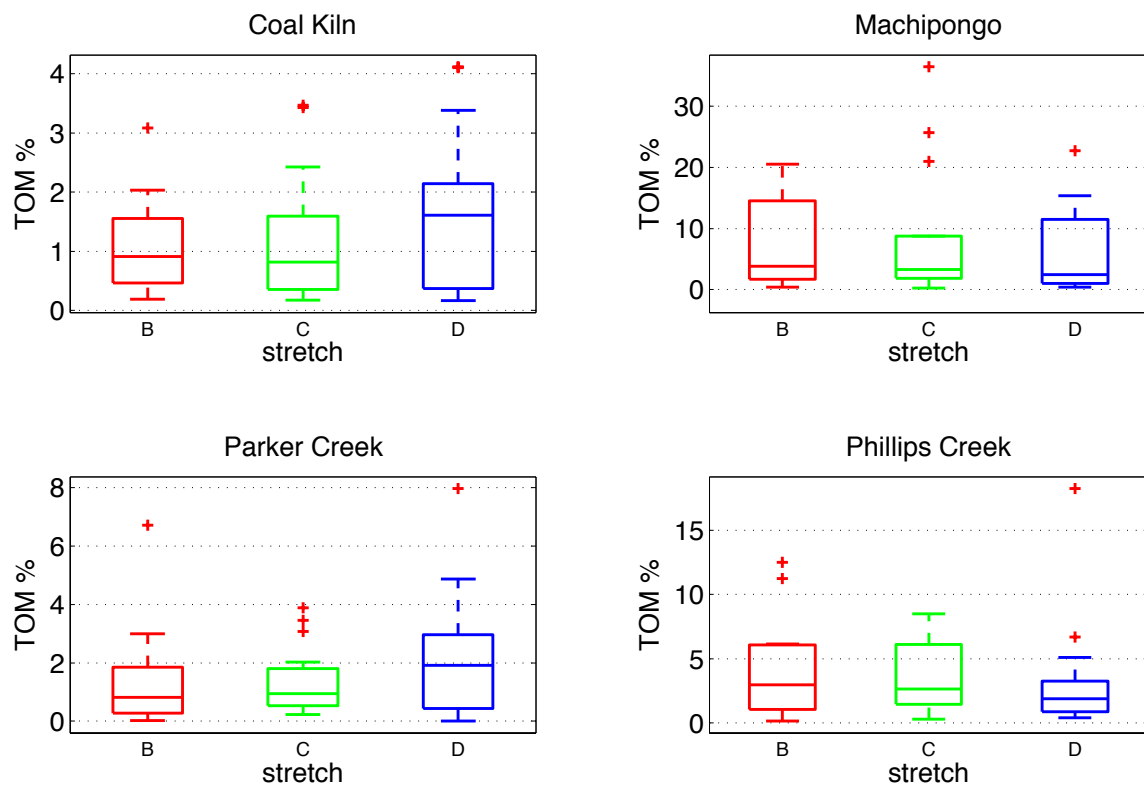


Figure 7-3. Boxplots of TOM% by location in the channel, stream stretch at each stream.

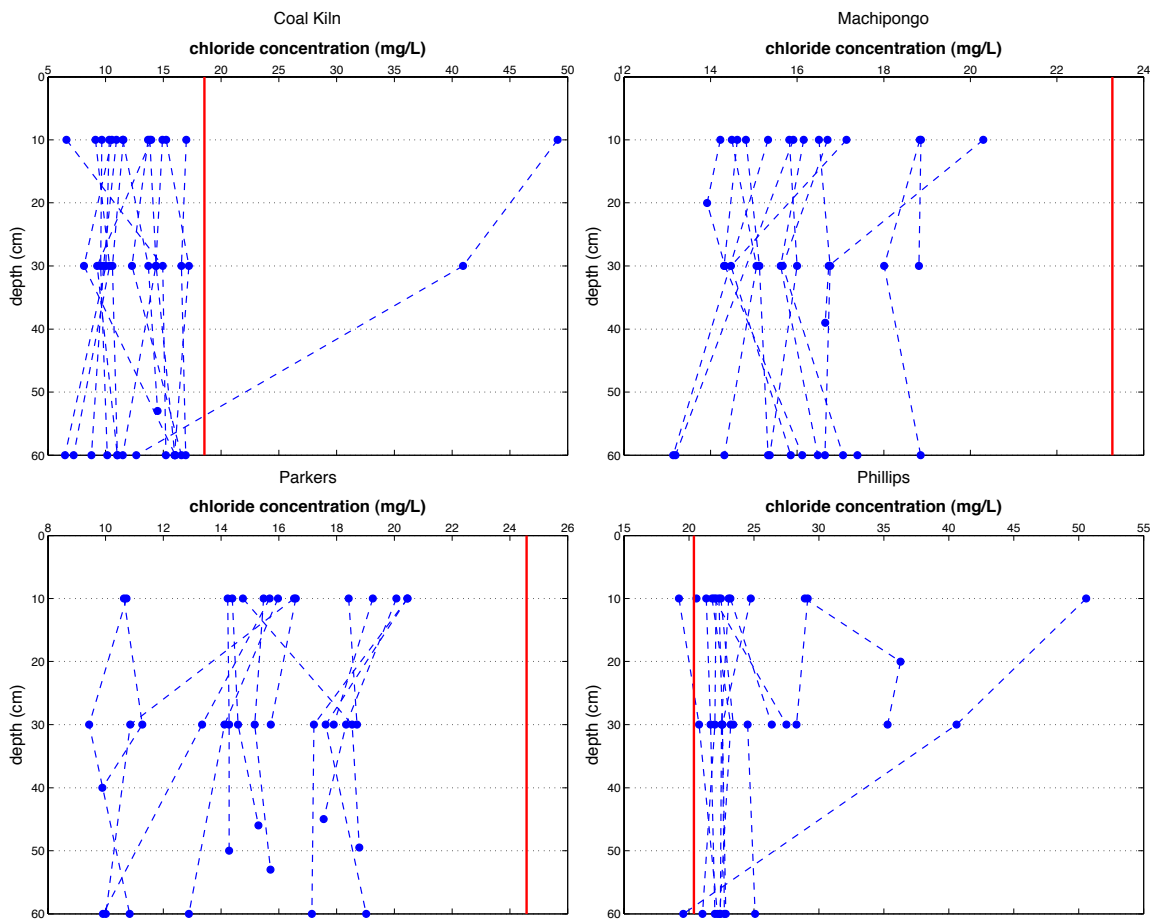


Figure 7-4. Chloride concentration vertical profiles at each stream.

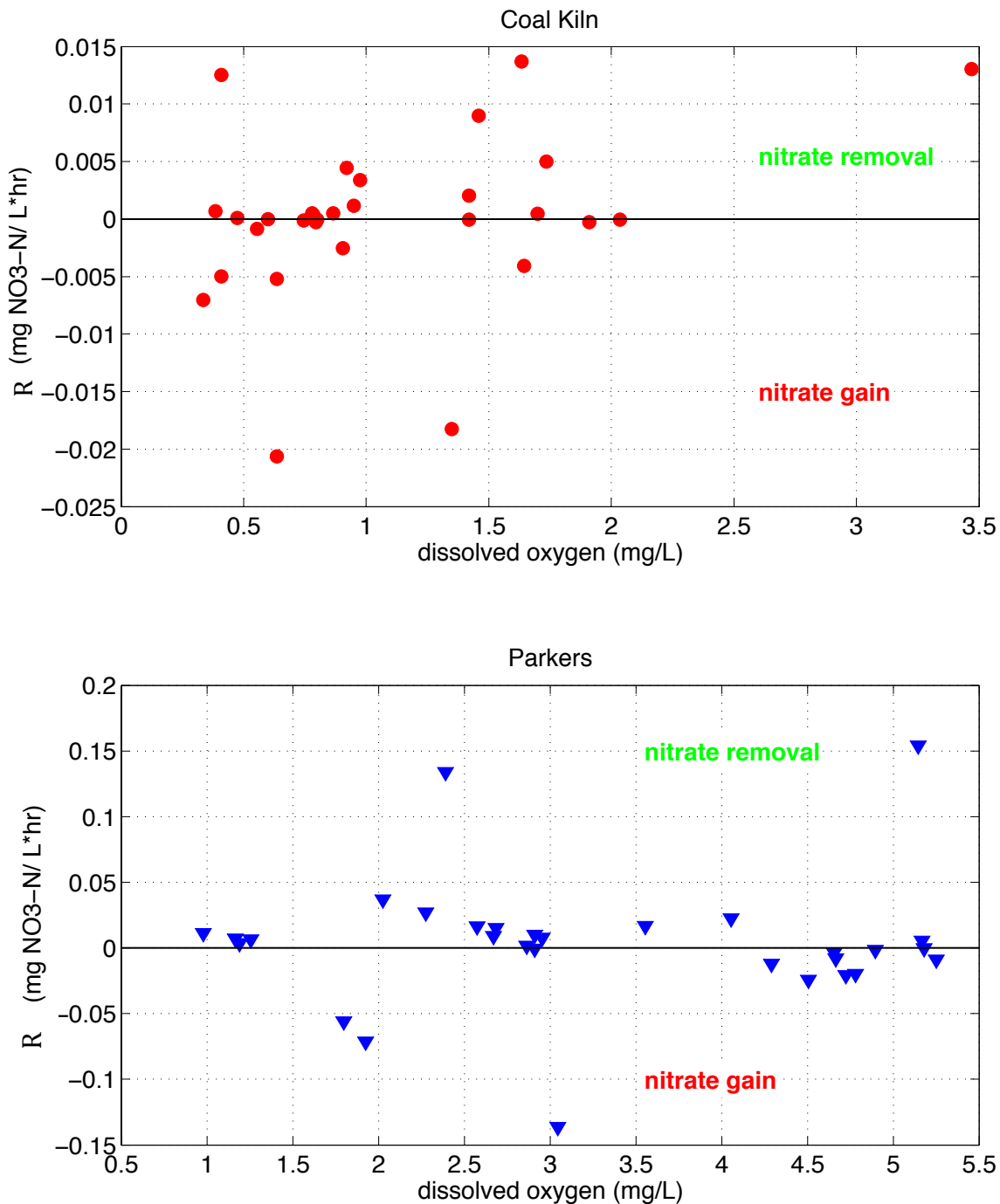


Figure 7-5. Scatter plot of *DO* to *R*. Nitrate removal rate, *R*, between depth intervals (between 10 and 30 cm and between 30 and 60 cm) was calculated according to flow direction, upward or downward. A corresponding *DO* value was calculated by averaging the *DO* of the two associated depth intervals (the mean *DO* at 10 and 30 cm or the mean *DO* at 30 and 60 cm).

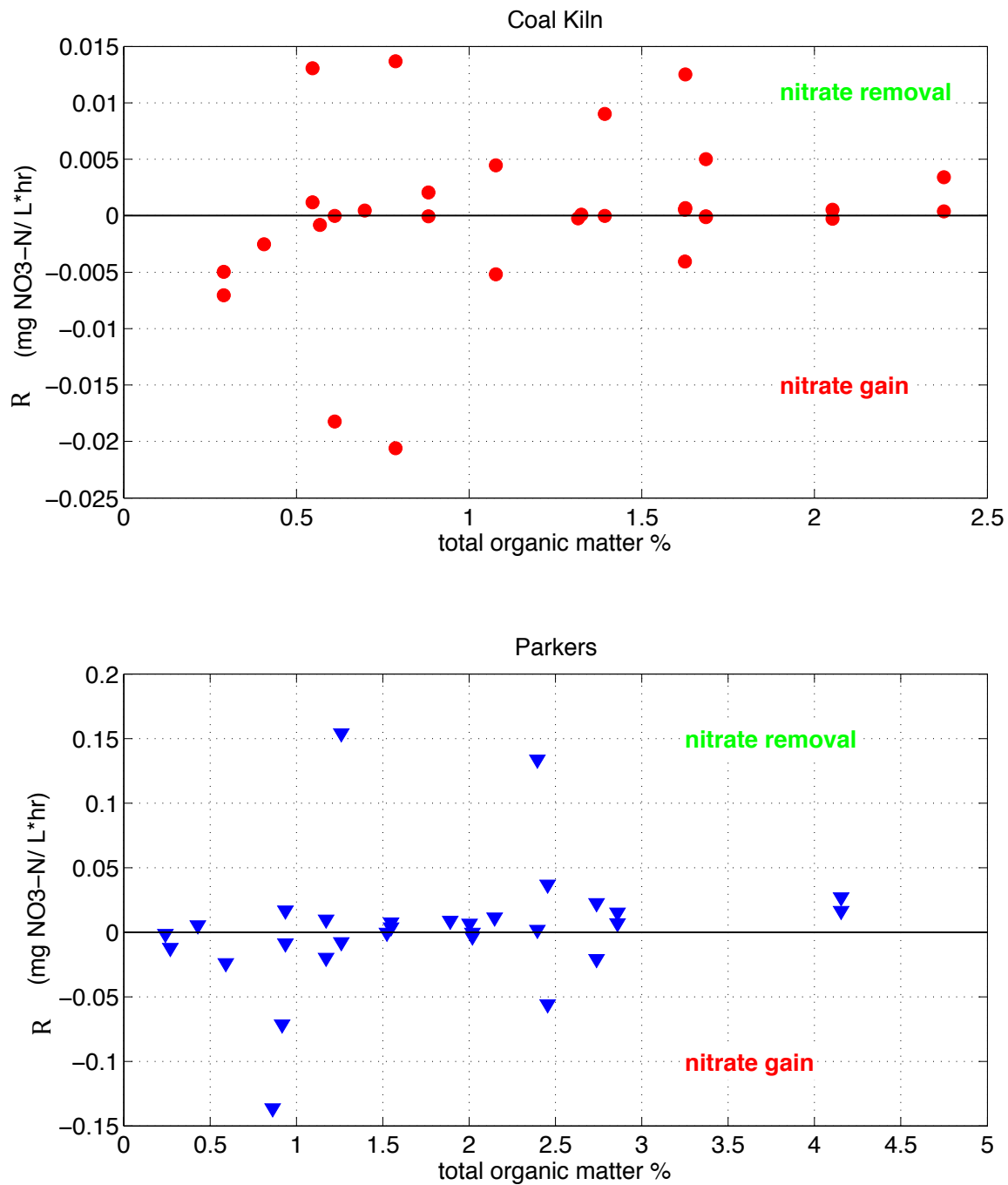


Figure 7-6. Scatter plot of TOM% to R . The same methods explained in Figure 7-2 were used here, but with TOM% instead of DO .

8 Appendix B

Groundwater temperature was used as a tracer to measure pore-water velocity of the visited streams. Pore-water velocities calculated using temperature profiles were compared for comparison to the oil-water manometer drive-point (piezomanometer) values. Using heat as a tracer to measure the complex flow paths of groundwater shows promise [Anderson, 2005], and the fieldwork is easy to perform.

At each location the piezomanometer was inserted, temperature profiles were measured immediately after the drive point was removed. The temperature profiles were analyzed using two Matlab models: a model by *Flewelling* [2009] and Ex-Stream [Swanson and Cardenas, 2011]. The *Flewelling* [2009] model uses the 1-D analytical solution for fluid flow by *Bredehoeft and Papadopoulos* [1965]. Within the Ex-Stream model, the Schmidt method was selected because the temperature data was more of a “snapshot” than a time series [Swanson and Cardenas, 2011]. In Figure 8-1, pore-water velocities from the *Flewelling* [2009] model were compared to piezomanometer values from the same location. The piezomanometer values from the 30 and 60 cm depths of each profile were averaged to provide one value. Only pore-water velocities from the 30 and 60 cm depths were used because of instrument issues at the 10 cm depth. Phillips Creek is not featured because the model returned errors and no velocities were calculated. None of the streams in Figure 8-1 had a 1:1 relationship between the different methods. The pore-water velocities at Parker Creek appear to have a slight linear relationship.

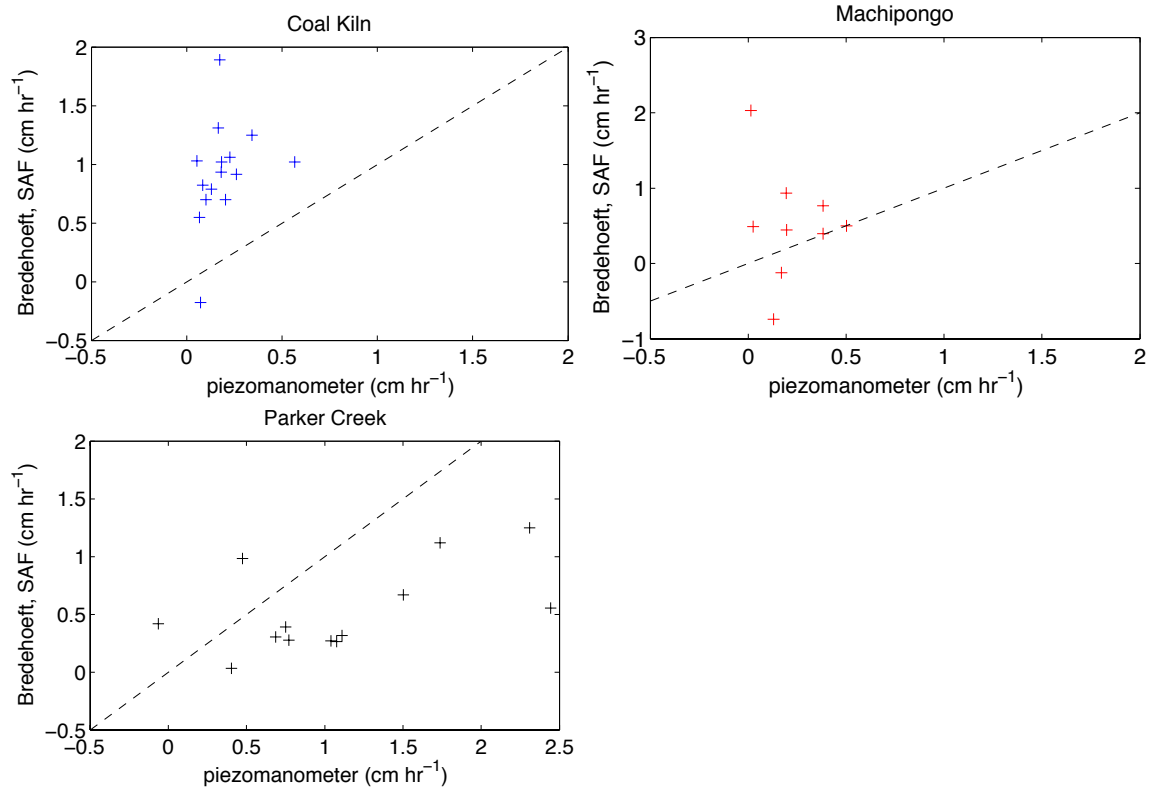


Figure 8-1. Pore-water velocity measured by the piezomanometer device compared to pore-water velocity calculated from temperature profiles using a Matlab program by *Flewelling* [2009].

The Ex-Stream model required temperature profiles to be averaged, thus one pore-water velocity value was produced for each stream. For comparison to the Ex-Stream method, the values from the *Flewelling* [2009] model and from the piezomanometer method were also averaged by stream. Again, for the piezomanometer method, only pore-water velocities from the 30 and 60 cm depths were used to calculate an average. Figure 8-2 compares the average pore-water velocities of the three methods. No pattern between methods appears. At each stream, the three methods have results within one order of magnitude. The comparison shows that temperature profiles provided pore-water velocities in close proximity to piezomanometer values.

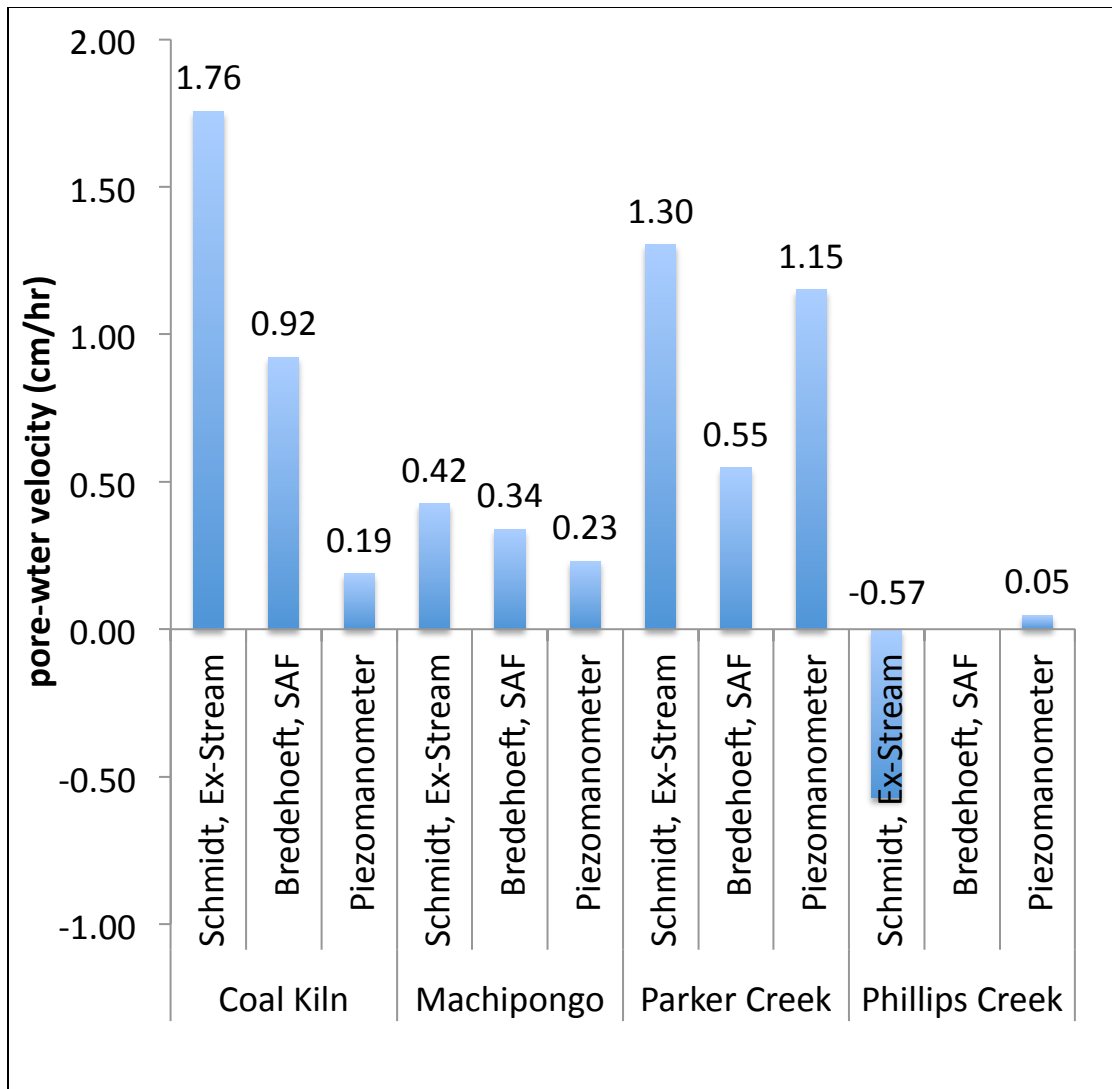


Figure 8-2. A comparison of methods for measuring pore-water velocity. The Schmidt method was completed using the Matlab program Ex-Stream; the Bredehoeft method was completed using a model by *Flewelling* [2009]; and the Piezomanometer method is also presented.